University of Stavanger

Faculty of Science and Technology

MASTER'S THESIS

Study program/Specialization: Petroleum Geoscience Engineering	Spring semester, 2019 Open
Writer: Benedicte Bleivik	Benedicte Bleivik …… (Writer's signature)
Faculty supervisor: Sylvia Nordfjord External supervisor(s): -	
Title of thesis: An Integrated Study of the Oligocene Sequence Stratigraphic Framework in the Egersund Basin, Norwegian North Sea	
Credits (ECTS): 30	
Key words: Sequence Stratigraphy Norwegian North Sea Egersund Basin Oligocene period Seismic interpretation	Pages: 110 Stavanger, 13.07.2019

AN INTEGRATED STUDY OF THE OLIGOCENE SEQUENCE STRATIGRAPHIC FRAMEWORK IN THE EGERSUND BASIN, NORWEGIAN NORTH SEA

By

BENEDICTE BLEIVIK

MASTER THESIS

Presented to the Faculty of Science and Technology

The University of Stavanger

THE UNIVERSITY OF STAVANGER

JULY 2019

Acknowledgement

This study was conducted at University of Stavanger, as a part of my master's degree in petroleum geoscience engineering. First, I would like to give a special thanks to my supervisor, Sylvia Nordfjord, for her helpful discussions, guidance, support and constructive feedback and comments throughout the process of writing the thesis. I would like to thank the University of Stavanger for providing me with necessary workstation facilities. I would also like to express my appreciation to my fellow students for their theoretical, technical and moral support. Finally, I thank my family for their support throughout my studies.

An Integrated Study of the Oligocene Sequence Stratigraphic Framework in the Egersund Basin, Norwegian North Sea

Benedicte Bleivik

The University of Stavanger, 2019

Supervisor: Sylvia Nordfjord

Abstract

The Oligocene interval of the Egersund basin in the Norwegian North Sea is under-studied stratigraphic successions due to its minor significance for the oil and gas industry. The purpose of this study was to improve the understanding of the sequence stratigraphic development in the area of the Egersund Basin.

The Oligocene succession formed as a response to an interplay between different controlling factors, such as tectonics, eustasy, sediment supply and accommodation space. The uplift of the mainland Norway and the thermal subsidence of the North Sea affected the sediment supply of the Oligocene interval. The succession of Oligocene deposition varies considerably in thickness from the Stavanger Platform to the northeast and further basinwards to the southwest.

Six key surfaces were mapped (Base Oligocene surface (MFS1), MFS2, SB1, MFS3, SB2 and Top Oligocene surface (MFS4)) within the post-rift Oligocene strata of the Egersund Basin and the nearby Åsta Graben in the Norwegian-Danish Basin. These key surfaces divide the Oligocene strata into seven seismic units (Units A-G), identified based on reflector terminations and internal reflector configuration.

Two complete, third-order cycle sequences bounded by a maximum flooding surface were identified in the study area. These sequences comprise two highstand systems tracts (HST2 and HST3), two lowstand systems tracts (LST1 and LST2) and two transgressive systems tracts (TST1 and TST2).

Table of Contents

Acknowledgement IV
Abstract V
1. Introduction 1
1.1 Objective 4
1.2 Previous Studies 4
2. Regional Geology 8
2.1 Tectonostratigraphy/Geological setting 9
2.1.1 Carboniferous to Permian 9
2.1.2 Triassic 9
2.1.3 Jurassic 10
2.1.4 Cretaceous 10
2.1.5 Cenozoic 11
2.2 Lithostratigraphy 15
2.2.1 Lark Formation 16
2.2.2 Skade Formation 18
2.2.3 Vade Formation (Upper Oligocene) 19
3. Sequence Stratigraphy 20
3.1 Seismic Stratigraphy 24
3.1.1 Key Stratigraphic Surfaces 24
3.1.2 Stratal Stacking Patterns 27
3.1.3 Systems Tracts 28
3.1.4 Stratal Terminations 31
3.1.5 Parasequences 32
3.1.6 Sequence Hierarchy 33
3.1.7 Clinoforms 33
3.2 Chronostratigraphic Charts 34
3.3 Seismic Facies Analysis 35
4. Data and methodology 36
4.1 Data 37
4.1.1 3D seismic data 37
4.1.2 2D seismic data 38
4.1.3 Well data 40

4.2 Methods 42
4.2.1 Tools 42
4.2.2 Seismic-to-well tie 42
4.2.3 Interpretation Strategy 43
4.2.4 Seismic Attributes 44
5. Observations and Interpretations 48
5.1 Subdivision and Seismic Stratigraphy 48
5.1.1 Subdivision of Surfaces 50
5.1.2 Subdivision of units 57
5.1.2.1Unit A 63
5.1.2.2 Unit B 65
5.1.2.3 Unit C 68
5.1.2.4 Unit D 69
5.1.2.5 Unit E 71
5.1.2.6 Unit F 73
5.1.2.7 Unit G 73
5.2 Seismic Facies Analysis 78
5.2.1 Seismic Facies 1 (SF1) 79
5.2.2 Seismic Facies 2 (SF2) 80
5.2.3 Seismic Facies 3 (SF3) 80
5.2.4 Seismic Facies 4 (SF4) 81
5.2.5 Seismic Facies 5 (SF5) 81
5.2.6 Seismic Facies 6 (SF6) 82
5.2.7 Seismic Facies 7 (SF7) 82
6. Discussion 83
6.1 Sequence Hierarchy 83
6.2 Temporal variability of the post-rift deposition 84
6.3 Controlling factors 86
7. Conclusion 88
References 90

List of Figures

Figure 1. The location of the study area is within the Egersund Basin 1

Figure 2. a) The position and extent of the cross-section (b) in the Norwegian North Sea. b) Cross-section extending from the Stavanger Platform in the NE to the Central Graben in the SW, within the Norwegian North Sea 3

Figure 3. a) Structural map showing the structural elements of the study area. 8

Figure 4. Paleocene times, showing the distribution of active structures, sediment facies and volcanic rocks associated with the North Atlantic mantle plume 11

Figure 5. Map showing the early Oligocene (36 Ma) and the distribution of active structures and sediment facies 12

Figure 6. Map for the early Miocene, that displays the distribution of active structures and sediment facies 12

Figure 7. a) Location of the seismic line going SW to NE, across the Central Graben. 14

Figure 8. Lithostratigraphic chart, ... 15

Figure 9. Sequence stratigraphic correlation scheme built for the North Sea Basin 17

Figure 10. Well 15/9-13 18

Figure 11. Well 2/3-2 19

Figure 12. Evolution of sequence stratigraphic approaches (from Catuneanu et al., 2010). 22

Figure 13. a) Nomenclature of systems tracts, and timing of sequence boundaries for various sequence stratigraphic approaches 23

Figure 14. Selection of sequence boundaries to the "depositional", "genetic stratigraphic" and "transgressive-regressive" sequence models. 26

Figure 15. a) Genetic types of deposits: normal regressive, forced regressive and transgressive. 28

Figure 16. The original three-tract model 29

Figure 17. The four-tract model 30

Figure 18. The Exxon depositional sequence model 31
Figure 19. Types of seismic stratigraphic reflection termination (from Catuneanu, 2002)..... 32
Figure 20. The concept of hierarchy is represented by this diagram. 33
Figure 21. a) Sequence stratigraphic model based on the principles of the Exxon model. b) Chronostratigraphic chart (Wheeler diagram) projected directly from a) above. Chris Kendall, 2001 after a larger scale version designed by Jerry Baum (USC website) http://www.sepmstrata.org/Terminology.aspx?id=chronostratigraphy 34
Figure 22. The basic types of reflection configuration in seismic facies analysis 35
Figure 23. The area of the 3D seismic data in the Norwegian North Sea. 36
Figure 24. The 3D seismic survey (PGS MC3D-EGB2005) used in this study. 37
Figure 25. Spectral analysis of the Oligocene interval 38
Figure 26. Map displaying the extent of the obtained 2D seismic data 39
Figure 27. The MN9206 and NSR04 2D seismic surveys 40
Figure 28. Map displaying the positions of the wells in this study 41
Figure 29. Seismic well-tie 45
Figure 30. Seismic section displaying the five key wells 46
Figure 31. Stratigraphic well correlation between the six key wells in the study area 47
Figure 32. Conceptual chronogram of seismic stratigraphic units and the interpreted surfaces 48
Figure 33. Well 9/2-11 with GR trace relative to the seismic data 49
Figure 34. Seismic section including well 9/2-1 49
Figure 35. Surface maps 53
Figure 36. The map to the left comprises many of the same features as the map to the right, indicating that these features are anomalies of shallow channels above the Oligocene interval, and is therefore seen as anomalies or disturbances on the left map. The orange color highlights one of the many channels. 54
Figure 37. Different maps of the top (1), middle (2) and base (3) Oligocene. 56
Figure 38. Location of the chosen 2D seismic lines within the study area 57

Figure 39. 2D seismic line I-I'. 58
Figure 40. 2D seismic line II-II' 59
Figure 41. 2D seismic line III-III' 60
Figure 42. 2D seismic line IV-IV' 61
Figure 43. 2D seismic line V-V' 62
Figure 44. Unit A 64
Figure 45. Unit B. 67
Figure 46. Unit C and Unit D. 70
Figure 47. Unit E. 72
Figure 48. Unit F and Unit G 75
Figure 49. Conceptual chronogram displaying the interpreted systems tracts and their bounding surfaces, together with the global sea-level curve modified from Hardenbol et al. (1998) 76
Figure 50. Direction of sediment supply 77
Figure 51. Seismic Facies 1. 79
Figure 52. Seismic Facies 2. 80
Figure 53. Seismic Facies 3. 80
Figure 54. Seismic Facies 4 81
Figure 55. Seismic Facies 5 81
Figure 56. Seismic Facies 6 82
Figure 57. Seismic Facies 7 82
Figure 58. Typical delta of the North Sea Cenozoic 87

List of Tables

Table 1. Various authors with their different definition of sequence stratigraphy 21

Table 2. The calculation of vertical and lateral resolutions of the 2D and 3D seismic surveys in the study area. The velocity value is based on the synthetic seismogram in the Oligocene interval. 38

Table 3. Six key wells in the area of the Egersund Basin, one of them located in the Åsta Graben 42

Table 4. The seven seismic facies recognized in the study area. They were identified based on the characteristics of the internal configuration, amplitude strength and continuity, based on Mitchum et al. (1977). Observations are mainly from the 2D seismic data. 78

1. Introduction

Sedimentary basins and highs in the North Sea have been of great interest for a long time, mainly due to being attractive areas for hydrocarbon exploration. Many fields have been discovered and developed in the Norwegian sector of the North Sea since the late 1960's, which have led to the search of more hidden resource potential. Several techniques for investigation of subsurface geology have been developed to assist the industry during this petroleum adventure. Analysis of sedimentology, stratigraphy and structures in the subsurface is important for the exploration, and

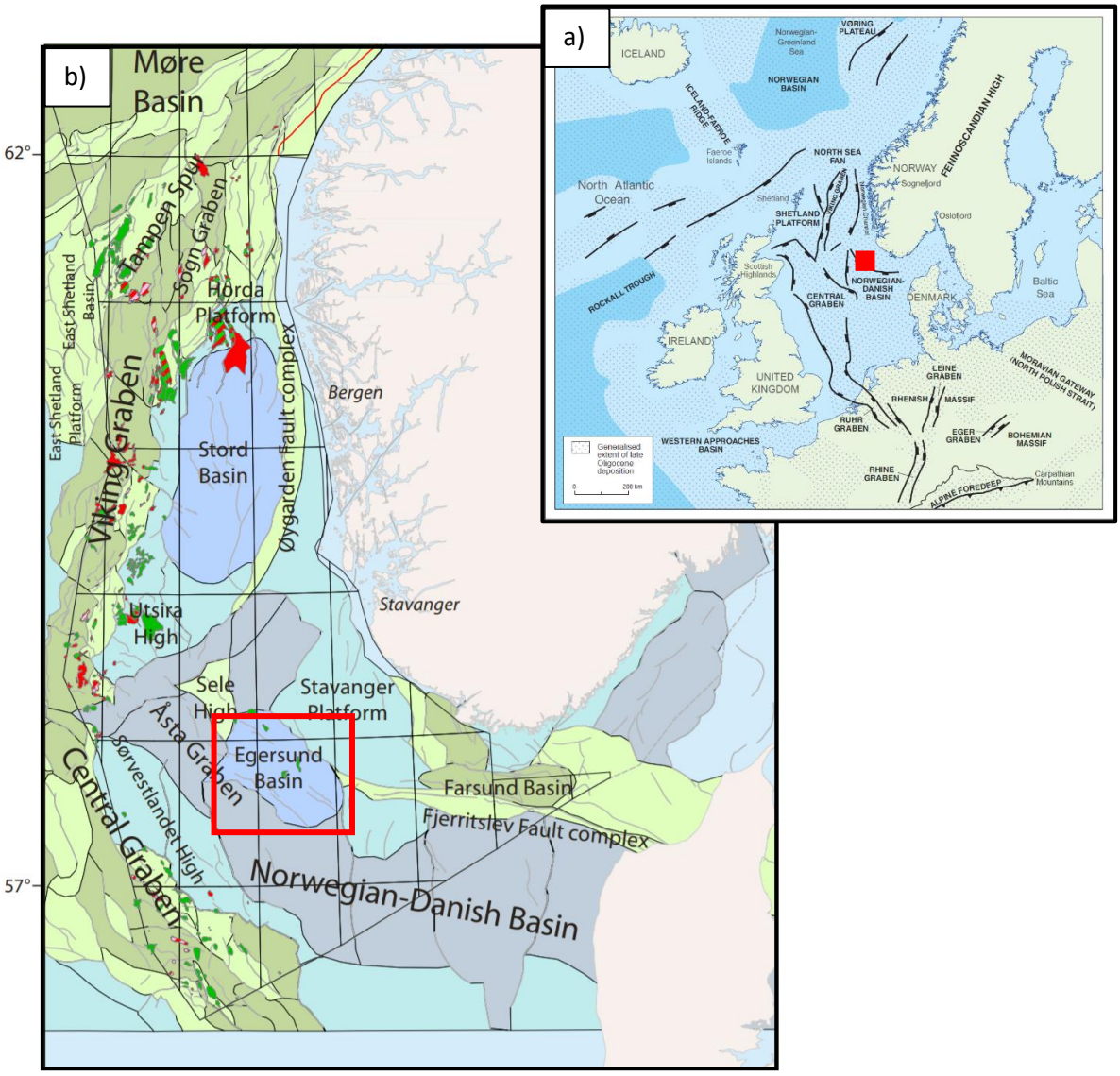

Figure 1. The location of the study area is within the Egersund Basin (red square). Figure a) illustrates the structural elements that were active during Oligocene and Pleistocene times (Modified from Fyfe et al. (2003), based on maps from Ziegler (1982,1989) and Udintsev and Kosminskaya (1982)). Figure b) displays the structural features in the Norwegian North Sea (modified from NPD).

through time it has led to a better understanding of the stratigraphy of sedimentary basins (Nichols, 2009). This study focuses on sequence stratigraphy analysis of the Oligocene sediments and development of the Egersund Basin by using well logs, 3D and 2D seismic data. The sequence stratigraphic framework of Cenozoic strata is generally less examined than the deeper, older sediments. A selection of key wells was used as control points for the stratigraphic and seismic interpretations.

The methods used, to carry out this study, include stratigraphic interpretation and correlation of key wells, seismic interpretation on 2D and 3D seismic, division in stratigraphic units, identifications of stratal terminations and finally interpreted systems tracts. This will contribute to the construction of structural and thickness maps, supplemented with attribute maps of the Oligocene epoch in the Egersund Basin.

Eidvin et al. (2013) investigated the Oligocene to Lower Pliocene deposits in the Nordic offshore area (East Greenland, Svalbard and the Norwegian shelf) and onshore Denmark. They claimed that a detailed understanding of the Oligocene to Pliocene stratigraphy is important in understanding the late geological history of the North Sea Basin, in particularly the uplift and erosion of the Fennoscandian Shield (Eidvin et al., 2013). According to Eidvin et al. (2013), there has been no production of hydrocarbons from post-Eocene sediments on the Norwegian continental shelf, even though there are several discoveries. The deposits of this age have also been far less sampled and examined than older sediments, since the older strata have been the main target for hydrocarbon exploration. This makes of the database poorer for these shallow sediments, e.g. biostratigraphic, pressure samples, etc. Investigation of the sequence stratigraphy of these shallower sediments, can be applied to petroleum exploration and possibly CO2 sequestration with predicting the sandy deposits as well as the sealing shales (Eidvin et al., 2013). In the area Eidvin et al. (2013) studied, several small gas discoveries have been recorded from the Vade Formation (formation within the Hordaland Group). In well 25/2-10 S, oil shows have been discovered below the Skade Formation in a sandy section. In a number of wells, shallow gas and oil have been reported in the shallower sections in the North Sea (NPD 2013). The focus on high-risk exploration targets have also increased in the recent years, which makes the investigation of e.g. the Oligocene sediments more interesting for the petroleum industry (Eidvin et al., 2013).

The Egersund Basin is in the southern part of the Norwegian North Sea, east of the Central Graben and ca. 115 km from mainland Norway (Figure 1, Mannie et al., 2014). The basin trends northwest-southeast and is an extension of the Norwegian-Danish Basin (Tvedt et al., 2013). It is bounded by the Sele and Flekkefjord highs, respectively in the west and south, the Stavanger Platform to the NE and the Lista Nose to the SE (Figure 1) (Sørensen et al., 1992). Several papers have been written about the Egersund Basin, common for many of them is the focus on the reservoir intervals in the Jurassic age sediments. There is one field in the Egersund basin, the Yme field, which was produced between 1987 and 2001 (Husmo et al., 2003).

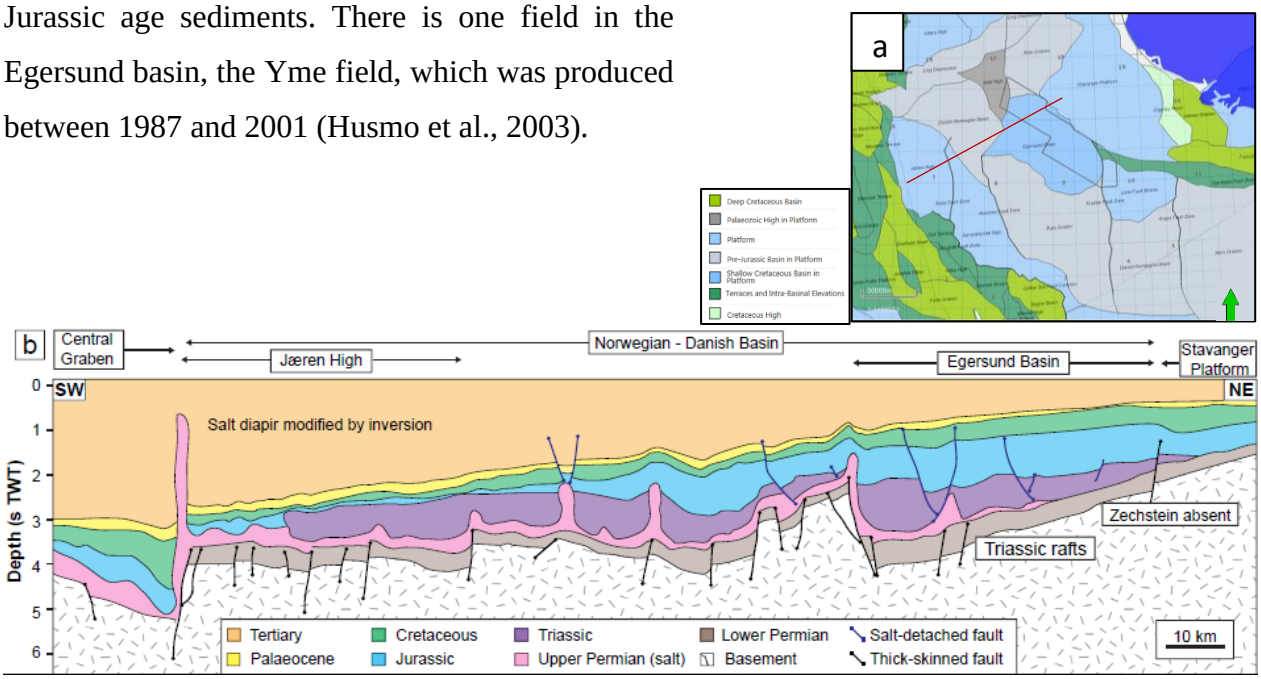

Figure 2. a) The position and extent of the cross-section (b) in the Norwegian North Sea. b) Cross-section extending from the Stavanger Platform in the NE to the Central Graben in the SW, within the Norwegian North Sea (the structures are based on the work by Zanella and Coward (2003), Jackson and Lewis (2013) and data from NPD. The figure is modified after Tvedt et al. (2016).

The main influence for the tectonostratigraphic development in the North Sea are the major rift phases that occurred during Permian to Early Triassic and Late Jurassic to Early Cretaceous (Hodgson et al., 1992; Ziegler, 1979, 1990). Another important aspect is that the Permian period was dominated by thick evaporitic successions (Zechstein Supergroup) that were deposited during periodic flooding and evaporation of the hypersaline waters (Glennie and Underhill, 1998; Hodgson et al., 1992; Ziegler, 1975, 1990). During the Late Jurassic to Early Cretaceous the most important structural development and basin accommodation occurred in the Central and Viking Graben (Faleide et al., 2010, Gabrielsen et al., 2001, Glennie and Underhill, 1998, Ziegler, 1975, Ziegler, 1990). In the Egersund Basin area the effects were more subtle with some reactivation of existing faults (Sørensen et al., 1992). Regional subsidence led to accommodation space and sediment fill in the Egersund Basin, which initiated salt movements and diapirism (Figure 2)

(Fjeldskaar et al., 1993; Sørensen et al., 1992; Sørensen and Tangen, 1995). The basin also experienced phases of uplift and erosion, as well as tectonic inversion (Fjeldskaar et al., 1993; Sørensen et al., 1992). One of the main events in the North Sea Basin during the Cenozoic was the significant change of direction in sediment transportation with a western source area during Paleocene to Eocene and a northern during the Oligocene (Jordt et al., 1995; Faleide et al., 2002; Michelsen et al., 1995; Anell et al., 2010).

1.1 Objective

The primary objective of this study is to further understand the sequence stratigraphic framework of the Oligocene. The limited research of Oligocene strata is mainly because of lack of interest compared to older and deeper lying strata, which has been considered to contain greater potential of hydrocarbon exploration. There have not been previous sequence stratigraphic studies focusing on the Oligocene in the Egersund Basin, therefore the aim of this thesis is to identify regional surfaces and units, mapping sequence stratigraphic boundaries and investigate the relationship between accommodation space and sediment supply of the Oligocene succession.

This study uses 3D seismic reflection survey (PGS MC3D-EGB2005), which is complimented by some 2D seismic lines and wells from quadrants 9, 17 and 18 on the Norwegian Continental Shelves (NCS). The well- and seismic data is released and therefore freely accessible. Schlumberger Plc. provide the Petrel 2018 software that was utilized for the interpretations. Sequence stratigraphic analysis of the Oligocene section over an extensive area, can be obtained from the high-resolution 3D seismic data, the 2D seismic data and well data, and again contribute to determining the timing of events. Also, the thickness and attribute maps produced from this data, are important to predict the depocenters and paleoenvironments of the area through the Oligocene time interval.

1.2 Previous Studies

Over the past decades, the Norwegian North Sea have been broadly studied. Although, the interest has been more concentrated in the northern and central parts of the Norwegian North Sea, e.g. the Viking Graben, than the southern areas, including the Egersund Basin. The studies published in the Egersund Basin, focuses mostly on the influence of the salt in the deeper parts of the basin and /or faults regarding the basin development. An example of this is the study by Tvedt et al. (2013), that investigated the structural style and evolution of salt-influenced, extensional fault array in the Egersund Basin. It concluded that the driving mechanisms behind fault activation and reactivation

is the combination of basement faulting and salt (re-)mobilization. Mannie et al. (2014) tried to determine the impact of syn-depositional salt-movement and associated growth faulting on the sedimentologic and stratigraphic architecture of the net-transgressive, syn-rift succession Middle-to-Upper Jurassic, by using data from the Egersund Basin. The study highlights the complexity of proposing a distinct depositional model for salt-influenced rift basins. In 2016, Tvedt et al. published a paper, where they illustrated how the multiphase salt mobilization influences the structural style and growth of supra-salt fault arrays in the Egersund Basin. All the studies mentioned above, look primarily at the strata of Permian to Cretaceous, with little to no focus on the overlying sediments of Cenozoic age.

Sørensen, Marizot and Skottheim created a tectonostratigraphic analysis of the southeast Norwegian North Sea Basin in 1992, that discussed the regional aspect of this area with respect to structural history, depositional history and stratigraphy. The Oligocene times and the area of Egersund Basin were also considered in this study. Sørensen et al. (1992) investigated the significant drop in sea level in the Early Chattian time and reported the development of Chattian sands along the eastern margin of the southeast Norwegian North Sea area, which they suggested were caused by the uplift of the Fennoscandian Shield to the east. They concluded their studies with a set of paleogeographic maps in their study area.

Investigations of the Cenozoic succession in the central and northern North Sea, were done by Jordt et al. (1995), with the aim of establishing a regional sequence stratigraphic framework. In their study they observed that the generation and therefore the ability to recognize depositional sequences are closely related to the area of origin. This means that sequence boundaries separating sequences consisting of sediments sourced from different areas are easier to identify, than the sequence boundaries separating sequences with sediments delivered from the same source.

They suggested that the development of depositional sequence boundaries is closely related to tectonic movements and to changes in sediment supply. By further investigation, Jordt et al. (1995) noticed that sequence boundaries developed close to significant sea-level falls, but also at times of regional tectonic movements associated with the development of the Atlantic continental margin. They concluded that the eustatic signal got overprinted by the tectonics linked to movements of continental plates, variations in spreading rates and to deep lithospheric processes.

Another study, focusing on younger strata was conducted by Danielsen et al. (1997), where they focused on the Oligocene sequence stratigraphy and basin development in the Danish North Sea sector. They based their interpretations on well logs, seismic and biostratigraphic data. During this study, they defined a total of five sequences in the Oligocene succession, whereas two of the sequences were identified onshore Denmark. They interpreted two types of lowstand prograding deposits, the first consisting of coarse grained, sandy deposits, that occurred in the proximal part of the sequence and comprised sharp-based forced regressive deposits covered with prograding lowstand deposits. The other type, located in the distal part of the sequence, is characterized by clayey and silty deposits and is interpreted as a lowstand prograding wedge (Danielsen et al., 1997). The highstand deposits are represented by thick prograding, sandy deposits in the proximal part of the sequence, and in the distal part these are characterized by thin and condensed intervals.

Danielsen et al. (1997) mapped a succession of lithofacies in each of the sequences, from shallow marine facies, dominated by sands, to outer shelf facies dominated by clays. They established that the main sediment input direction was from the north and northeast, based on the observed decrease in grain-size in a south and southwestward direction. They concluded with an overall southward progradation of the shoreline occurring during the Oligocene, with minor interruptions of shoreline retreats.

Jarsve et al. (2014) studied the Oligocene succession in the eastern North Sea. They revised and re-interpreted the Oligocene sedimentary succession by combining seismic sequence stratigraphy, renewed interpretations, biostratigraphy and Sr-isotope stratigraphy from three key wells and published climate data. This work provided an improved understanding of the link between tectonic and climatic influence of the Oligocene source to sink system in the eastern North Sea area. One of their main findings were that the sediment progradation from the southern Norway was initiated during the earliest Oligocene and continued until the earliest of Eocene. They also suggested that the observed significant increase in water depths during the deposition of Oligocene sequences were associated with basin subsidence that exceeded the generally shallowing eustatic sea level. Jarsve et al., 2014 demonstrates that the creation and infill of accommodation space are both related to tectonic processes and climate changes, during Oligocene in the eastern North Sea.

The results of an integrated study of the Oligocene to Pliocene basins around Norway (including the Norwegian continental shelf, Norwegian Sea, Svalbard and Denmark) were provided in the

paper by Eidvin et al. (2014). Eidvin et al. (2013d) synthesizes data from 47 wells and boreholes from the entire Norwegian shelf, one outcrop from northwestern Svalbard and two stratigraphic boreholes from onshore Denmark. They identified three main depocenters within their study area, where sandy sediments accumulated throughout the Oligocene to Early Pliocene period. These depocenters are in the Norwegian-Danish Basin, the basinal areas of the UK and Norwegian sectors of the North Sea, north of 58°N. Sandy sedimentation in other local depocenters along the west coast of Norway, occurred only in parts of the period. Changes in the paleogeography in the source areas affected shifts in local depocenters.

2. Regional Geology

The Egersund Basin is located in the central Norwegian North Sea, to the east of the UK Central Graben and approximately 115 km offshore south-western Norway (Mannie et al., 2014). The basin is trending NW-SE and is the northwest extension of the Norwegian-Danish Basin (Tvedt et al., 2013). The Egersund Basin is bounded by the Sele High to the north-west, the Stavanger Platform to the northeast, Lista Nose to the southeast, and the Flekkefjord High to the southwest (Figure 3)

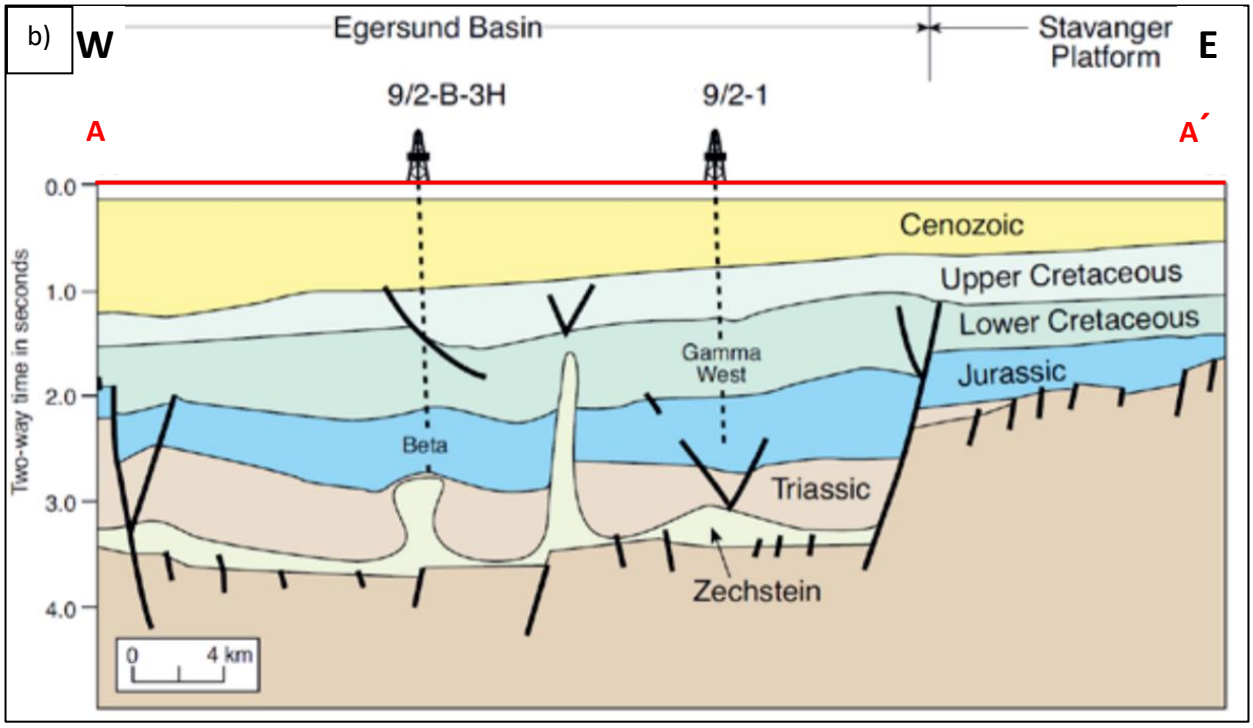

Figure 3. a) Structural map showing the structural elements of the study area. The location of the cross-section in b) is marked as A-A' (modified after Kalani et al., 2015). b) Cross-section of the Egersund Basin, which clearly displays a gradual thickening of the Cenozoic strata towards the west. The older strata within the Egersund Basin have a relatively continuous thickness in the basin, with thinner strata at the Stavanger Platform, caused by uplift and erosion. The observed salt structures located in the northeastern part of the Egersund Basin, are from west to east identified as a salt wall (Beta), salt diapir (Omega or Epsilon) and a salt wall (Gamma) (Mannie et al., 2014). Thick-skinned faults can be observed to the east, separating the Stavanger Platform from the paleo-Egersund Basin, which have been active until the beginning of Late Cretaceous, and to the west, where the Flekkefjord High is situated, which have been active until the end of Jurassic times. Thin-skinned faults are located in shallower strata directly overlying the salt structures, at the base of the Zechstein Salt and at the "base" of Stavanger Platform (Permian deposits) (modified from Millennium Atlas, Evans et al., 2001).

(Sørensen et al., 1992). The Egersund Basin mainly formed in response to the rift events occurring in the Late Permian to Early Triassic and the Middle Jurassic to Early Cretaceous. The second rifting event were partly controlled by the older structural elements (Jackson et al., 2013).

2.1 Tectonostratigraphy / Geological setting

The geological setting sub-chapter briefly explains how the basin has developed from Carboniferous until recent times (Figure 7). More details are included the Cenozoic settings, because th focus on the Oligocene interval for this thesis.

2.1.1 Carboniferous to Permian

The Egersund basin was initially created in response to Carboniferous-to-Permian rifting (Sørensen et al., 1992; Ziegler, 1992), that led to opening and subsidence of this area. This rifting occurred as a result of the syn- to post-orogenic collapse of the Variscan Orogeny (Hodgson et al., 1992; Sørensen et al., 1992). Series of normal faults were generated including the Sele High Fault System and the creation of the North and South Permian Basins were formed due to this Carboniferous-to-Permian rifting. The Egersund Basin represented a sub-basin of the North Permian Basin at this time (Sørensen et al., 1992; Ziegler, 1992). A thick succession of continental sediments (eolian and fluvial sandstones) was deposited (the Rotliegend Group) in the two Permian basins during the Early Permian, (Sørensen et al., 1992). Later, during Late Permian, deposition of thick evaporate sequences, Zechstein Supergroup, accumulated in the basins after a major transgressional event in the North Sea (Hodgson et al., 1992; Sørensen et al., 1992; Davidson et al., 2000b; Glennie et al., 2003). Today, the evaporitic deposition of the Zechstein Supergroup is relatively thick in the center of the Egersund basin, while it is absent or very thin on the structural highs surrounding the basin (Jackson and Lewis, 2013; 2016; Sørensen et al., 1992; Tvedt et al., 2016; Tvedt et al., 2013).

2.1.2 Triassic

The major N-S to NE-SW rifting of early Triassic resulted in the development of a series of NW-SE trending half-grabens and triggered the mobilization and flow of the Zechstein Supergroup. The salt mobilization led to the formation of a variety of salt structures, where several are located above basement-involved normal faults (Sørensen et al., 1992; Jackson et al., 2013). In the Egersund Basin, the Sele High Fault System and the Stavanger Fault System were reactivated due to this rifting event, causing tilting of the Zechstein salt layer and gravity-gliding, together with stretching and normal faulting of the overburden (Sørensen et al., 1992; Tvedt et al., 2013; Mannie et al., 2014; Jackson and Lewis, 2016). During Late Triassic, an increased sediment input from the east,

resulted in the deposition of coarse-grained alluvial fans and fluvial systems (Skagerrak Formation) along rift margins, grading into finer deposits in the center of the basins in the North Sea (Sørensen et al., 1992; Lewis et al., 2013). A widespread transgression occurred in the end of Triassic transitioning to the Early Jurassic, from both north and south (Halland et al., 2011).

2.1.3 Jurassic

The marine transgression was followed by the plume related crustal rise, called the Mid-North Sea Dome, or uplift, that was centered over the North Sea triple junction (point between the Viking Graben, the Central Graben and the Moray Firth Basin) in the Central North Sea in Early Jurassic. This doming or crustal rise caused uplift and widespread erosion, especially affecting the area of the North Sea Rift triple junction (Underhill and Partington, 1993). This is the reason for absence of Lower Jurassic deposits in the Egersund Basin (Husmo et al., 2003).

In the Middle Jurassic, the Mid-North Sea Dome began to reduce or deflate, as a new event of rifting initiated (Underhill and Partington, 1993; Husmo et al., 2003). That caused the reactivation of major NW-SE-striking normal faults, such as the basin-bounding Sele High Fault System in the Egersund Basin (Sørensen et al., 1992; Underhill and Partington, 1993; Husmo et al., 2003). The reactivation during the Middle to Late Jurassic also generated renewed salt mobilization and associated fault growth (Tvedt et al., 2013; Mannie et al., 2014).

Fault slip, extension and subsidence rates were large during the Late Jurassic (Vollset and Doré, 1984). During this time a significant rifting phase occurred in the North Sea area, that lasted until the beginning of Early Cretaceous. Major block faulting happened during this tectonic episode, causing uplift and tilting, creating erosion on the local topography and considerable sediment supply (Halland et al., 2011).

2.1.4 Cretaceous

During the Early Cretaceous the extension rates decreased (Møller and Rasmussen, 2003), followed by a marine transgression and deposition of deep-water mudstones and marls (Flekkefjord, Åsgård, Sola and Rødby Formations) (Vollset and Doré, 1984; Isaksen and Tonstad, 1989). Later in Early Cretaceous the rifting ceased, before a period of post-rift subsidence, inversion and basin shortening occurred in response to the Alpine orogenic event in Late Cretaceous (Ziegler, 1992; Vejbæk and Andersen, 2002; Jackson et al., 2013). This led to folding, reverse reactivations of the pre-existing faults, and rejuvenation of the Zechstein salt and its pre-existing salt-structures,

observed as squeezing and narrowing of some of the larger salt structures (Sørensen et al., 1992; Jackson and Lewis, 2012; Jackson et al., 2013; Dooley et al., 2009). The inversion is assumed to have continued until Miocene times (Sørensen et al., 1992). The shortening was relatively mild (<0.56%), so the Stavanger Fault System in the Egersund Basin, only underwent minimal reverse reactivation (Jackson et al., 2013). The Upper Cretaceous deposits in the North Sea, varies considerably, from deposition of chalk south of 61°N including the Egersund Basin (south of 58°N), while more siliciclastic, clay-dominated sediments are deposited to the north of 61°N (Halland et al., 2011).

2.1.5 Cenozoic

The structural provinces surrounding and including the Egersund Basin (Åsta Graben, Fiskebank Basin and part of the Norwegian-Danish Basin) experienced thermal subsidence during the Cenozoic period, according to Sørensen et al. (1992). There were major earth movements during Cenozoic, among some of the events were closing of the Tethys Ocean to the south-east, sea floor spreading in the North Atlantic Ocean to the north and west and mountain building in the Alps and Himalaya (Halland et al., 2011; Coward et al., 2003). During this time the landmasses surrounding the North Sea Basin were uplifted and the basin deepened, resulting in progradation of deltaic sequences from the Shetland Platform and western onshore Norway into the deep basin (Eidvin and Rundberg, 2001, 2007; Gregersen and Johannessen, 2007).

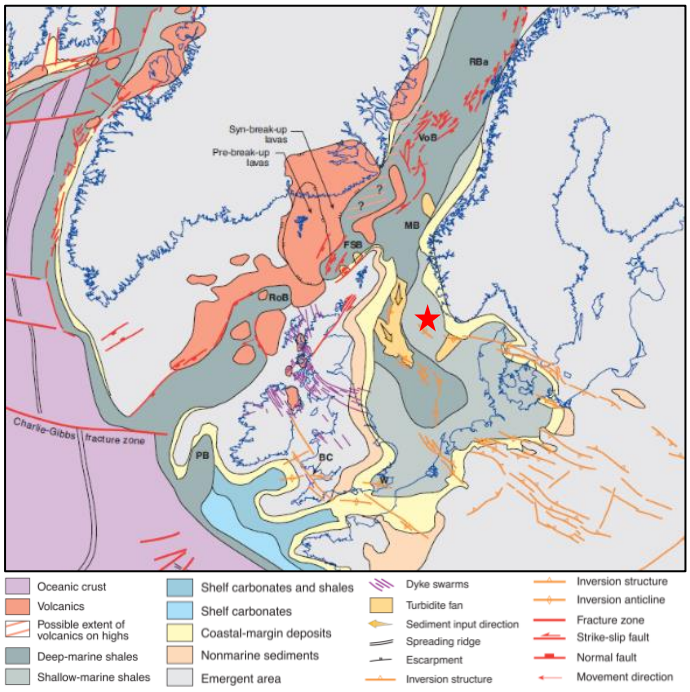

Figure 4. Paleocene times, showing the distribution of active structures, sediment facies and volcanic rocks associated with the North Atlantic mantle plume (modified from Coward et al. (2003)). Red star indicates location of the Egersund Basin.

The eastern part of the Egersund Basin was uplifted during the Paleocene (Figure 4) (Jacobsen, 1982), and this led to deposition of condensed sequences of Lista and Sele Formations. The deposition of the Balder formation, consisting of mainly claystones and a high content of tuffaceous material, represents the boundary between Paleocene and the Eocene, but it can also be observed in the earliest Eocene strata (Sørensen et al., 1992). The sandy deposits of the Fiskebank Formation were deposited in the southeastern part of the Egersund Basin during the Eocene (Deegan and Scull, 1977).

The North Atlantic Ocean developed between Greenland and Scotland during Eocene and Oligocene (Figure 5). The rifting and spreading activity at the Kolbeinsey Ridge, west of Jan Mayen was initiated during this time, and the estimated Eocene-Oligocene boundary is assumed to correspond to this event (e.g. Faleide et al., 1996; Eidvin et al., 1998b). The deposits accumulating from the Late Eocene and Early Oligocene were dominantly shaly (Figure 5).

A significant drop in sea level occurred in the Early Chattian time (Sørensen et al., 1992), and this could be associated with

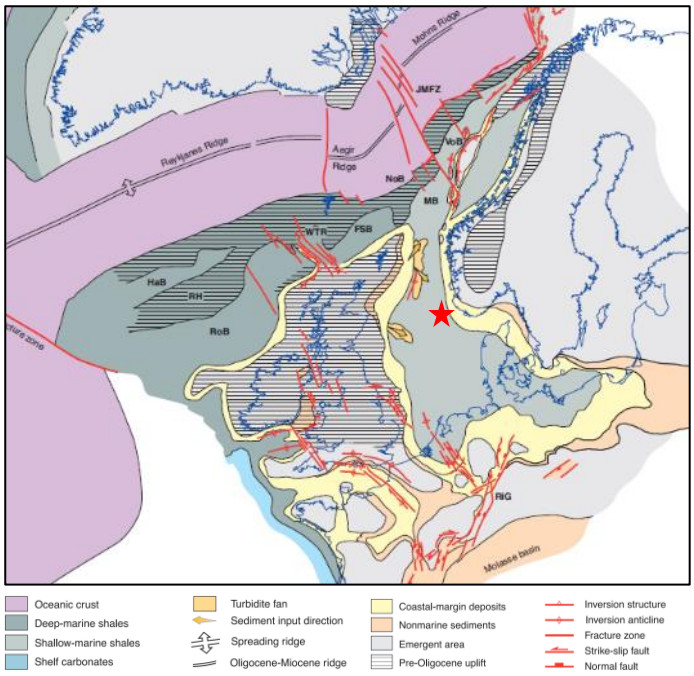

Figure 5. Map showing the early Oligocene (36 Ma) and the distribution of active structures and sediment facies (modified from Coward et al. (2003)). Red star marks the Egersund area.

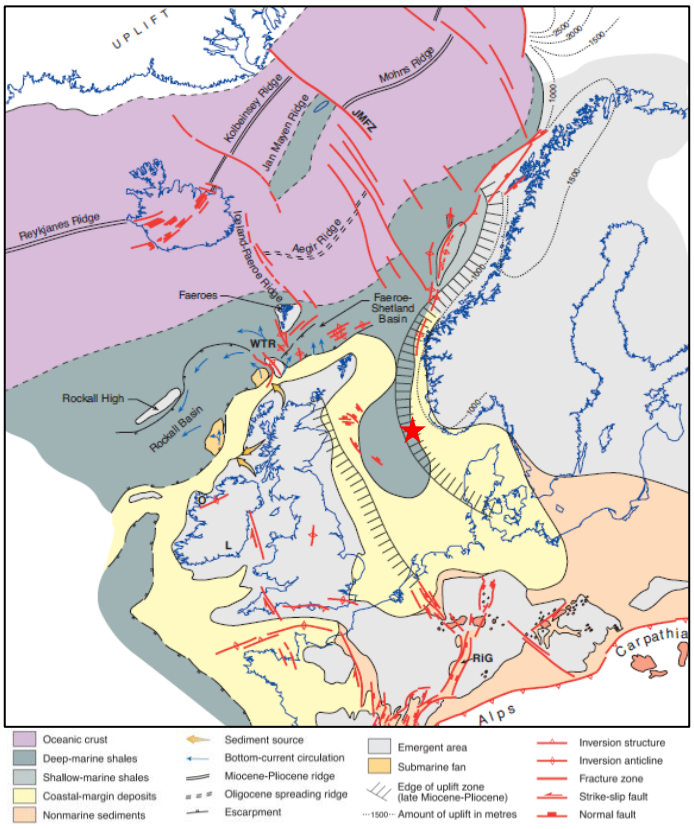

Figure 6. Map for the early Miocene, that displays the distribution of active structures and sediment facies (modified from Coward et al. (2003)). Red star marks the Egersund area.

the uplift of the Fennoscandian Shield. This uplift was due to regional compressive stress formed by the linkage between parts of the North Atlantic rift zone and Alpine collision in southern Europe (Zanella and Coward, 2003). Ziegler (1982) assumed that the fall in eustatic sea level, caused a local hiatus in parts of the central North Sea. Another explanation for this hiatus is that the opening of the North Atlantic Ocean in the Greenland-Norwegian Sea, which influenced the ocean circulation (Jordt et al., 1995).

In the North Sea Basin and the Norwegian-Danish Basin, the deposition occurred in a tectonically quiet, passive margin setting during Oligocene and Miocene epochs (Figure 6). Offshore Norway was affected by basin inversion, due to compression of large transform faults (Doré et al., 1999), but only minor inversion affected parts of the northeastern North Sea, including the Egersund Basin (Zanella and Coward, 2003).

Progradation of sediments into the deeper basins continued into the Oligocene and Miocene. In the sedimentary record from this time, several pulses of coarse clastics have been observed in this area (Eidvin et al., 2014; Rundberg and Eidvin, 2005). The clastic input to the basins during this time interval could be interpreted as a response to uplift of the Scandinavian hinterland or the Shetland platform together with the Quaternary glacial erosion. Other alternatives for this event are non-tectonic processes such as eustatic changes and/or climate changes, sedimentary progradation or rearrangement of ocean current (Laberg et al.,2005b; Eidvin et al., 2014). In the North Sea, the subsidence continued during Late Oligocene and Miocene times, that together with abundant sediment supply from the uplifted margins, resulted in accumulation of significant thickness of mudstones (Fyfe et al., 2003; Sørensen et al., 1992; Eidvin et al., 2014). As clearly observed in the Egersund Basin, the Upper Cenozoic units gradually thins towards the east and the Fennoscandian Shield, whereas the units are more complete in the west. This difference in thickness is due to non-deposition or erosion, that might be related to the continued uplift (Sørensen et al., 1992). It is assumed that the Fennoscandian Shield and Shetland Platform have contributed to the deposition of clastic sediments into the North Sea Basin throughout Oligocene to early Pleistocene (Fyfe et al., 2003).

The late Pliocene and early Pleistocene were times of uplift of the old landmasses surrounding the North Atlantic (Doré et al., 1999). At the same time the global climate continued to cool, which led to the development of a Scandinavian ice cap in the Pleistocene. Periods of more temperate climate caused repeated retreats and advances of the ice sheets, that led to erosion and deposition of ice-related sediments until recent times (Holmes, 1997).

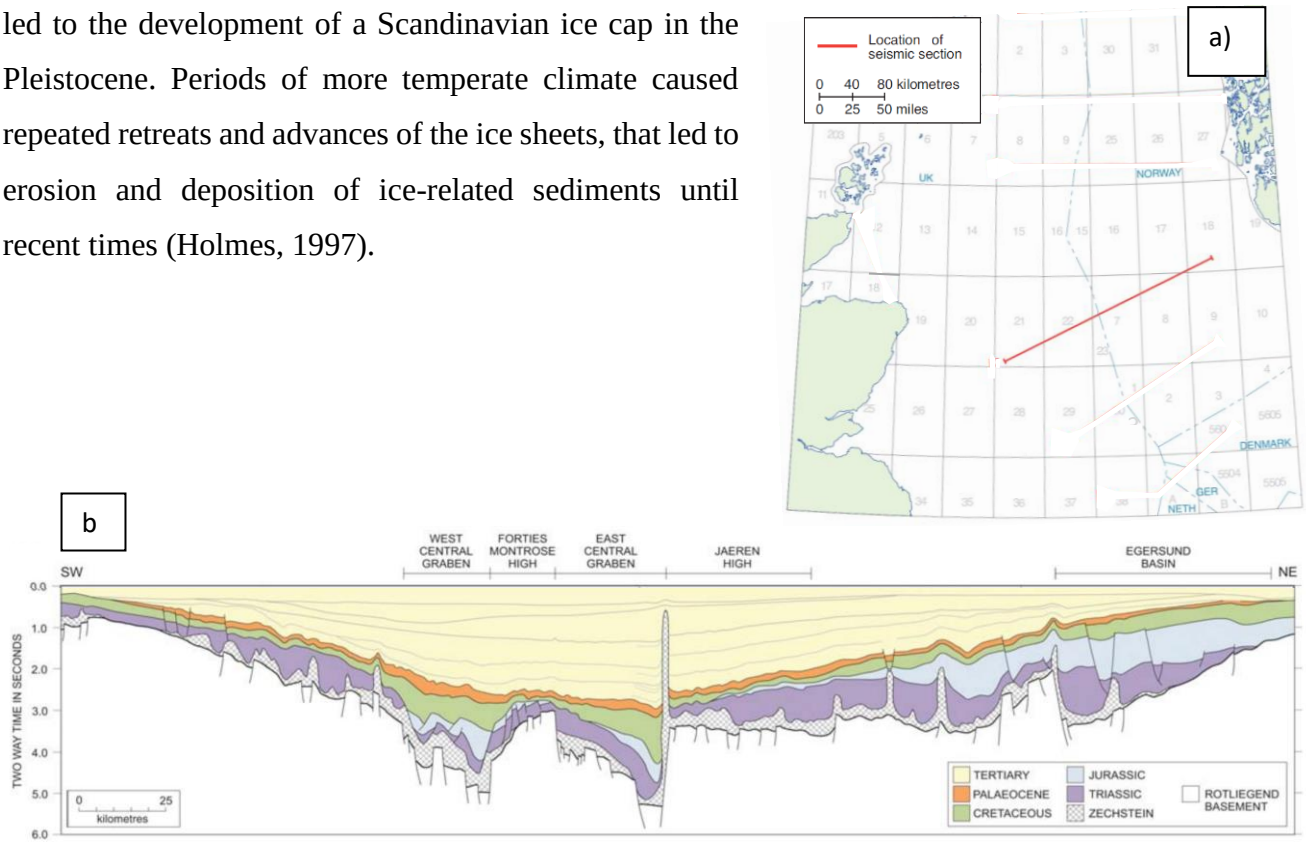

Figure 7. a) Location of the seismic line going SW to NE, across the Central Graben. b) Geoseismic interpretation highlighting structural and stratigraphic elements. The structural style of the central North Sea is characterized by halokinetic deformation due to Zechstein salt movements. The Egersund Basin is located to the NE in this cross section. Modified from Erratt et al. (1999) and Zanella and Coward (2003).

2.2 Lithostratigraphy

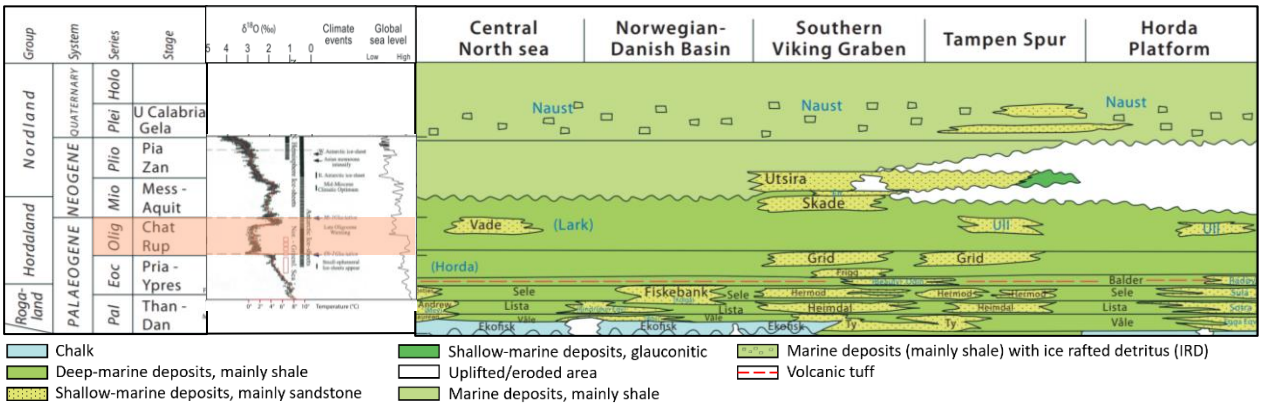

Figure 8. Lithostratigraphic chart, modified from NPD, 2014, paleoclimatic data after Zachos et al. (2001), and the global sea-level curve after Hardenbol et al. (1998).

Stratigraphy is defined as the science describing rock bodies, based on observed properties and attributes that the rocks possess. Lithostratigraphy is a sub-discipline of stratigraphy, and it is the study of stratified rock bodies, that are characterized based on the observable lithological properties (Salvador, 1994). In lithostratigraphy, there is a classification system that divide the rock bodies into unit-terms, which includes, groups, formations, members and beds. These terms are based on the lithological composition and stratigraphic position of the rock bodies. Associated formations with similar distinctive lithological properties are collected into one group. And the same principals are applied for members, which are gathered into one formation, and can be distinguished from the adjacent parts of the formation. Beds are of the lowest rank and, which divides the members into smaller sections (Salvador, 1994).

Deegan and Scull (1977) executed the first study regarding the lithostratigraphy of the central and northern North Sea, that covered the Norwegian and the UK sectors, with special interest for Mesozoic and Cenozoic strata. They named the interval from Eocene to lower Miocene as the Hordaland Group. The sediments of this group consist dominantly of marine shales and mudstones, with some occurrences of sandstones and thin limestone bands. That include some important sandstone formations, called the Skade Formation and Vade Formation.

Alterations of the lithostratigraphy of primarily Paleogene and lower Neogene, in the central and northern North Sea area has been published by Isaksen and Tonstad (1989) for the Norwegian sector, and for the UK sector, by Knox and Holloway (1992). Four sandstone formations were recognized within the Hordaland Group in the Norwegian sector (Frigg, Grid, Skade and Vade

Formations) (Halland et al., 2011), while Knox and Holloway (1992) divided and replaced the Hordaland Group into two groups in the UK sector. These groups are named the Stronsay Group, covering the Eocene, and the Westray Group, that covers the Oligocene to middle Miocene. The Hordaland Group is not divided for the Norwegian Sector, (except for the occurrences of sandstones), it is therefore easier to distinguish what part of the Hordaland Group that is in question when referring to e.g. the Westray Group (UK term for early Oligocene to middle Miocene deposition). Since this thesis focuses on the Oligocene times, only the Westray Group or this time period within the Hordaland Group, will be explained further.

The Westray Group (UK sector) or the early Oligocene to middle Miocene part of the Hordaland Group (Norwegian and Danish sector), have been subdivided into formations with dominantly argillaceous and arenaceous components. The Group is characterized by a relatively symmetrical basin fill, with the greatest thickness being in the deepest parts of the basin over the Central and Viking grabens.

In the Westray and parts of the Hordaland Groups, three formation have been recognized; the Lark Formation (dominated by mudstone), and the Skade and Vade Formations (composed of shallow-marine sands and sandstones) (Fyfe et al., 2003, Ch. 16). The timeframe of the Westray Group, early Oligocene to middle Miocene (Figure 8), comprises the laterally equivalents of Jordt et al. (1995), CSS-3 to CSS-6.

2.2.1 Lark Formation

The Lark Formation is defined in the UK sector, and its equivalent is assumed to be mapped into Norwegian and Danish sectors. However, it has not been distinguished as a formation within the Hordaland Group in these areas. The formation is characterized by its brownish grey mudstone lithology, separated from the underlying greenish grey silt mudstones belonging to the Hordaland Formation of Eocene age. The gamma-ray response for the Lark formation is generally higher than the underlying Eocene formation, but lower than the response from the overlying Nordland Group mudstones.

The lower part of the Lark Formation and its lateral equivalents is of early Oligocene age, and correlates with the Sequence CSS-3, defined by Jordt et al. (2005) (Figure 9). Areas where deposition of Sequence CSS-3 is discovered, are in the eastern part of the northern North Sea, sourced by the Fennoscandian Shield, the North Viking Graben, where sediments built out from

the East Shetland Platform, and the Norwegian-Danish Basin sourced from the north and the central North Sea.

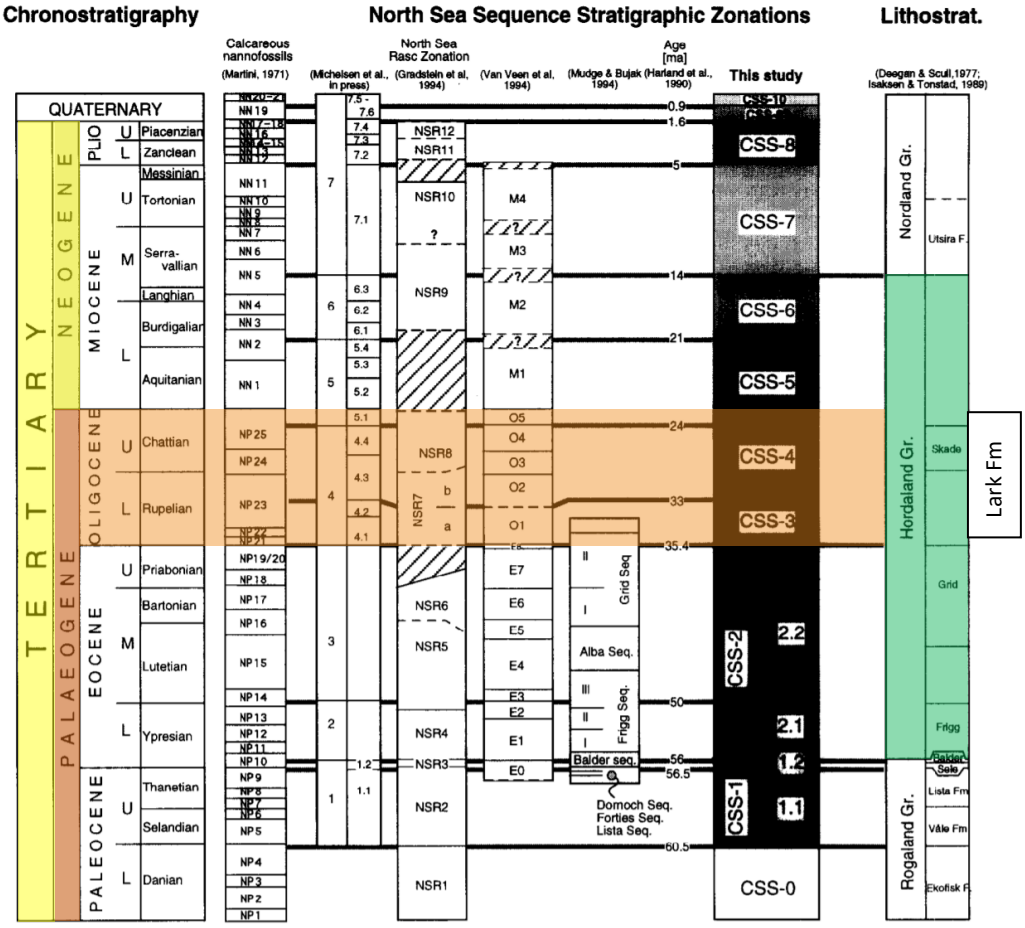

Figure 9. Sequence stratigraphic correlation scheme built for the North Sea Basin, modified from Jordt et al., 1995. The age of the CSS sequences is based on fossil zonations correlated with nannofosssil zonations of Martini (1971). The interval of interest is marked in orange.

Sequence CSS-3 is overlain by Sequence CSS-4 (Jordt et al., 2005), and was deposited late in Early Oligocene until late Oligocene. This sequence is also time equivalent to the Lark Formation, but it also correlates laterally to the Vade Formation in the central North Sea and to the Skade Formation in the northern North Sea. The Lark Formation has only been observed in the deeper parts of the basin in the central North Sea. Towards the west it intersects the Skade Formation and in the Norwegian-Danish Basin it interacts with the Vade Formation. The Sequence CSS-4 is characterized by its more uniform deposition than the rest of Cenozoic succession characterized by its even aggrading reflections. The nature of this sequences suggests a reduced basin relief and an

increased accommodation space. This sequence progrades mainly from the west into the Viking Graben, but progradation has also been recognized south-westward into the Norwegian-Danish Basin, as well as north-westwards off the Stavanger Platform. The presence of CSS-4 above the lower Oligocene CSS-3 deposits, indicate an occurrence of a regional marine transgression. The sequences CSS-5 and CSS-6 of Jordt et al. (1995), lies above the Skade and the Vade formations, where the Hordaland and Westray groups are represented by the Lark Formation (Figure 8). Sequence CSS-5 is of latest Oligocene to earliest Miocene age in the central North Sea (Eidvin, 1993), and CSS-6 is of late Early Miocene to early Middle Miocene. CSS-5 pinches out eastward, north of the Stavanger Platform, and in the Norwegian Danish Basin, silty clay deposits of the CSS-5 built out from the north-east. According to Jordt et al. (2005), this sequence is below seismic resolution along the Fjerritslev Fault, partly as a result of the gradual thinning of deposition towards land and erosion. A hiatus has been identified in the Miocene and it is assumed to correlate with the top of CSS-6. This unconformity is supported by a pinch-out northwards and the missing section in the northern North Sea (Eidvin and Riis, 1992). The upper sequence boundary of CSS-6, correlates to the lithostratigraphic boundary between the Hordaland Group/Westray Group and the overlying Nordland Group (Eidvin et al., 2014; Ziegler, 1981).

2.2.2 Skade Formation

The Skade Formation, defined by Isaksen and Tonstad (1989), can be recognized in wells by a blocky gamma-ray log pattern, possibly representing deeper-water turbiditic sandstones. This formation comprises up to 200 m of fine-to-medium grained sandstones (Fyfe et al., 2003), that overlays the Oligocene mudstones in the North Sea (Figure 10). In the Gullfaks area in the Norwegian sector, thick sandstones of the Skade Formation were deposited during almost the entire Oligocene, while in the UK sector the formation was deposited around middle Oligocene time. In a large area in the Viking Graben, the sandy section of the Skade Formation has been identified to be sourced from the East Shetland Platform. This succession consists of sandstones with occasionally thinner mudstone beds (Eidvin et al., 2014). The deposition of the Skade Formation is in most parts turbiditic in

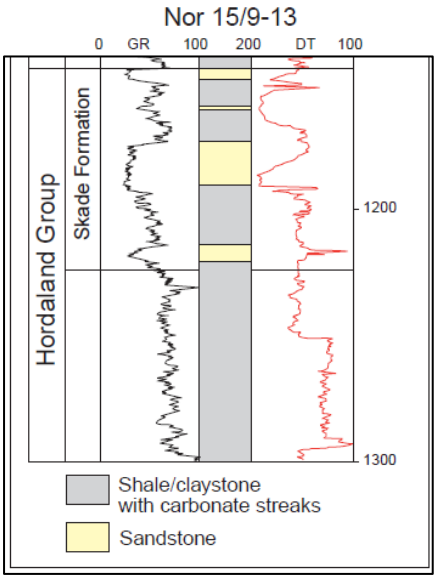

Figure 10. Well 15/9-13, example of the GR log response for the Skade Formation (Fyfe et al., 2003).

origin and assumed to have been deposited on the outer shelf. However, the formation has also been encountered in wells where it has probably been deposited in shallower water in proximity to a delta (Eidvin et al., 2013a and d). The Hutton sandstones (Gregersen and Johannessen, 2007) found in the UK sector, extends into the Norwegian sector and can be correlated with the Skade Formation. The Skade sandstones pinches out to the east and north.

2.2.3 Vade Formation (Upper Oligocene)

The Vade Formation is also defined by Isaksen and Tonstad (1989 as an additional formation within the Hordaland Group, and it is only recognized in the Norwegian continental shelf, (Fyfe et al., 2003,). It is composed of shallow-marine sandstones deposited during the late Oligocene. The Vade Formation occurs in the southern part of the Norwegian sector of the North Sea (Isaksen and Tonstad, 1989), and it is found in the well 2/3-2 (Fyfe et al., 2003) with a total thickness of 72 meters (Figure 11). The gamma-ray response in this well clearly displays the top and base of the sandy Vade Formation interbedded with the mudstones of the Hordaland Group (Isaksen and Tonstad, 1989).

The Vade Formation forms part of Sequence CSS-4 in parts of the central North Sea, where it is identified by laterally continuous, even reflectors. Westward-prograding reflectors in the northern North Sea is absent, which could indicate an end of the sediment supply from the Fennoscandian High. There is evidence of erosion on the eastern margin of the basin, which have removed the stratigraphic succession and thus any potential progradational record from the east (Fyfe et al., 2003).

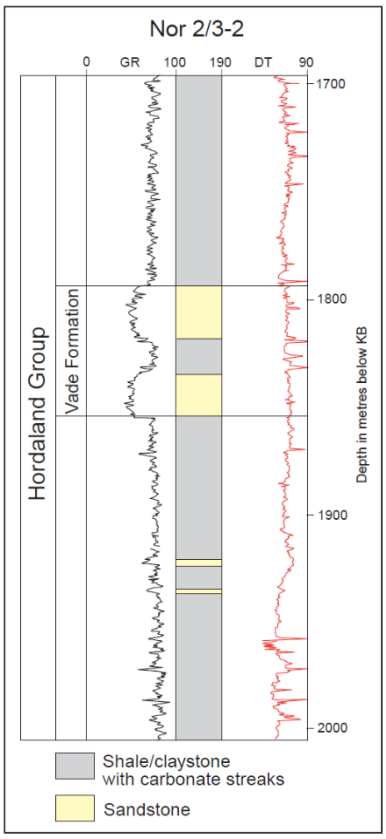

Figure 11. Well 2/3-2, example of the GR log response for the Vade Formation (Fyfe et al., 2003).

3. Sequence Stratigraphy

Sequence stratigraphy is an acknowledged analytical approach for analyzing rock successions. Helland-Hansen et al. (2009) described it as a "branch of stratigraphy that focuses on the subdivision of sedimentary successions into genetic units with chronostratigraphic significance bounded by surfaces of nondeposition or erosion". The technique focuses on analyzing changes in facies and geometric character of strata, together with identification of key surfaces to determine the chronological order of basin filling and erosional events (Catuneanu et al., 2009). Van Wagoner et al. (1988) suggested a division of sedimentary layers (sequence stratigraphic unit) into sequences, parasequences and systems tracts, where each type of unit is defined by its stratal stacking patterns and bounding surfaces (Catuneanu et al., 2011). The tools and concepts used for sequence stratigraphy has been gradually developing from the beginning (Mitchum et al., 1977) until today, in order to keep up with the new data, new analytical methods, new scales of investigation and an improved understanding of how sediments are partitioned from source to sink (Nystuen, 1998). During this time, the definition of sequence stratigraphy has been developed by several authors. Below is a table (Table 1) outlining the different authors definitions of sequence stratigraphy following the age from 1988 until recent time. Catuneanu et al. (2009), discovered that all current definitions share common principles. These four principles, that were most commonly addressed in publications, were:

(1) Cyclicity (that a sequence represents the product in the rock record of a stratigraphic cycle)
(2) Temporal framework (the mapping of sedimentary facies or depositional systems in time)
(3) Genetically related strata (within a systems tract, no significant hiatuses are recognized, relative to the chosen scale of observation)
(4) The relationship between sedimentation and accommodation

Table 1. Various authors with their different definition of sequence stratigraphy

Authors	**Definition of Sequence stratigraphy**
Posamentier et al., 1988 and Van Wagoner, 1995	*The study of rock relationships within a time-stratigraphic framework of repetitive, genetically related strata bounded by surfaces of erosion or nondeposition, or their correlative conformities.*
Galloway, 1989	*The analysis of cyclic sedimentation patterns that are present in stratigraphic successions, as they developed in response to variations in sediment supply and space available for sediment to accumulate.*
Posamentier and Allen, 1999	*The analysis of cyclic sedimentation patterns that are present in stratigraphic successions, as they develop in response to variations in sediment supply and space available for sediment to accumulate.*
Catuneanu, 2006	*The analysis of the sedimentary response to changes in base level, and the depositional trends that emerge from the interplay of accommodation (space available for sediment to fill) and sedimentation.*
Emery and Myers, 2009	*The subdivision of sedimentary basin fills into genetic packages bounded by unconformities and their correlative conformities.*
Catuneanu, 2011	*A methodology that provides a framework for the elements of any depositional setting, facilitating paleogeographic reconstructions and the prediction of facies and lithologies away from control points.*

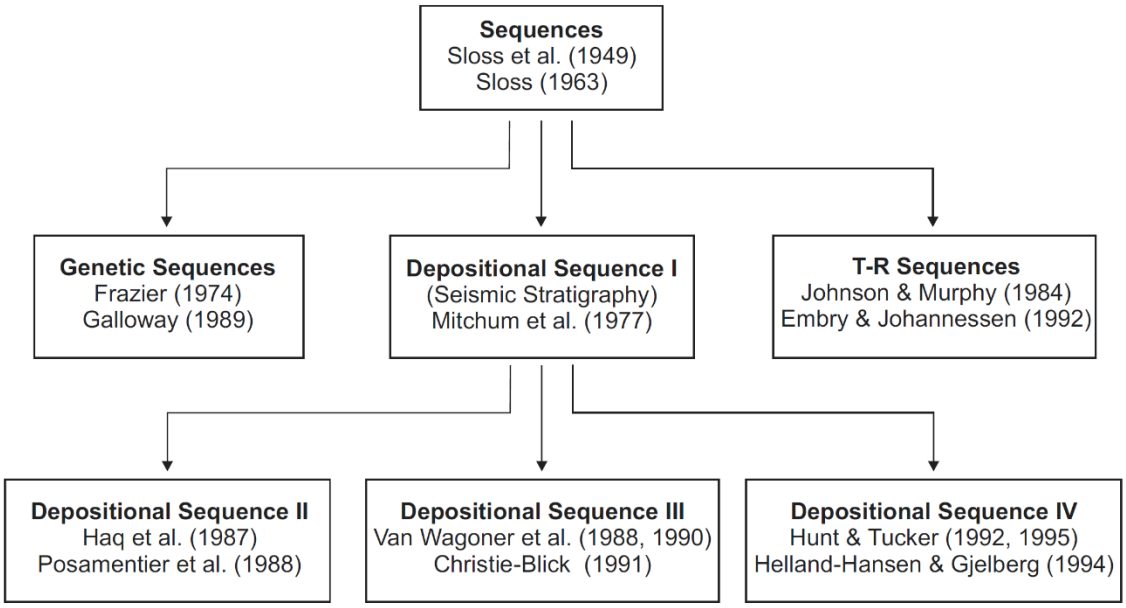

Figure 12. Evolution of sequence stratigraphic approaches (from Catuneanu et al., 2010).

Seismic sequence stratigraphy is extensively used to subdivide the stratigraphic record into units bounded by unconformities (and correlative conformities) (Mitchum et al., 1977a). Several sequence stratigraphic models have been suggested (Nystuen, 1998; Catuneanu, 2002), but common for all the varies models (mentioned below), is that they all focus on recognizing stratigraphic surfaces, that are defined by stratal differences (Martinet al., 2009). The different models include the depositional sequence model (Vail et al., 1977; Posamentier and Vail, 1988; Van Wagoner et al., 1988, 1990), the genetic stratigraphic sequence model (Galloway, 1989), the transgressive-regressive (T-R) sequence model (Embry, 1993, 2003), and the forced regression sequence model (Hunt and Tucker, 1992; Helland-Hansen and Gjelberg, 1994) (Figure 12.).

Catuneanu et al. (2009) highlighted the three first models mentioned above; the depositional, genetic and the transgressive-regressive sequence models (Figure 12). The description of the depositional sequence is that the sequence uses subaerial unconformities and their marine correlative conformities as sequence boundaries (Figure 13a) (Posamentier et al., 1988). The second model is the genetic sequence defined by Galloway (1989) as a sequence bounded by maximum flooding surfaces (MFS) at the top and base (Figure 13a, b). It is usually a practical model, because maximum flooding surfaces are easy to objectively observe in marine environments. The last model Catuneanu et al. (2009) focused on, was the transgressive-regressive (T-R) sequence model of Embry (1993), where the sequence boundary includes the maximum

regressive surface (MRS) linked by the subaerial unconformity (SU) (Figure 13a). Figure 11 displays the different sequence stratigraphic models, with highlighted the systems tracts and the timing of the sequence boundaries used for each type of the models. In this study, the genetic sequence model has been applied to the interpretation of the seismic data in the area of the Egersund Basin, because the maximum flooding surfaces are relatively apparent markers in the well logs.

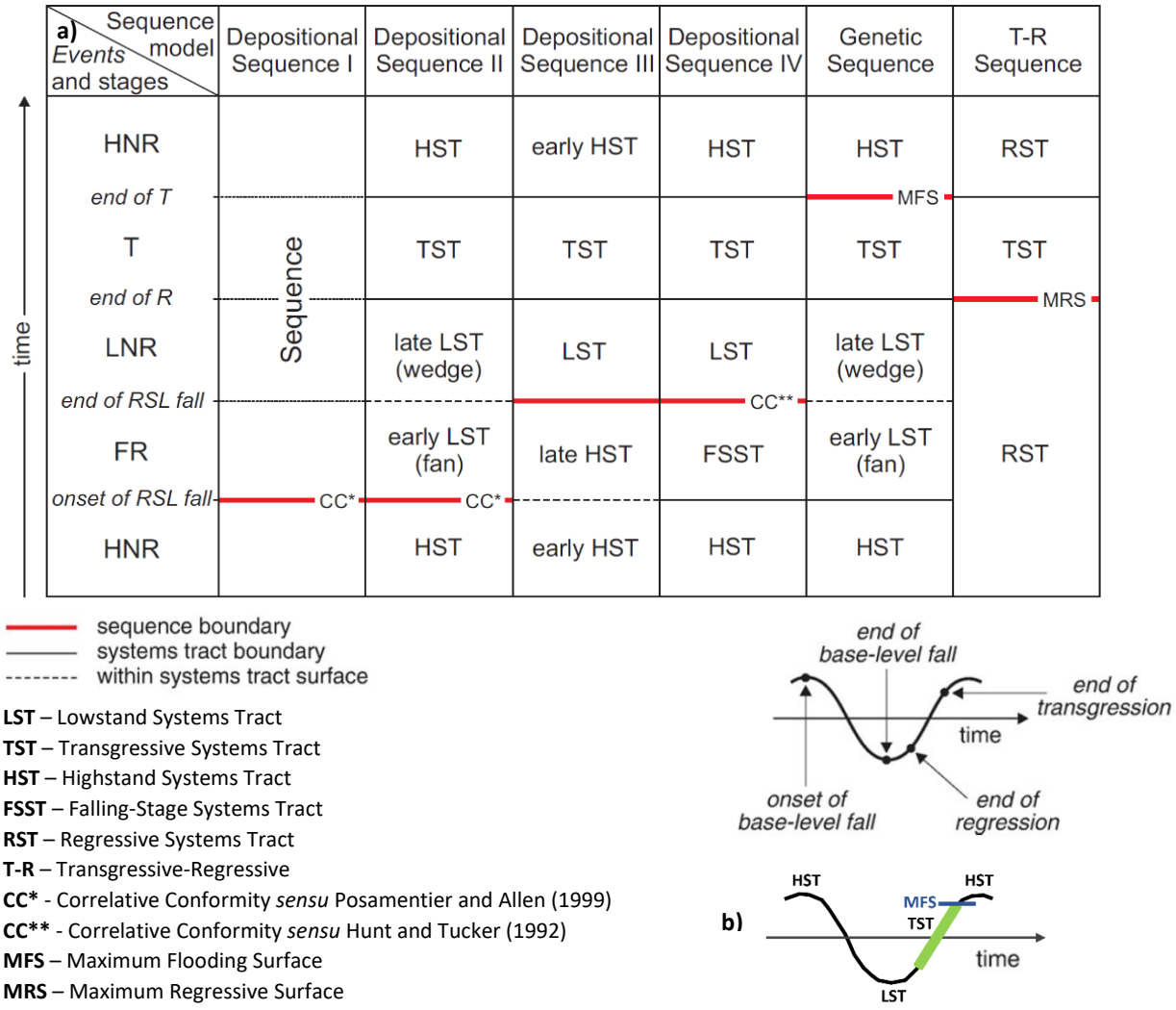

Figure 13. a) Nomenclature of systems tracts, and timing of sequence boundaries for various sequence stratigraphic approaches (modified from Catuneanu et al., 2010). Figure b) is based on the genetic stratigraphic sequence approach, defined by Galloway (1989), with maximum flooding surface as sequence boundary placed at the end of a transgression.

3.1 Seismic Stratigraphy

Mitchum et al. (1977) states that "*seismic stratigraphy is the study of stratigraphy and depositional facies as interpreted from seismic data*", while Cross and Lessenger (1988) explains seismic stratigraphy as the study of stratigraphic units that are defined based on their seismic characters. Seismic stratigraphy is a good tool for interpretation of structural trends, stratal stacking patterns, stratal termination relationships, stratal geometries, depositional features and geomorphology in the subsurface (Catuneanu et al., 2009). Key stratigraphic surfaces can be applied as systems tract boundaries, because the surfaces mark changes in stratal stacking patterns (Catuneanu et al., 2011). As mentioned, systems tracts are recognized by bounding seismic reflectors, as different systems tracts refer to deposition during different positions of relative sea level (Catuneanu, 2002). The term seismic reflection termination, or stratal terminations, is applied to define the stacking pattern units and to present characteristic features in recognizing different surfaces and systems tracts (Van Wagoner et al., 1988). Another important feature in seismic stratigraphy is the concept of seismic facies (Vail et al., 1977), or seismic facies units, that are units consisting of reflection configurations, that are interpreted to determine lateral lithofacies variations (Mitchum et al., 1977).

3.1.1 Key Stratigraphic Surfaces

Sequence stratigraphic surfaces are fundamental for identifying and recognizing key stratigraphic contacts such as the sequence boundary, maximum flooding surface (MFS) and unconformities. These surfaces also mark changes in stratal stacking patterns or genetic deposit types, e.g., lowstand and highstand systems tracts (LST and HST), forced and normal regressive, and transgressive packages, that are also linked to shoreline trajectories (Catuneanu et al., 2009; Catuneanu et al., 2011; Zecchin and Catuneanu, 2012). A stratigraphic surface or a conceptual horizon usually displays a change in acoustic impedance or clear unconformable relationship (Carter et al., 1998) identified in well logs and seismic data. Six stratigraphic surfaces used in sequence stratigraphy are: subaerial unconformity, correlative conformity, maximum flooding surface, maximum regressive surface, transgressive ravinement surfaces and regressive surface of marine erosion, and these will be further discussed in the following subchapters.

3.1.1.1 Subaerial Unconformity (SU)

A subaerial unconformity (SU) is defined as an unconformable, erosional (Nystuen, 1998) or non-depositional surface, with erosion being due to continental processes such as fluvial erosion or

bypass, pedogenesis, wind degradation, or dissolution and karstification (Sloss et al., 1949). The subaerial unconformity is formed during base level fall and may be extended further basinward during forced regression and continuous to the end of base-level fall, where it reaches its maximum basinward extent (Posamentier et al., 1988; Wheeler, 1958; Jervey, 1988). Overlying the subaerial unconformity is strata of non-marine to brackish origin and it represents a significant gap in the stratigraphic record, while the underlying strata is highly variable (Embry, 2009; Shanmugan, 1988). This unconformable surface is represented by stratal truncations below (top laps) representing seaward movements of the shoreline.

3.1.1.2 Correlative Conformity

The term correlative conformity has been interpreted differently by varies authors (Figure 12). Hunt and Tucker (1992) and Catuneanu (2002) explains that the correlative conformity forms within the marine environment at the end of base level fall at the shoreline, in other words, it marks the change in stratal stacking patterns from forced regression to lowstand normal regression. This is the palaeo-seafloor at the end of forced regression, and it correlates with the seaward termination of the subaerial unconformity. While Posamentier et al. (1988), suggested that the correlative conformity was a marine stratigraphic surface that marks the change in stratal stacking patterns from highstand normal regression to forced regression.

3.1.1.3 Maximum Flooding Surface (MFS)

The maximum flooding surface (MFS) (Figure 11) corresponds to the seafloor at the time of maximum shoreline transgression. It marks the change between transgressive (below MFS) and normal regressive (above MFS) shoreline trajectories (Posamentier et al., 1988; Van Wagoner et al., 1988; Helland-Hansen and Martinsen, 1996; Catuneanu, 2006). In seismic stratigraphic terms, maximum flooding surfaces are identified as a downlap surface marking the base of the highstand prograding clinoforms (Figure 12) (Zecchin and Catuneanu, 2013). Maximum flooding surfaces are good markers to map, because of it is widespread in nature and consist of distinctive facies that are represented by a condensed, marine shale bed deposited (Miall, 2016).

3.1.1.4 Maximum Regressive Surface (MRS)

The maximum regressive surface (MRS) (Helland-Hansen and Martinsen, 1996) marks the change between regressive deposits below to transgressive deposits above (Figure 14). The main characteristic for identification of a maximum regressive surface in marine settings is a conformable shift from progradational stacking pattern to a retrogradational stacking pattern. This also marks the change in trend from coarsening- (and shallowing) upward to fining- (and deepening) upward successions (Catuneanu et al., 2009).

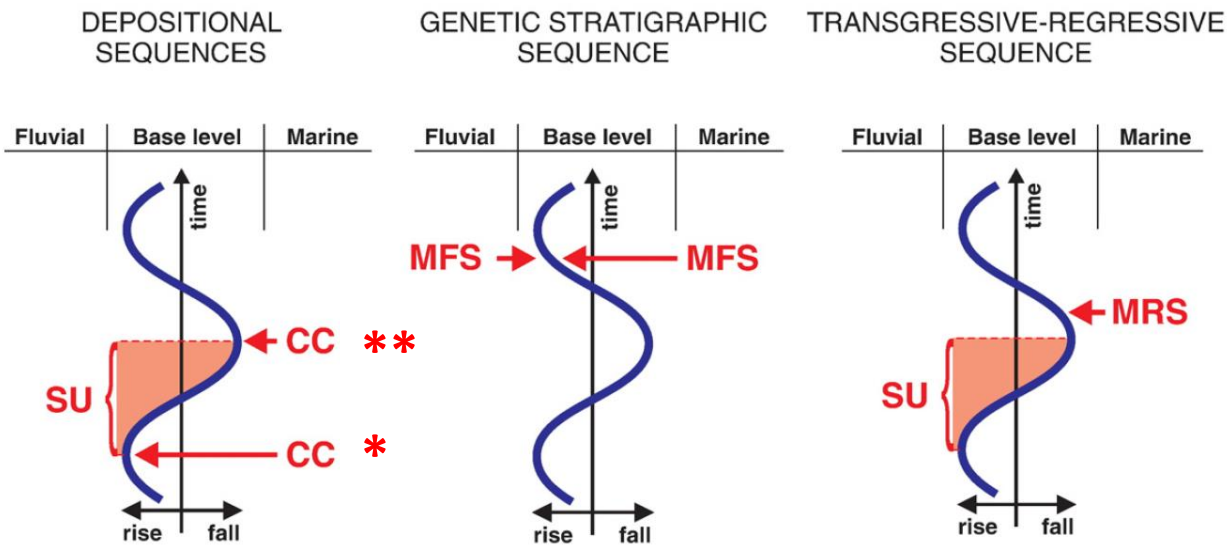

Figure 14. Selection of sequence boundaries to the "depositional", "genetic stratigraphic" and "transgressive-regressive" sequence models. The subaerial unconformity (SU) is a stage-significant surface, whereas all other surfaces displayed in this figure are event-significant. Modified from Catuneanu et al. (2009).

3.1.1.5 Transgressive Ravinement Surface (TRS)

The transgressive ravinement surface (TRS) is expressed by Nummedal and Swift (1987) as an erosional surface created by waves action in a shallow-marine setting or by tidal currents in eustarine settings during a transgressive setting (Allen and Posamentier, 1993). The two types of transgressive ravinement surfaces, wave-ravinement surface and tidal-ravinement surface, are both diachronous and younging towards the basin margin (Nummedal and Swift, 1987; Catuneanu et al., 2011). These surfaces merges into the maximum flooding surface (MFS) in a landward direction and into the maximum regressive surface (MRS) in a basinward direction.

3.1.1.6 Regressive Surface of Marine Erosion (RSME)

The regressive surface of marine erosion (RSME) is formed during times of base-level fall (Plint, 1988). It is an erosional surface which is carved by submarine erosion by wave and current action

on the inner part of the marine shelf during seaward movement of the shoreline during the entire interval of base-level fall. It is progressively covered by prograding shoreface deposits. The RSME is a highly diachronous diastem, the surface is youngest towards the basin (Catuneanu et al., 2011). Due to the diachronuosity, this surface should not be treated as a significant unconformity (Embry, 2009).

3.1.2 Stratal Stacking Patterns

Stratal stacking patterns are defined by the geometries and facies relationships that occurred from the interplay of sediment supply and accommodation space during the time of deposition. Stratal stacking pattern can be defined either independently of or in relation to shoreline trajectories (Catuneanu et al., 2011).

Shoreline-related stacking patterns are defined by their depositional trends. The common shoreline-related stacking patterns are forced regression, normal regression and transgression (Figure 13a). The forced regression stacking pattern is defined as progradation with downstepping at the shoreline, which is driven by relative sea-level fall and induced negative accommodation (Catuneanu, 2002). The normal regression stacking pattern has a depositional trend of progradation to aggradation at the shoreline, where the progradation is driven by sediment supply. This leads to positive accommodation due to sedimentation rates outpace the rates of relative sea-level rise (Catuneanu, 2002). Two types of normal regression stacking patterns have been identified, lowstand normal regression and highstand normal regression (Figure 13b). In both cases, the progradation is driven by sediment supply, but they show a different shape of the shoreline trajectory (Catuneanu, 2011). The last shoreline-related stacking pattern, transgression, has a retrogradational trend. The backstepping is driven by relative sea-level rise and that accommodation outpaces the sedimentation rates at the shoreline (Catuneanu, 2002).

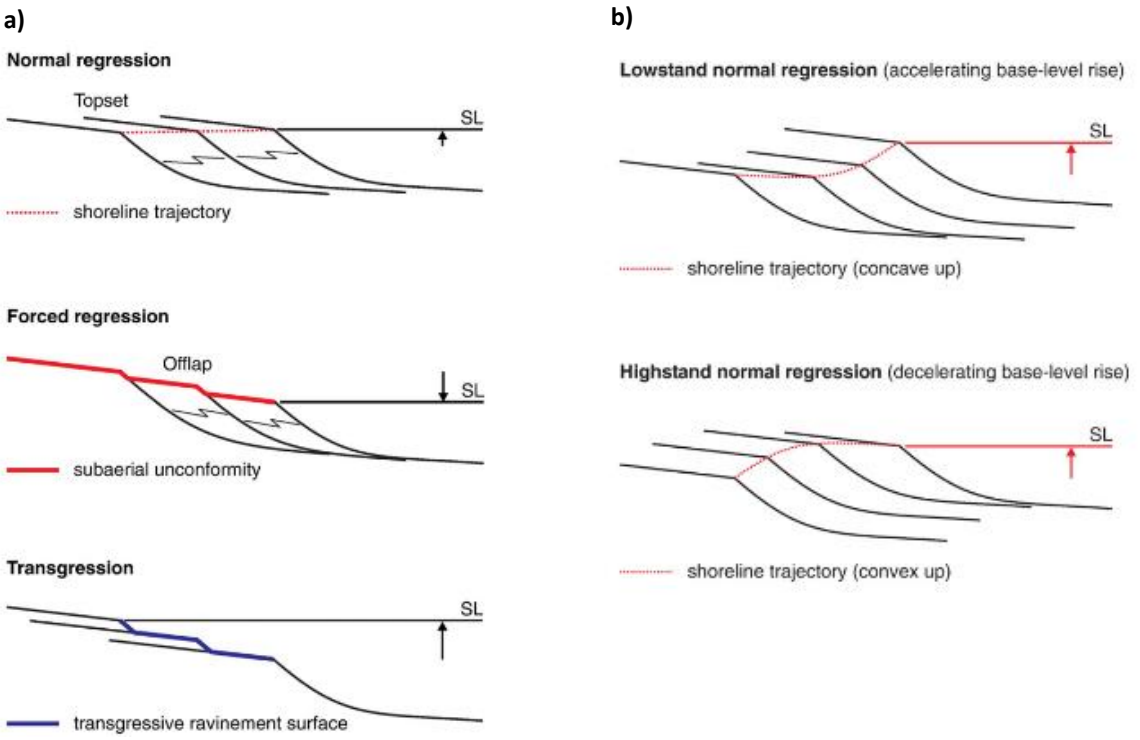

Figure 15. a) Genetic types of deposits: normal regressive, forced regressive and transgressive. The figure displays the types of shoreline trajectory during changes (rise/fall) in base level. Lateral changes in facies within the same sedimentary bodies are indicated by zigzag lines. (From Catuneanu et al., 2009) b) Stratal stacking patterns of "lowstand" and "highstand" normal regressions (modified from Catuneanu, 2006). In both cases progradation is driven by sediment supply, where sedimentation rates outpace the rates of base-level rise at the shoreline.

3.1.3 Systems Tracts

Brown and Fisher (1977) defined systems tracts as "*a linkage of contemporaneous depositional systems*", which can be described by geometry and facies associations and forms the subdivision of a sequence (Van Wagoner et al., 1988; Posamentier et al., 1988). A systems tract consists of a relatively conformable succession of strata bounded by conformable or unconformable sequence stratigraphic surfaces. The internal architecture of a systems tract varies with the scale of observation from a succession of facies to a parasequence set (Catuneanu et al., 2011). Systems tracts are identified and interpreted based on their stratal stacking patterns, types of bounding surface and the position within the sequence (Van Wagoner et al., 1987, 1988, 1990; Posamentier et al., 1988; Posamentier and Allen, 1999). The main systems tracts, that will be used in this study are the falling stage systems tract (FSST), lowstand systems tract (LST), transgressive systems tract (TST) and highstand systems tract (HST) (Figure 17).

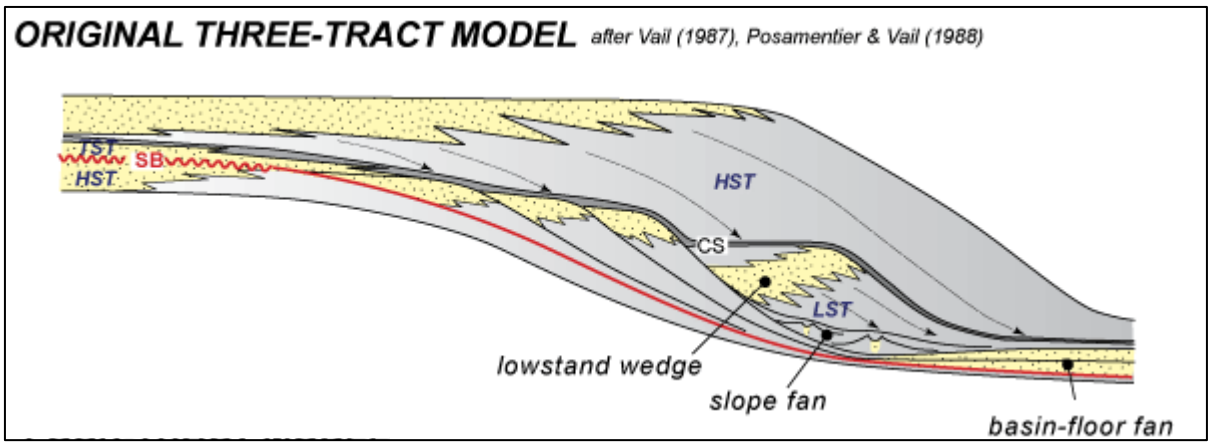

Figure 16. The original three-tract model based on the studies by Vail (1987), Posamentier and Vail (1988). This model contains three systems tracts, LST, TST and HST, and the sequence boundary (SB) is located between the highstand systems tract and the overlying LST towards the basin (left) and TST further up the shelf. Modified from Holland, 2008. http://www.sepmstrata.org/Terminology.aspx?id=sequence%20boundary.

3.1.3.1 Falling-Stage Systems Tract (FSST)

The falling-stage systems tract (FSST) (Figure 17) is formed during relative sea-level fall when the shoreline is forced to prograde regardless of the sediment supply (Catuneanu, 2002, 2006). This displays a foreshortening ("*Stratigraphic sections where the decompacted thickness of a shoaling upward section is significantly less than the difference in palaeo-water depth from base to top (where the top is at or near the sea level) are said to be foreshortened*" (Posamentier and Allen, 1999, p. 140)) at the shelf because of the progressive decrease in accommodation with time. The forced regressive deposits display a thinning in seaward direction (Posamentier and Allen, 1999), and are represented by offlapping stacking pattern without topset development, due to the conditions of negative accommodation (Hunt and Tucker, 1992; Helland-Hansen and Gjeberg, 1994). Different approaches have been used to define the falling stage systems tract. Posamentier and Allen (1999) interpreted the FSST to lie directly on the sequence boundary, terminated by the overlying lowstand systems tract deposition. While Hunt and Tucker (1992) positioned the sequence boundary above the FSST, based on the idea that the boundary marked the termination of one cycle of deposition and the start of another.

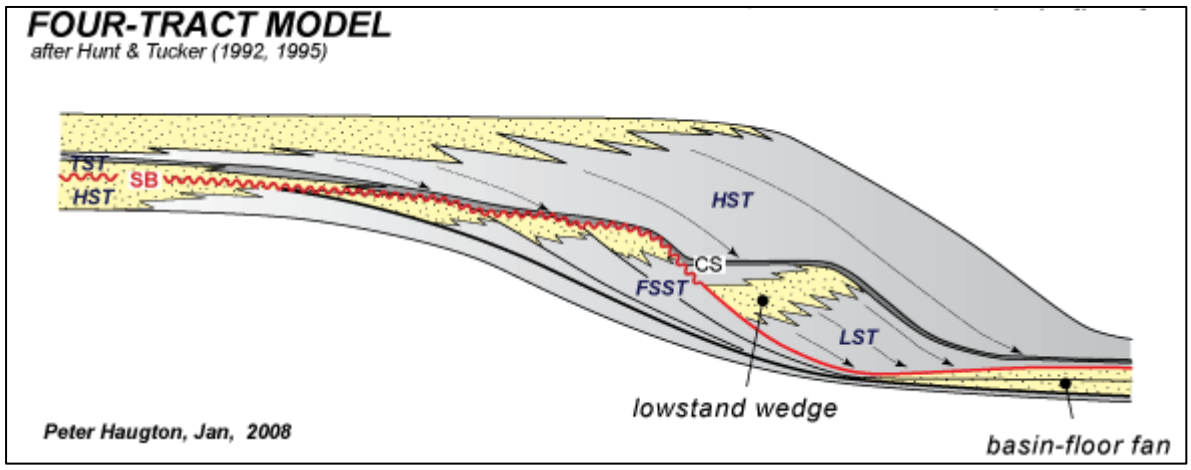

Figure 17. The four-tract model suggested by Hunt and Tucker (1992, 1995), that includes: FSST - falling-stage systems tract, LST - lowstand systems tract, TST - transgressive systems tract and HST - highstand systems tract. Notice that the sequence boundary (SB)/ correlative conformity is positioned at the top of the FSST. Modified from Holland, 2008. http://www.sepmstrata.org/Terminology.aspx?id=sequence%20boundary

3.1.3.2 Lowstand Systems Tract (LST)

The lowstand systems tract (LST) is created during normal regression, where sediments are deposited after the start of relative sea-level rise (Catuneanu et al., 2011). The stacking pattern of the LST is characterized by aggrading clinoforms that shows a thickening downdip, and a topset of fluvial, coastal plan and/or delta plain deposits (Posamentier et al., 1988). Different types of deposition within the lowstand systems tracts include basin-floor fans, slope fans and lowstand wedges (Van Wagoner et al., 1990). This systems tract is bounded by a subaerial unconformity at the base and by the maximum regressive surface at the top (Catuneanu, 2002) (Figures 16, 17 and 18).

3.1.3.3 Transgressive Systems Tract (TST)

The transgressive systems tract (TST) (Figure 16) consists of sediments that accumulated at the beginning of transgression until the time of maximum transgression of the coast, and prior to the regression and development of the highstand systems tract (Catuneanu et al., 2011). The stacking pattern of the TST involves backstepping, onlapping and retrogradational clinoforms, that displays a thickening and younging of strata landwards. The stacking pattern can be aggradational in areas where there is a high sediment supply (Galloway, 1989; Catuneanu et al., 2011). The transgressive systems tract is bounded by the maximum regressive surface (also termed a transgressive surface) below and by the maximum flooding surface (downlap surface) above (Van Wagoner et al., 1990).

3.1.3.4 Highstand Systems Tract (HST)

The highstand systems tract (HST) is characterized by the deposits formed when the rates of sediment supply are higher than the rate of accommodation space creation, which takes place during the late stages of relative sea-level rise (Catuneanu et al., 2011). The stacking pattern of the HST shows both prograding and aggrading clinoforms (Figures 16,17 and 18). The highstand systems tract lies directly above the maximum flooding surface (MFS) and is bounded on top by the next sequence boundary (Van Wagoner et al., 1990) or subaerial unconformity and its correlative conformity (Posamentier and Allen, 1999).

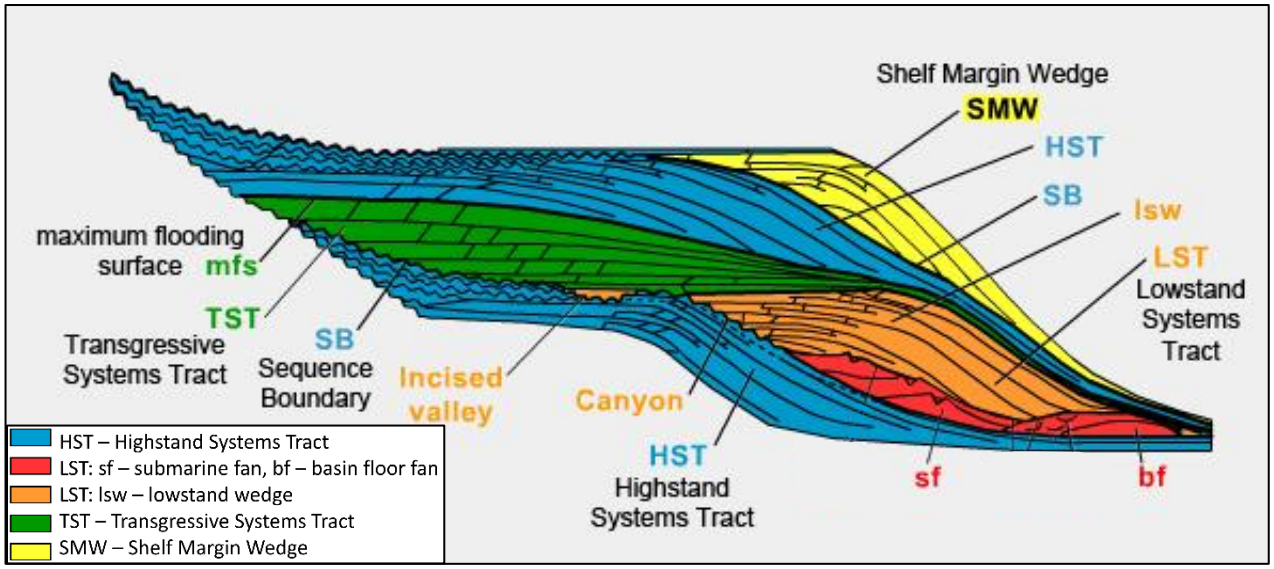

Figure 18. The Exxon depositional sequence model of 1988, that shows the different systems tracts. Modified from Vail et al., 1997.

3.1.4 Stratal Terminations

Mitchum et al. (1977) originally defined stratal terminations, when interpreting reflection seismic profiles. Reflection terminations were explained by Emery and Myers (2009) as "*a two-dimensional seismic section by the geometric relationship between the reflection and the seismic surface against which it terminates"*. Stratal terminations can be used to recognize sequence stratigraphic surfaces, e.g., by onlap and downlap (occurring above a surface), truncation and toplap (occurring below a surface) and offlap. These termination patterns can be used to identify forced regressions and the delineation of subaerial unconformities and their correlative conformities (Catuneanu et al., 2009). Onlap (Figure 19) is the termination of low-angle strata against an underlying steeper surface (Mitchum et al., 1977), which results from sedimentation during relative sea-level rise (Catuneanu et al., 2009). Downlap (Figure 19) is termination of inclined strata against an underlying lower angle or initially horizontal surface (Mitchum et al.,

1977). This is a product of sediment progradation during relative sea-level rise or fall. Truncation (Figure 19) is termination of strata against an overlying erosional surface (Mitchum et al., 1977). Toplap (Figure 19) is termination into the upper boundary of a depositional sequence, where inclined strata terminate against an overlying lower angle bypass surface. Toplap is an indication of sediment supply greater than the accommodation space (Mitchum et al., 1977; Emery and Myers, 2009). Offlap is an outcome of sedimentation during relative sea-level fall, normally occurring due to forced regression (Mitchum et al., 1977). It displays termination of low-angle strata against an underlying steeper surface (Figure 19), where the progressive offshore shifts within a conformable sequence of rocks (Catuneanu, 2002). Surfaces and systems tracts can be defined by stratal termination together with stratal geometries, but it can also express something about the accommodation conditions at the time of deposition (Catuneanu et al., 2009).

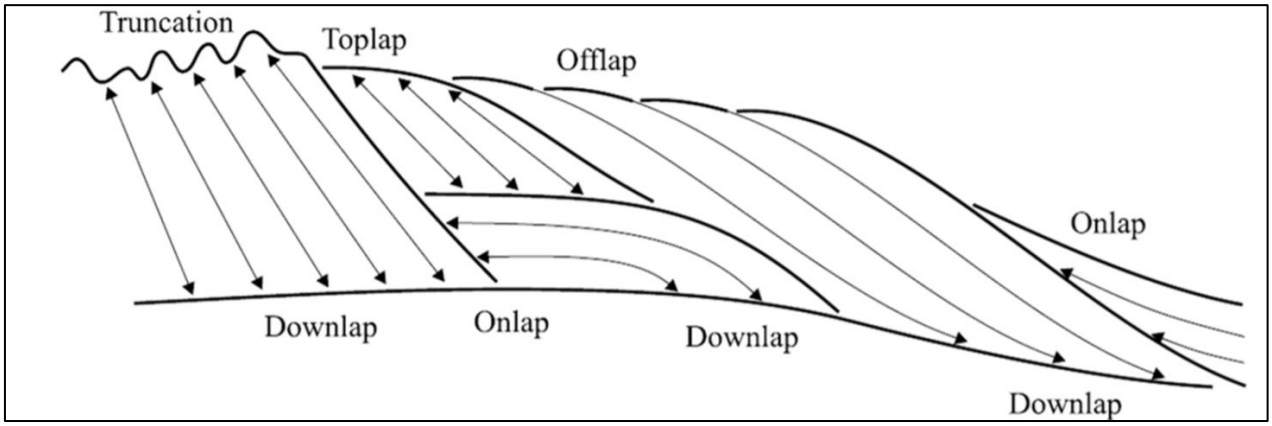

Figure 19. Types of seismic stratigraphic reflection termination (from Catuneanu, 2002).

3.1.5 Parasequences

Van Wagoner et al. (1988) originally defined the term parasequence and describe it as "*a relatively conformable succession of genetically related beds or bedsets bound by marine flooding surfaces".* It is also characterized as units of shallowing-upward strata, and typically coarsening-upward, that is separated by surfaces which marked transgression (Van Wagoner et al., 1990; Embry, 2009; Zecchin and Catuneanu, 2012).

3.1.6 Sequence Hierarchy

The concept of hierarchy refers to the classification of sequences based on their relative scale, duration of cycles and stratigraphic significance (Van Wagoner et al., 1990; Mitchum and Van Wagoner, 1991). There is a great variation in magnitude of sequence stratigraphic surfaces, therefore it is necessary to separate large magnitude sequences/ sequence boundaries from the ones with much smaller scale, using a hierarchical system and divide them into different orders (Embry, 2009). High-order sequences or those of lower rank (Figure 20), e.g. fourth and fifth order, occur more frequently than those of lower orders (e.g., third, second and first) in the rock record (Catuneanu et al., 2011). The first order (Figure 20) is of highest rank, which means that it is of greater importance than smaller scaled sequences, due to its low frequency in the rock record, that usually makes the surface more easily correlated over a larger area (Embry, 1995; Catuneanu, 2006).

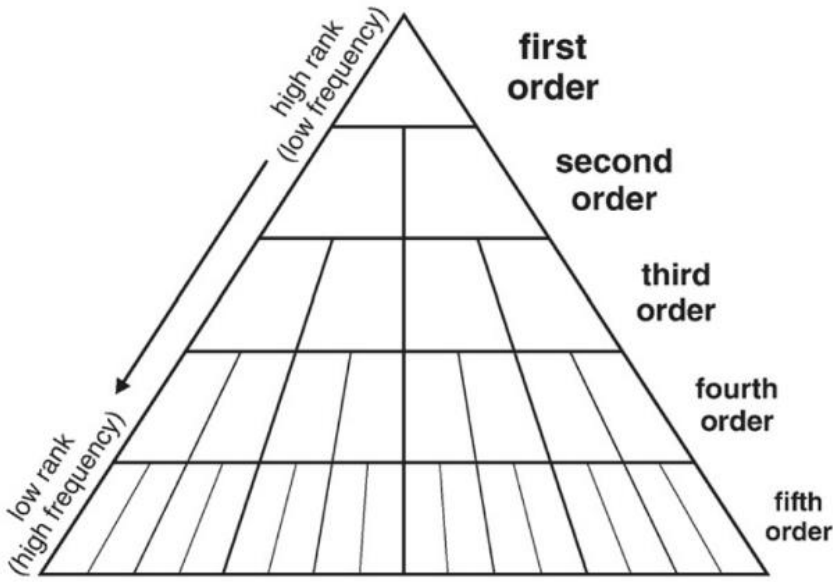

Figure 20. The concept of hierarchy is represented by this diagram. The terms of "high rank" versus "low rank"make reference to the position of the cycle within the hierarchy pyramid. The use of hierarchial orders ("low" versus "high") is inconsistent, some authours prefer first order as a "high order", while others prefer first order as a "low order". From Catuneanu et al. (2011).

3.1.7 Clinoforms

Rich (1951) originally defined the term clinoform as dipping, prograding units that downlaps onto the maximum flooding surface as lateral progradation occur (Miall, 2016). Another explanation used for the term is full sigmoidal "topset-foreset-bottomset" depositional profile (Steel and Olsen, 2002). Clinoforms can be recognized by identifying break-in-slope and their migration patterns. They range widely in scale due to the difference in depositional environment, so Helland-Hansen and Hampson (2009) divided the clinoforms into two systems, (1) shelf-slope-basin clinoforms (building out into the ocean) and (2) shoreline clinoforms (prograding into shallow water). Where the clinoforms created at the shelf-margin (1), can reach a vertical height from hundreds of meters

up to several kilometers, and the clinoforms developed at the shoreline (2), usually has a scale of a few tens of meters. Different combinations of sediment supply, subsidence rates, depositional energy, water depth and sea-level position is reflected in the variations of clinoforms architectures (Miall, 2016).

3.2 Chronostratigraphic Charts

Chronostratigraphic charts (Figure 21), also known as Wheeler diagrams (Mitchum et al., 1977a,b; Vail et al., 1977a), initially described by Wheeler (1958), is constructed in order to display the time relationships of depositional systems, their relationships to surfaces of erosion, condensation and non-deposition (Emery and Myers, 2013). The vertical axis in the stratigraphic cross-section (Wheeler diagram) displays time and the horizontal axis plots distance relatively to the area of interest (Figure 19b) (Miall, 2016). Due to the focus on time instead of thickness, time gaps or unconformities, become more apparent. That again makes it easier to determine the relative positions of the depositional units in time and space from seismic data (Emery and Myers, 2013).

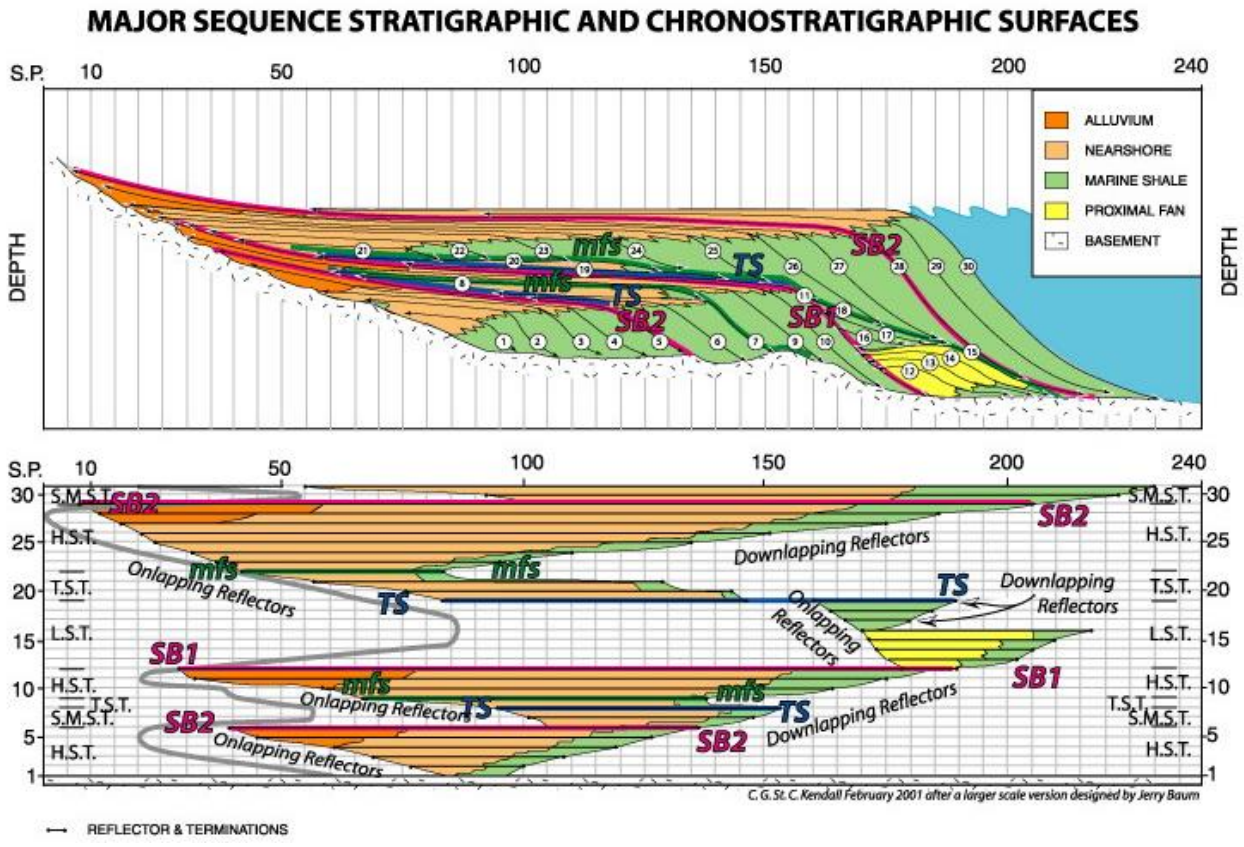

Figure 21. a) Sequence stratigraphic model based on the principles of the Exxon model. b) Chronostratigraphic chart (Wheeler diagram) projected directly from a) above. Chris Kendall, 2001 after a larger scale version designed by Jerry Baum (USC website) http://www.sepmstrata.org/Terminology.aspx?id=chronostratigraphy

3.3 Seismic Facies Analysis

Roksandic (1978) defined a seismic facies unit as a sedimentary unit which is different from the adjacent units in its seismic characteristics (Figure 22). These characteristics may include geometry and structure, lateral facies relationships, reflection configuration, nature of bounding surfaces, amplitude and continuity (Ryan et al., 2009). The results of the seismic facies analysis can be shown on seismic facies maps and seismic facies cross-sections, depending on the available seismic data and geological conditions in the area of interest. Seismic facies maps illustrate the lateral relationships and aerial extent of the individual seismic facies in each of the seismic units (Ryan et al., 2009). A seismic facies unit have an overall geometry consisting of the external form and the internal reflection configuration of the unit. These are used to explain the geometric interrelation and depositional setting of the facies units (Mitchum et al., 1977). Within a given external form, one or more internal reflection configurations may occur. Ramsayer (1979) indicated that because the reflections follow the bedding planes, the reflection geometry equals the depositional geometry, and that this knowledge could be used to further interpret depositional environments, facies unit and possible reservoir rocks, based on the internal reflection patterns of a sequence and their distribution.

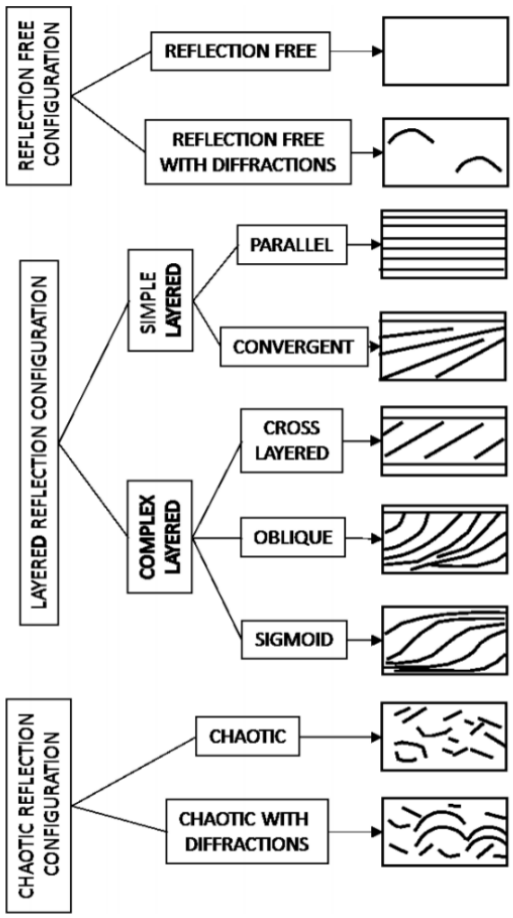

Figure 22. The basic types of reflection configuration in seismic facies analysis (Roksandic, 1978). Reflection free, layered and chaotic reflection forms/configurations can be utilized in analyzing sedimentary facies.

4. Data and methodology

This study is based on a 3D seismic reflection survey, which is complemented by two 2D seismic surveys surrounding the Egersund Basin. Together with key wells, lithostratigraphic and chronostratigraphic well tops, provided by NPD (NPD, 2019) and the University of Stavanger/TGS-Nopec, since this data is freely accessible. This data will be presented and further applied for seismic interpretation in software Petrel E&P 2018.

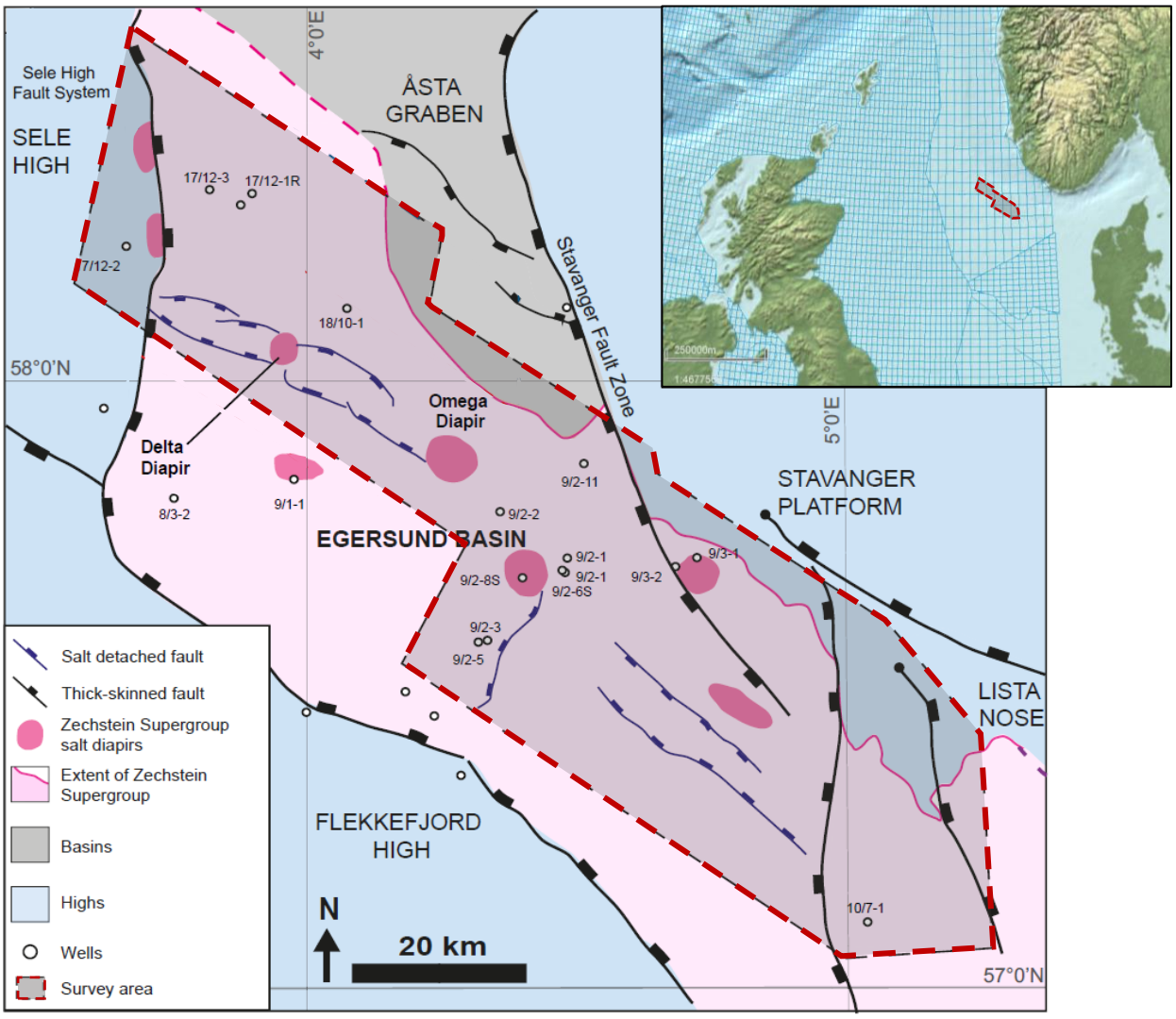

Figure 23. The area of the 3D seismic data in the Norwegian North Sea. a) The location of the 3D seismic data in the Norwegian North Sea. b) Structural map of the area of the 3D seismic data. Modified from Tvedt et al. (2016).

4.1 Data

4.1.1 3D seismic data

This study is primarily based on a pre-stack time migrated, three-dimensional reflection seismic survey (PGS MC3D-EGB2005). The 3D seismic survey was acquired by PGS NOPEC in 2005 and covers an area of approximately 3 550 km^2 in the north-eastern part of the Egersund Basin, Norwegian North Sea. Figure 23 displays the position and extent of the entire 3D seismic survey.

The data has a crossline and inline spacing of 25 m, a record length of 6656 ms and a vertical sample rate of 2 ms. The inlines are oriented NW-SE and crosslines are oriented NE-SW. The geodetic datum and projection of this survey are ED50 (European Datum 1950) and UTM zone 31N.

The seismic sections of this 3D seismic data are displayed with reverse polarity, where the trough is blue (seabed), and peak is red in this dataset (Figure 24). An increase in acoustic impedance is presented by a trough (blue), while a decrease in acoustic impedance is represented by a peak (red) (SEG European Convention).

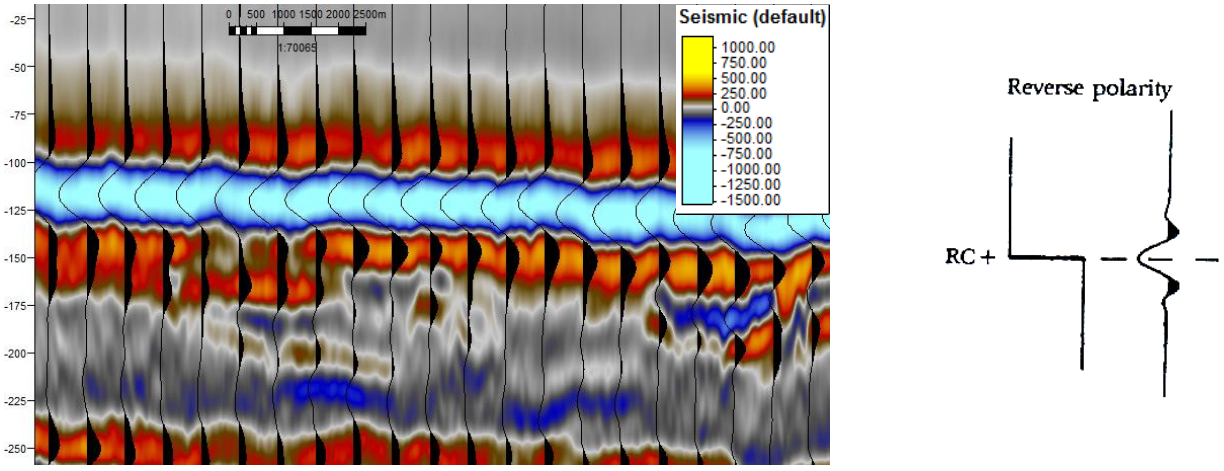

Figure 24. The 3D seismic survey (PGS MC3D-EGB2005) used in this study. The seafloor reflector shows zero-phase signal and reverse polarity, based on Sheriff (2006). The blue color represents negative amplitude and the red color correlates with positive amplitude.

The average velocity for the Oligocene strata is measured from synthetic seismograms from several wells, and ranges from 1900 m/s to 2050 m/s. The depths or interval used for the calculation ranges from ca. 400m to 900m (TWT). The curve below (Figure 25) displays the dominant frequency in

the interval of interest, formed by using spectral analysis. From this plot a frequency range of 25-40 Hz is observed. The vertical resolution calculated within the area and strata of interest (Oligocene interval) is approximately 12 to 20.5 m (Table 2.). This good resolution is most likely a result of high frequencies and relatively shallow sampled seismic data, which allows for detailed mapping of the interval.

Table 2. The calculation of vertical and lateral resolutions of the 2D and 3D seismic surveys in the study area. The velocity value is based on the synthetic seismogram in the Oligocene interval.

Parameters	**Values & Calculation**
Average Velocity	1900 – 2050 m/s
Dominant Frequency	25 – 40 Hz
Wavelength (λ)	= 1900-2050 m/s / 25-40 Hz = 47.5-82 m
Vertical Resolution	= 47.5-82 m / 4 = 11.9-20.5 m

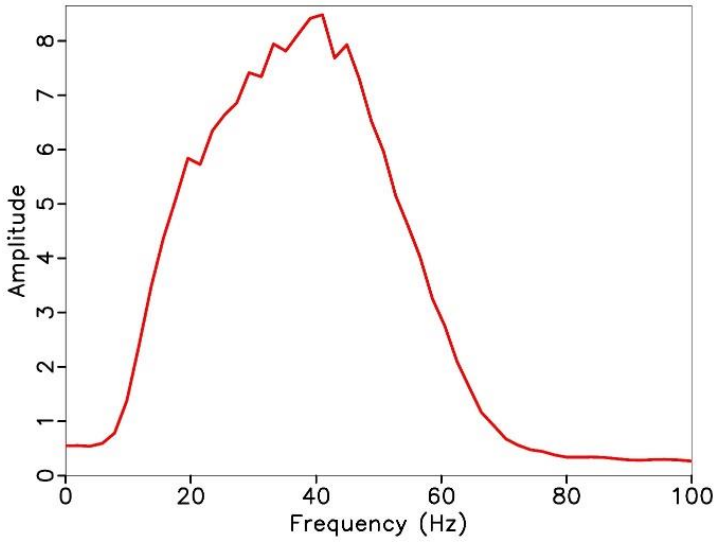

Figure 25. Spectral analysis of the Oligocene interval from the 2D and 3D seismic surveys depicting the dominant frequency between 25 and 40 Hz. The maximal peak frequency is used to identify the lateral and vertical resolution of the seismic survey of the Oligocene interval

4.1.2 2D seismic data

The 2D seismic data available for this study are the surveys NSR04 (NSR: North Sea Renaissance) and the MN9206 (Figure 26). The data survey NSR04 was acquired by TGS-NOPEC in 2004 on the Norwegian continental shelf. Additionally, the MN9206 survey was acquired by Mobil Exploration Norway INC in 1992.

The NSR04 seismic survey includes several 2D lines that again covers the study area, with some exceptions in the north-western part of the Egersund Basin, but the 3D seismic survey, MC3D EGB2005, fulfills this area. The 2D lines going NE-SW, provides more information in the basin, outside the 3D seismic data area, which ultimately gives a better understanding of the area and stratigraphic events. The 2D seismic lines also contributes to the identification of key surfaces, stratal terminations and this information contributes to the interpretation of systems tracts.

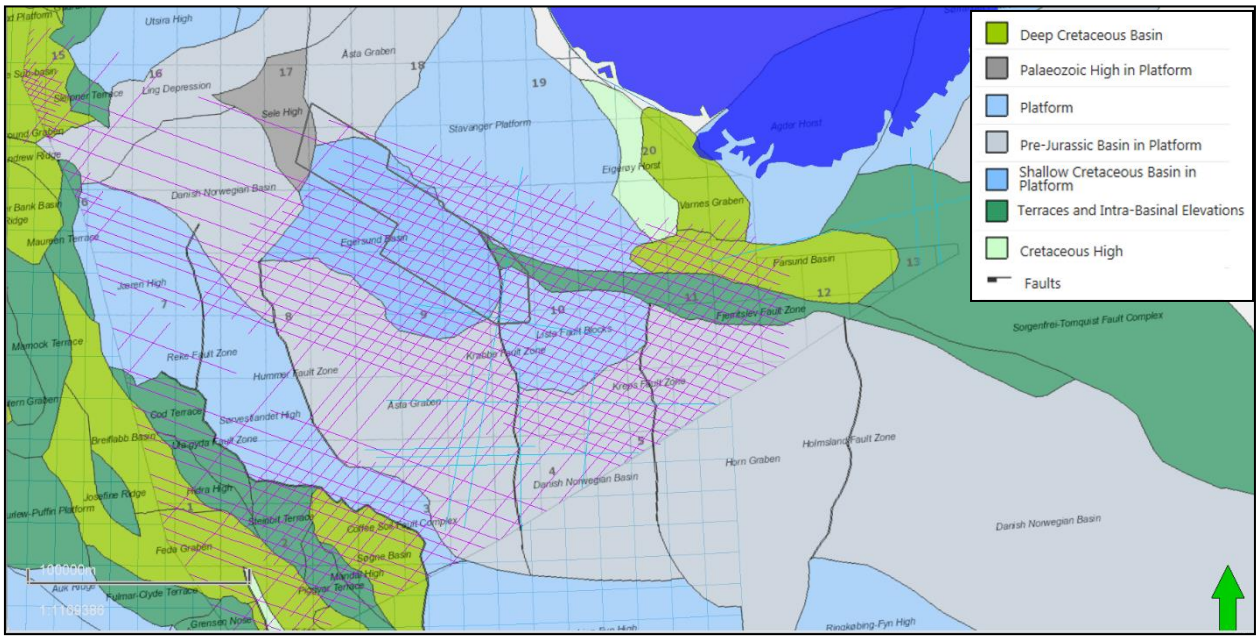

Figure 26. Map displaying the extent of the obtained 2D seismic data of the NSR04 seismic survey (purple) and MN9206 seismic survey (light blue) in the Norwegian North Sea.

Most of the given 2D seismic lines of the MN9206 seismic survey is located in the Åsta Graben. The only 2D seismic line of this survey, crossing through the 3D cube, was the MN9206-605, which were used to make a well-tie with the well 9/12-1 located in the area of Åsta Graben, south of the 3D data cube. Besides this application, the survey has not been further used.

The phase and polarity of the two 2D seismic surveys were determined by the interface between the seawater and seafloor. The NSR04 seismic survey has been acquired with a normal polarity and zero-phase signal, which is opposite of the 3D seismic data. The seafloor in this survey is displayed as a peak (red) and has an increase in acoustic impedance (Figure 27a). While the MN9206 has the same polarity and phase as the 3D data, reverse polarity and zero-phase signal. With the seafloor being a trough (blue) with an increase in acoustic impedance (Figure 27b) (SEG European Convention).

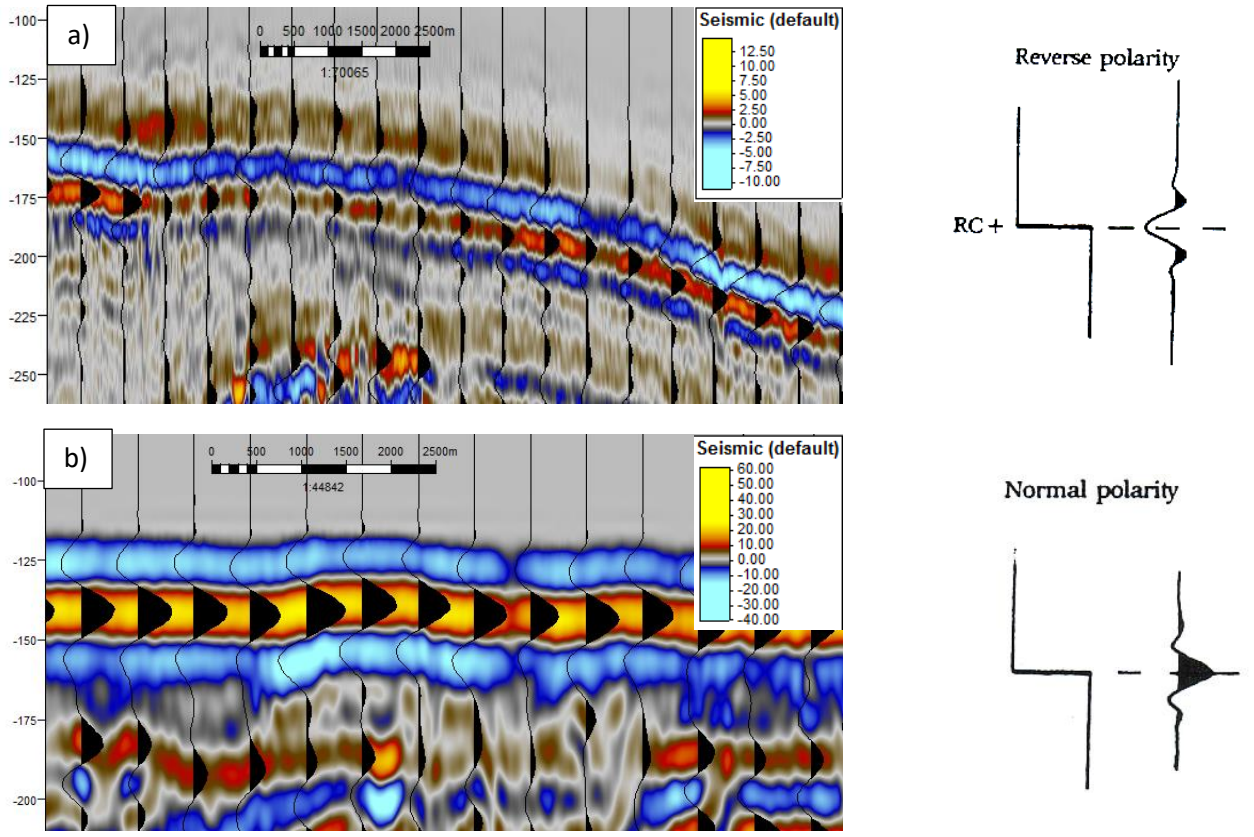

Figure 27. The MN9206 and NSR04 2D seismic surveys , used in this study. a) MN9206: The seafloor reflector shows zero-phase signal and reverse polarity, based on Sheriff (2006). The blue color represents negative amplitude and the red color correlates with positive amplitude. b) The seafloor reflectors (red color) in this survey display zero-phase signal, normal polarity model based on Sheriff (2006).

4.1.3 Well data

A total of 22 wells were used in this study. The wells are spread out in the area, but mostly inside the 3D seismic cube. In the area of the 3D seismic data, the well control is better in the middle and northern parts, than in the southern part (Figure 28). From these wells a few key wells were picked to represent the main trends and the variety of deposition throughout the study area. They were selected based on the diverse deposition and to cover most of the study area, with special focus within the 3D seismic area. Some of the key exploration wells covers some former hydrocarbon producing fields, such as the Yme field (Figure 28). The data included in the well logs differs, but all includes gamma ray, density and resistivity. Some of them also contains check-shot data that has been used in seismic-to-well tie and in stratigraphic well correlation (18/10-1 and 9/12-1).

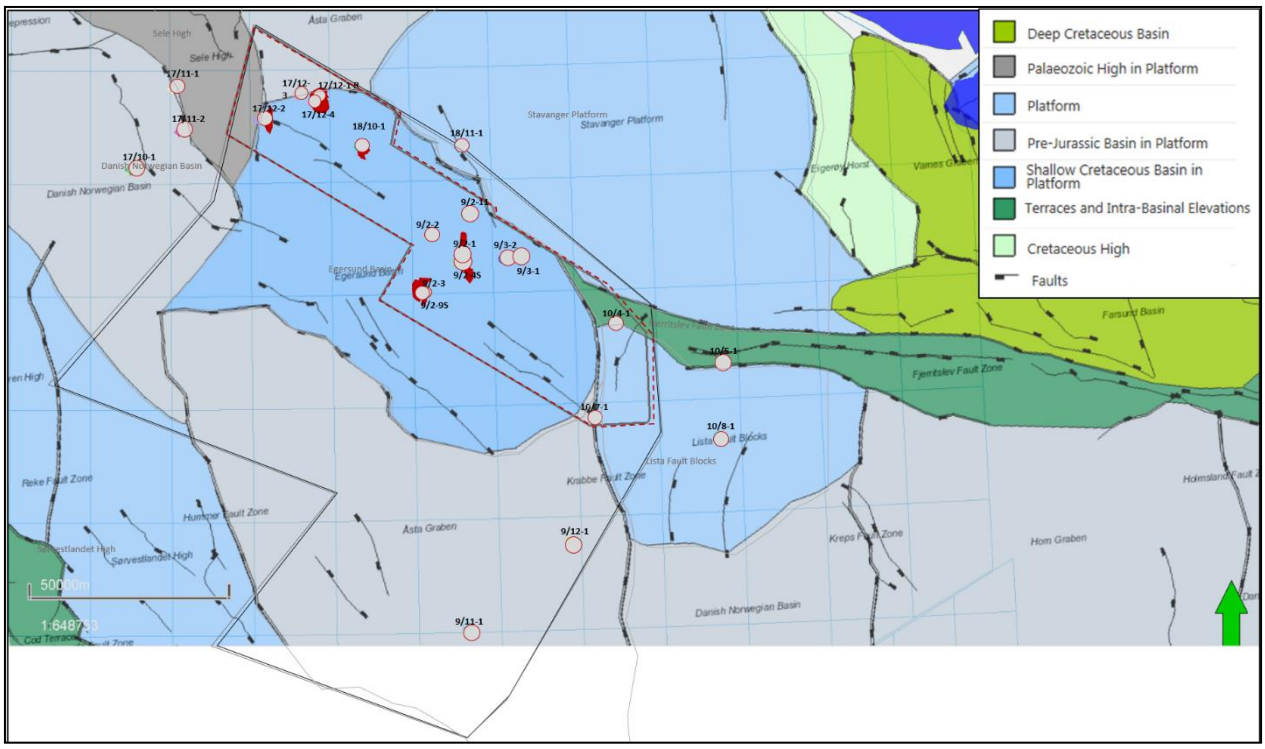

Figure 28. Map displaying the positions of the wells in this study, together with the area of the 3D seismic data (red lined box), the extent of the total study area (grey lined box) and the position of the oil and gas fields in the Egersund Basin (red).

The key wells are listed in Table 3, which includes information about the well's location, entered year, its purpose, the thickness of the whole Hordaland Group based on the information from NPD, and the approximate thickness of the Oligocene sediments, which were estimated based on the interpretations in the seismic and completion reports from NPD. From the table, it is easy to observe that the overall thickness of Hordaland Group gets thicker towards the deeper parts of the basin, in south-west direction. The well containing the thickest deposition of Hordaland Group is 9/11-1, with a thickness of 675 m according to NPD, the second thickest is well 9/12-1, which is located further in on the shelf in the Åsta Graben in the Norwegian-Danish Basin.

Only a few of these 22 wells comprised complete gamma ray, density, sonic and resistivity logs. Especially for the interval of the Oligocene epoch, there were many wells with no available data, making it difficult for good well control within these sediments. The uncertainty is also so greater when interpreting the different surfaces based on this limited data.

Table 3. Six key wells in the area of the Egersund Basin, one of them located in the Åsta Graben

Well bore name	Location	Year	Purpose	Thickness of Hordaland Gp (m)	Approx. thickness of Oligocene sediments (m)
9/12-1	Åsta Graben	1969	Wildcat	400→987= 587 m	350 m
10/7-1	Lista Fault Block/Åsta Graben	1992	Wildcat	451→652= 201 m	130 m
9/2-3	Southwestern part of the 3D seismic cube	1989	Wildcat	410→938 = 528 m	235 m
9/2-2	In the middle of the 3D cube	1987	Wildcat	406→747= 341m	210 m
18/10-1	Northern part of 3D cube	1980	Wildcat	369→709 = 340 m	150 m
17/12-2	Close to Sele High	1973	Wildcat	707→924 = 217 m	205 m

4.2 Methods

4.2.1 Tools

The software Petrel E&P 2018 was used in this study as the main software when interpreting well logs and seismic reflection data. The seismic surveys MC3D-EGB2005, NSR04 and MN9206, were loaded into the Petrel Software, together with the given wells. This was done to produce seismic-to-well tie, well correlations and seismic interpretations. By the use of this software, structural, thickness and attribute maps were created, which aided further interpretation and analyzing in the study area. Seismic facies analysis was also done to identify the depositional environment based on seismic characterization.

4.2.2 Seismic-to-well tie

The seismic-to-well-tie process is done to provide a time-depth relationship between the well data and the seismic data, as well as to identify relevant reflectors. The interval of interest, Oligocene, was defined by first determining the top and base of Hordaland Group, which it lies within. This was necessary to shorten the relevant extent in the well logs. Some information regarding lithostratigraphy and depths of the Oligocene interval were provided from the Norwegian Petroleum Directorate (NPD) and was used as a guide on interpreting this chronostratigraphic succession.

A total of five well-ties were executed, but when observing the relations of the wells and the seismic reflections, some of the different wells display e.g. Top Hordaland Group at a different reflection

than in other areas, so the surface does not correlate and cannot be interpreted at the same seismic reflector. All the well tops of the Hordaland Group are collected from NPD, but as observed it seems that Top Hordaland Group has been interpreted differently at the different location, some defining one reflection as this top and some as another reflection. It could also be due to previous interpretation from areas far away from the Egersund Basin, that resulted in "wrong" interpretation due to lack of data or well control. Because of the uncertainty regarding the differently interpreted well tops in the shallower intervals (Eocene, Oligocene, Miocene etc.), only two wells have initially been the foundation for the interpretation of the seismic data in this study, well 9/12-1 (southeast of the Egersund Basin) and 18/10-1 (inside the 3D seismic cube). The synthetic seismograms were produced by convolving the sonic and density logs, with a Ricker wavelet to generate the synthetic predicted traces. The power spectrum shows that the peak frequencies are approximately 30-40 Hz (Figure 29), which is similar to the highest seismic frequencies from the spectral analysis (Figure 25). The synthetic seismogram in Figure 29 displays the correlation between one of the key wells (18/10-1) and seismic data in the Oligocene interval.

The seismic-to-well tie analysis is done to ensure that the borehole seismic and the surface seismic at the borehole trajectory look as similar as possible, making a good connection between the well data in the depth domain and the seismic data in the time domain (Figure 29). This also assists in the identification of the key reflectors for interpretation.

4.2.3 Interpretation Strategy

To develop the stratigraphic framework in the study area, mainly two stratigraphic surfaces were recognized; the maximum flooding surface and sequence boundary (erosional unconformity). These key horizons can be identified from the seismic data (Figure 30) and partially in the stratigraphic well correlation (Figure 31).

In the seismic data, stratal terminations guided the definition of the key stratigraphic surfaces. These stratigraphic surfaces determined several units in the Oligocene strata and assisted in analyzing the tectono-stratigraphic sequences of this interval. The analysis was done by using mainly the time depth surface maps and thickness maps for each interval or unit bounded by the stratigraphic surfaces in the area of the 2D seismic data, but some information was also suggested from the attribute maps created in the area of the 3D seismic data. By seismic facies analysis,

internal seismic reflectors were linked to depositional environment. This analysis was based on parameters such as reflection amplitude and reflection continuities (Roksandic, 1978).

4.2.4 Seismic Attributes

The seismic attribute maps were used to explain geological features. The variance attribute measures discontinuity of seismic data from surrounding area by using a statistical method (Schlumberger, 2016). The amplitude map can be used as a facies map if the amplitude of the reflection is correlated to the geological features, explained by Emery and Myers (2009), put in other words attributes should aid in enhancing the seismic resolution. RMS amplitude, the root-mean square of the amplitude, can be used to differentiate intervals of different seismic amplitudes. The characteristics of seismic amplitude depends on the density and/or velocity contracts in the layer, which is mostly associated with depositional facies.

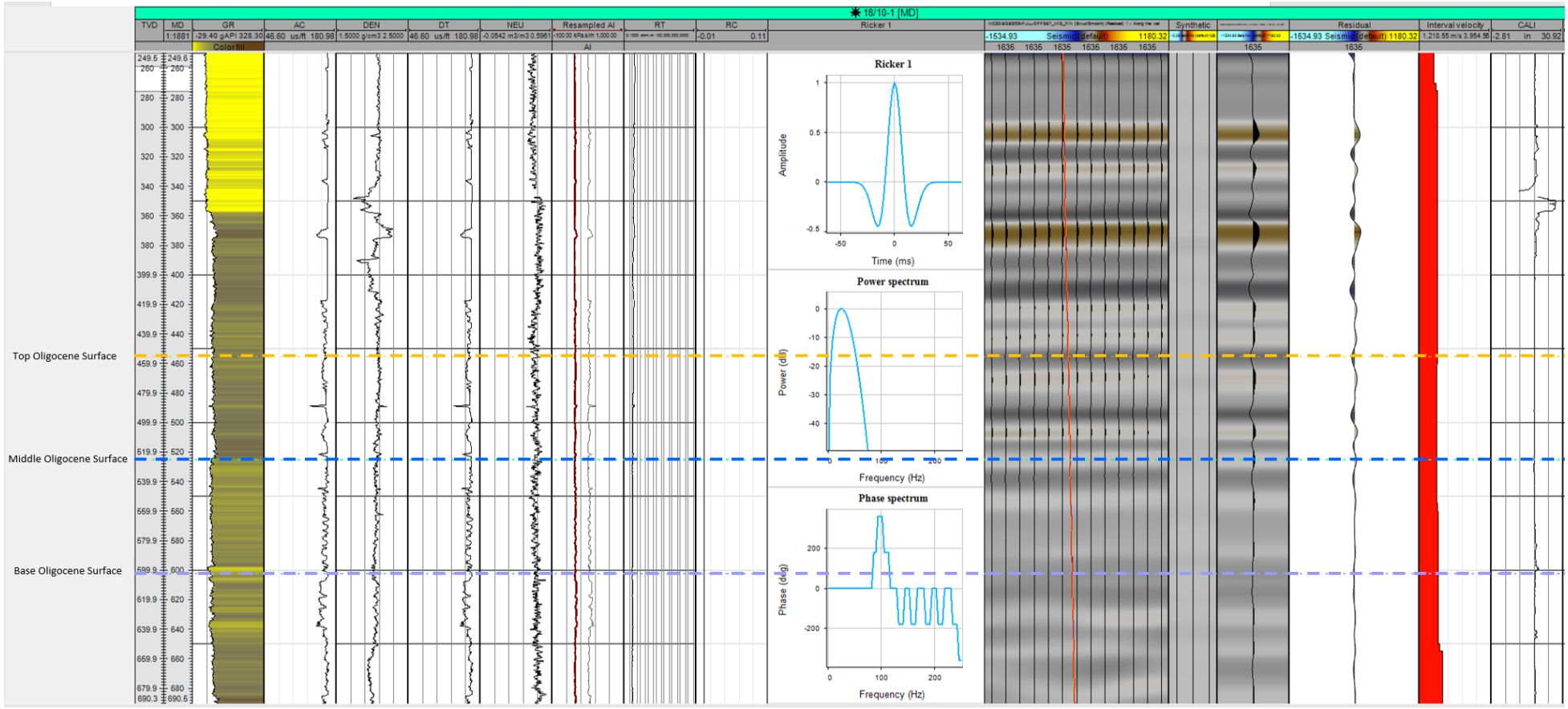

Figure 29. Seismic well-tie with well 18/10-1. The synthetic seismogram is depicted here, together with the seismic section, wavelet, power and phase spectrum. The peaks are characterized by the red color, whereas the troughs are identified with red color. The location of the well is shown in Figure 28.

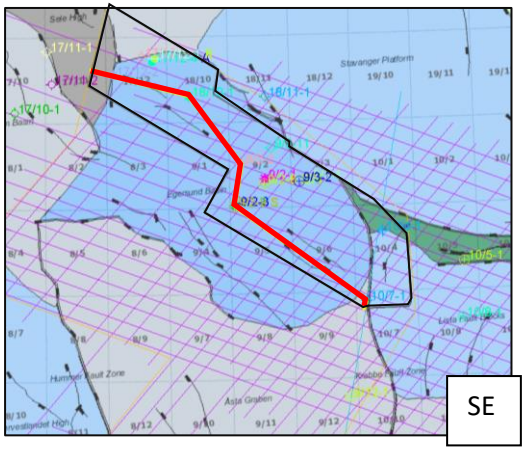

NW

SE

Well 17/12-2 Well 18/10-1 Well 9/2-2 Well 9/2-3 Well 10/7-1

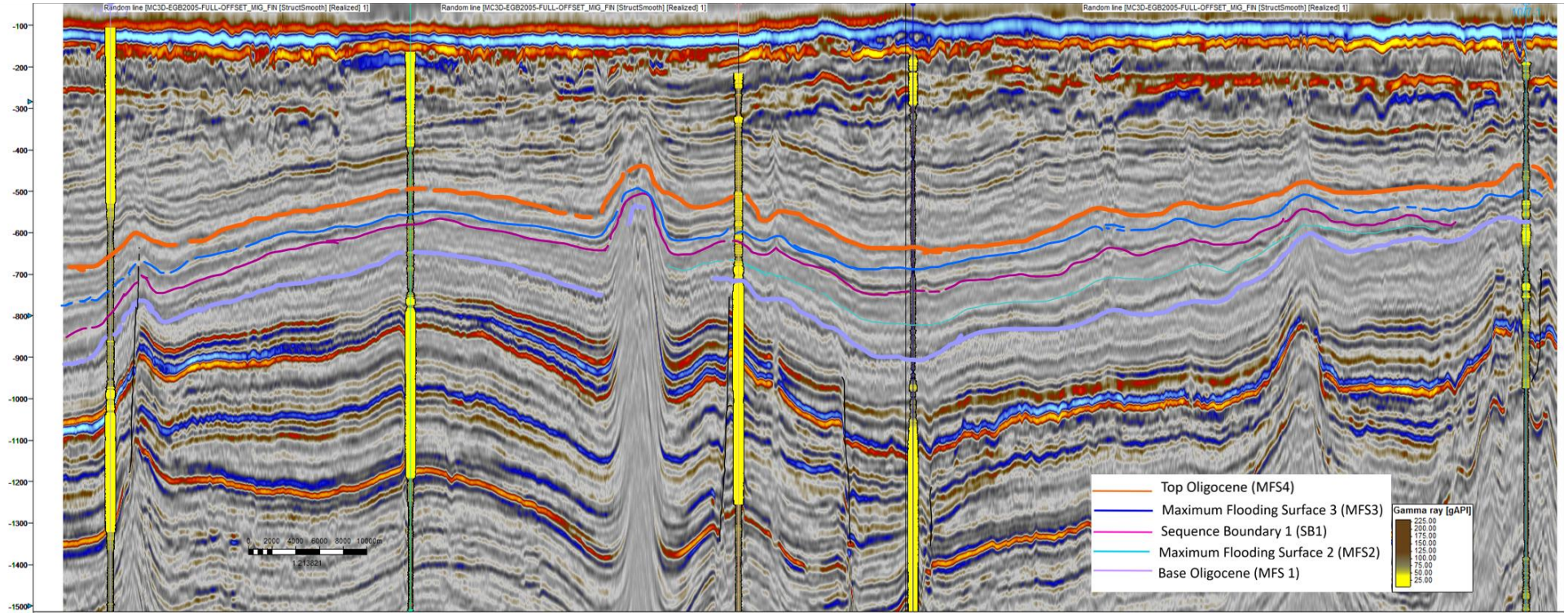

Figure 30. Seismic section displaying the five key wells (with GR trace) within the area of the 3D seismic data. The different interpreted surfaces of Oligocene age within this area, are also shown. The location of this seismic section is displayed in the map in the upper right corner.

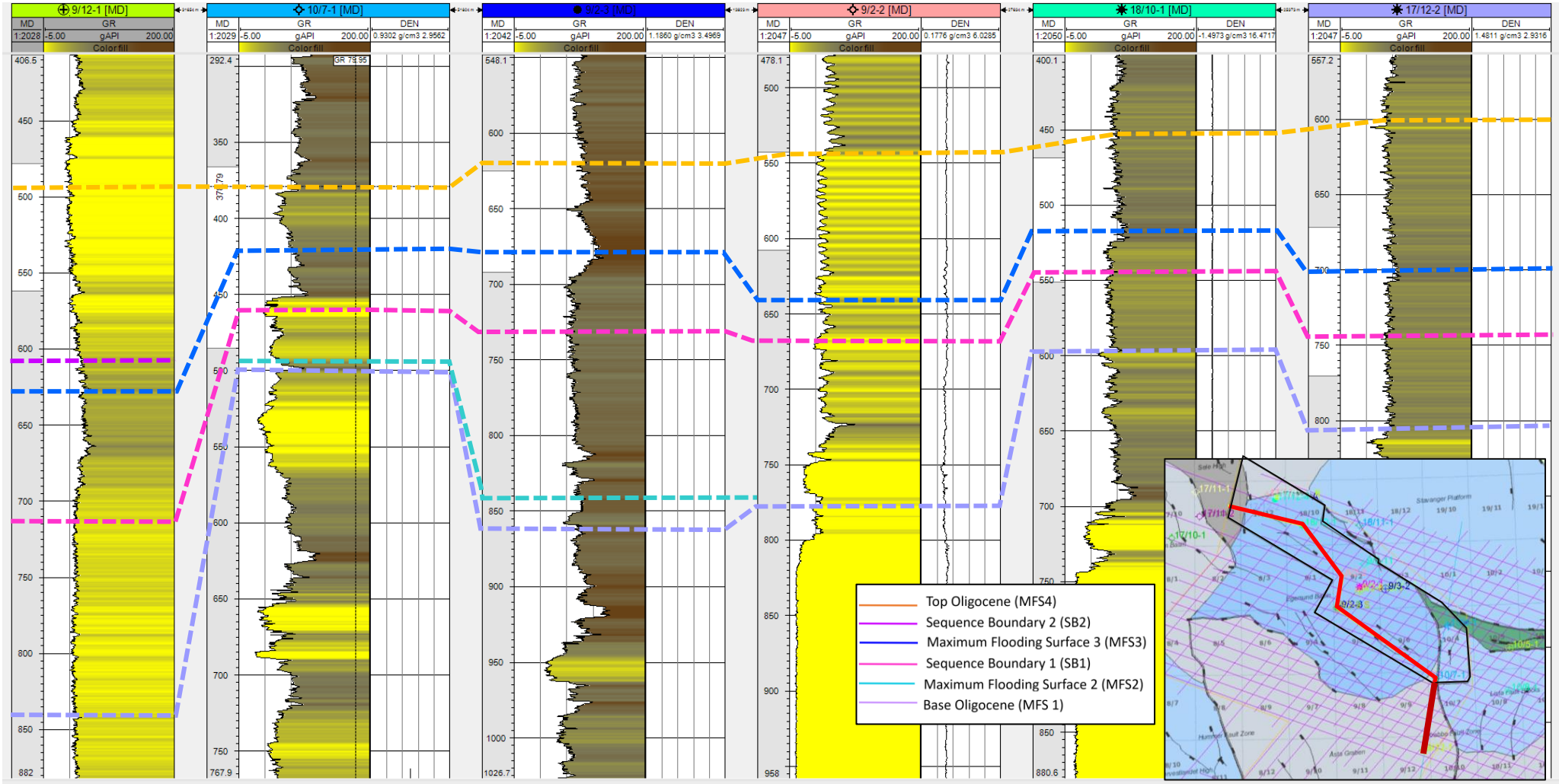

Figure 31. Stratigraphic well correlation between the six key wells in the study area and the interpreted surfaces. Notice the significant change in thickness from well 9/12-1, which is located in Åsta Graben to well 10/7-1 and well 18/10-1, which are located on structural highs (Lista Fault Block and the edge of the Stavanger Platform). The location of the chosen wells is seen in the map in the lower right corner.

5. Observations and Interpretations

5.1 Subdivision and Seismic Stratigraphy

The subdivision of seismo-stratigraphic units was identified based on continuity and amplitude of the bounding reflectors, the nature of the bounding surfaces, the geometries and lateral extension. Based on this, the Oligocene interval, in the Egersund Basin and further southwest into Åsta Graben/Danish Norwegian Basin (Figure 1 and 35), was divided into seven systems tracts. Each of the interpreted seismic systems tracts have been named a unit ranging from A to G. Bounding surfaces are named Maximum Flooding Surface (MFS) and Sequence Boundary (SB).

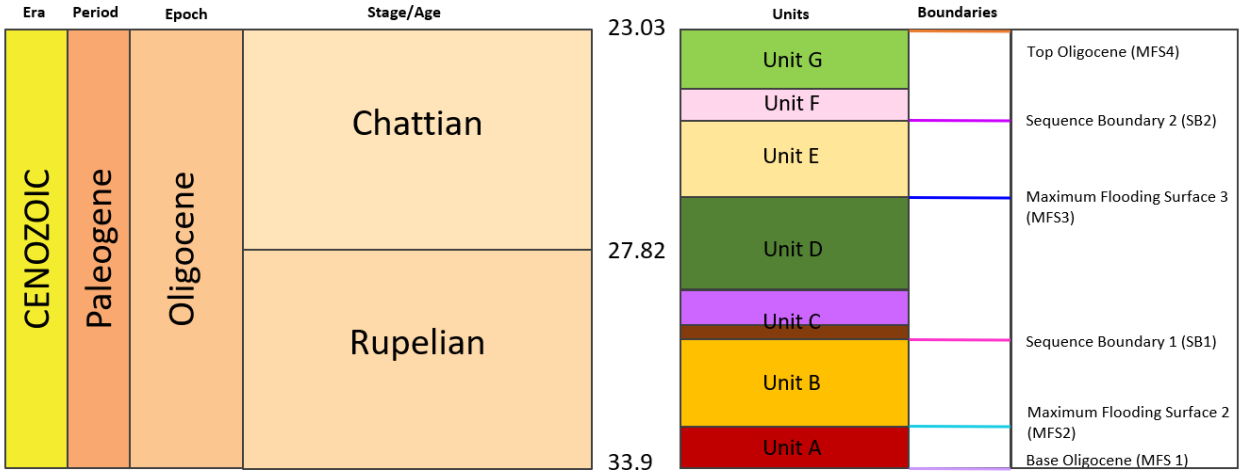

Figure 32. Conceptual chronogram of seismic stratigraphic units and the interpreted surfaces

The subdivision is based on the interpreted surfaces inside the 3D seismic cube and extrapolated out on the 2D seismic lines, where the well control is poor. The well logs inside the 3D cube is positioned high up on the shelf, so the interval of interest is significant thinner in the well logs here (Figure 31), than potential wells closer to the Central Graben. The 2D seismic lines assist the 3D seismic data, to get a better understanding of the sequence stratigraphy of the Oligocene interval in the Egersund Basin and its surroundings. The Egersund Basin was almost entirely filled with sediments before Oligocene times, causing limited accommodation space in the basin. This has led to strata of relatively limited thicknesses within the 3D cube area, whereas greater deposition is observed further downdip in the study area based on the 2D seismic lines. To locate important

downlapping reflectors, it was necessary to follow the reflectors further out into the Åsta Graben (Figure 1, 35 and 41). By doing this, it was easier to recognize the different systems tracts within the Oligocene interval. The 2D seismic sections in Figures 39-43 displays data in a northeast to southwest direction, with deposition from the Stavanger Platform towards Åsta Graben/Danish Norwegian Basin. All created surfaces display a deepening towards the southwest, which is the same direction of deposition in a basinward orientation.

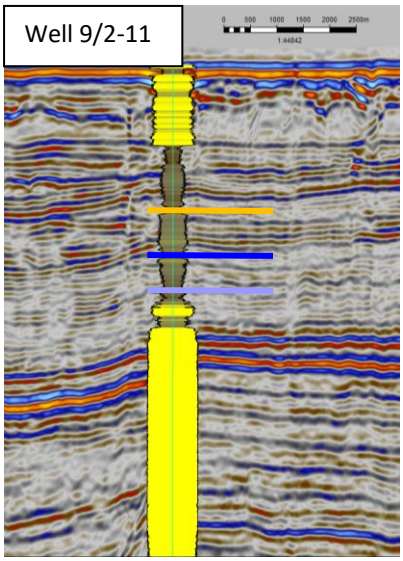

Figure 33. Well 9/2-11 with GR trace relative to the seismic data

The different surfaces were correlated with most of the well within the 3D seismic area. In well 9/2-11 (Figure 33), also seen in seismic line II, the top Oligocene surface is illustrated as orange, and based on the increase in the GR log, this surface is interpreted to be a maximum flooding surface. The blue mark represents an interpreted MFS during the transition from Rupelian to Chattian age, where an increase of GR indicative of deposition of finer sediments, is also observed for this surface. The bottom line is the base Oligocene surface, which is also based on this significant fining of sediments recorded in the log and also by features that will be further explained in the following sub-chapters. Some of the surfaces and units, later explained in greater detail, are not present in some of the well logs, because of the extent of the surface and unit that does not cover the area of the 3D seismic data.

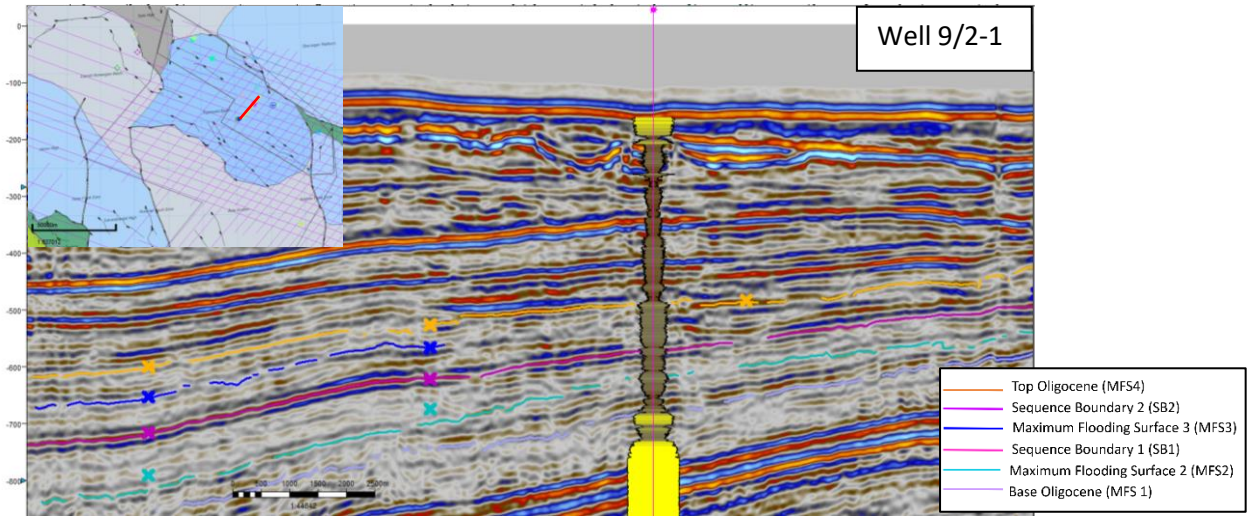

Figure 34. Seismic section including well 9/2-1 and its GR trace, together with the interpretations of the different surfaces located in this area. Location of section is displayed on the map in the upper left corner

5.1.1 Subdivision of Surfaces

A total of six surfaces have been created with the assistance of 3D seismic data in the Egersund Basin and 2D seismic data extending in SW direction into Åsta Graben/Danish Norwegian Basin. All the surfaces have an overall dip direction towards the southwest/west and in a basinward orientation. They are named A-F, where A is the oldest and F is the youngest. The shallowest part for all surfaces is in the North-Eastern corner of the study area. Salt diapirs can be observed imprinted on all the surfaces, as small rounded highs and dark to black circular features.

5.1.1.1 Observations

Surface A is a downlapping surface and the base of the Oligocene interval (Figure 35a). This surface is displayed with a variance map overlain in the area where the 3D seismic data is located. This surface is the deepest interpreted surface in this study, with a maximum depth at approximately 2000 ms (3810 m), which covers a fair amount of the southwesterly area. The highest elevated area is around -400 ms (760 m).

Surface B (Figure 35b) is only interpreted to exist in a more limited area than the outlined study area. The depth reaches around 1100 ms (2100m) and the highest point is located at ~500 ms (950 m). There are only a few wells penetrating this surface. This surface separates Unit A from Unit B.

Surface C (Figure 35c) covers again the study area and is also displayed with a variance map. The surface is interpreted to be of Middle Oligocene age, around 27 Ma. Depth ranges from ~2000 ms (3810 m) to ~450 ms (860m) is observed on the elevation time map. The thickness between this surface and the next surface D, is relatively small within the 3D seismic cube, where most of the wells are located. Surfaces C and D are more easily differentiated at greater depth, where the thickness between them is thicker. This surface separates Unit B, from Unit C and Unit D.

Surface D (Figure 35d) also extends over the entire outlined study area and displays backstepping features. There is not much difference in dip direction separating this surface and the underlying surface C. Surface D was developed after surface C and is reasonable to be at shallower depths than surface C. Surface D separates Unit C and D from Unit E, Unit F and partially Unit G in North-East.

Surface E (Figure 35e) covers only the outer part of the study area, with an exception in the south-western corner. This surface is limited by onlaps on the underlying surface D in NE direction, and downlaps in the opposite direction (Figures 39-43). There are only two wells located in the

southeastern part, making the well control poor for this surface. The observed maximum depth of this surface is from ~1500 ms (2860 m) to somewhere between -600 ms (1140 m) and -500 ms (950 m). Surface E separates Unit E from Unit F and G.

The last interpreted surface F is the top of the Oligocene interval (Figure 35f), which again covers the entire study area. The variance map also displayed on this surface. The deepest part of this surface is ~1900 ms (3620 m), and the shallowest part is around ~300 ms (570 m) to ~350 ms (670 m).

5.1.1.2 Interpretation

The different surfaces were interpreted based on the characteristics of the surrounding seismic reflections, based on the observations from mainly the 2D seismic data and some of the wells closer to the platform. The interpretation is described in greater detail below, when the interpretations of the different units are explained.

Surface A interpretation is based on well data together with the characteristics downlapping reflectors onto this surface in the seismic data (Figures 39-43). The well logs (Figure 33 and 34) show a characteristic and significant fining upwards followed by a coarsening upwards cycle. This infers that the deposition during this time were consisting of fine-grained materials which could have been caused by relative sea level rise. The base of Oligocene is interpreted as a Maximum Flooding Surface, in this study it is referred to as MFS1 or the Base Oligocene surface.

Surface B is interpreted based on the identified downlapping reflectors further landward and up onto the shelf (Figures 40-43). The extent of this surface is limited but based on the geometry and surrounding seismic configurations (Figures 40a-43a), this surface are interpreted as a short time interval of backstepping and transgression. Therefore, this surface is named MFS2 in this study and it is described in greater detail in the interpretation of Unit A.

Surface C is interpreted as a sequence boundary, named SB1. This interpretation is based on the onlapping reflectors close to slope of the shelf (Figures 39-43) and the regional extent of the reflectors.

Surface D is interpreted as a maximum flooding surface, called MFS3. This interpretation is based on the characteristics in the well logs (Figure 33) and the interpretation of a significant transgression during the middle Oligocene in the Egersund Basin published in previous studies in

this area (Jarsve et al., 2014 and Eidvin et al., 2014). This is also supported by the downlapping reflectors on top of this surface observed in the seismic (Figures 39-43), together with the its regional extent.

Surface E has a more limited extent than the underlying MFS3 but does still cover a considerable area (Figure 35e). Onlapping terminations onto this surface further out in the basin is also observed (Figures 39-43). This surface is interpreted as a sequence boundary, referred to as SB2 in this study.

Surface F, representing the top of the Oligocene interval, has been interpreted to be another maximum flooding surface (MFS4). This interpretation is mainly based on the used well logs (Figure 33 and 34) and their significant increase in gamma-ray values, which indicate fine-grained deposits. In addition, downlapping features has been observed on top of this surface.

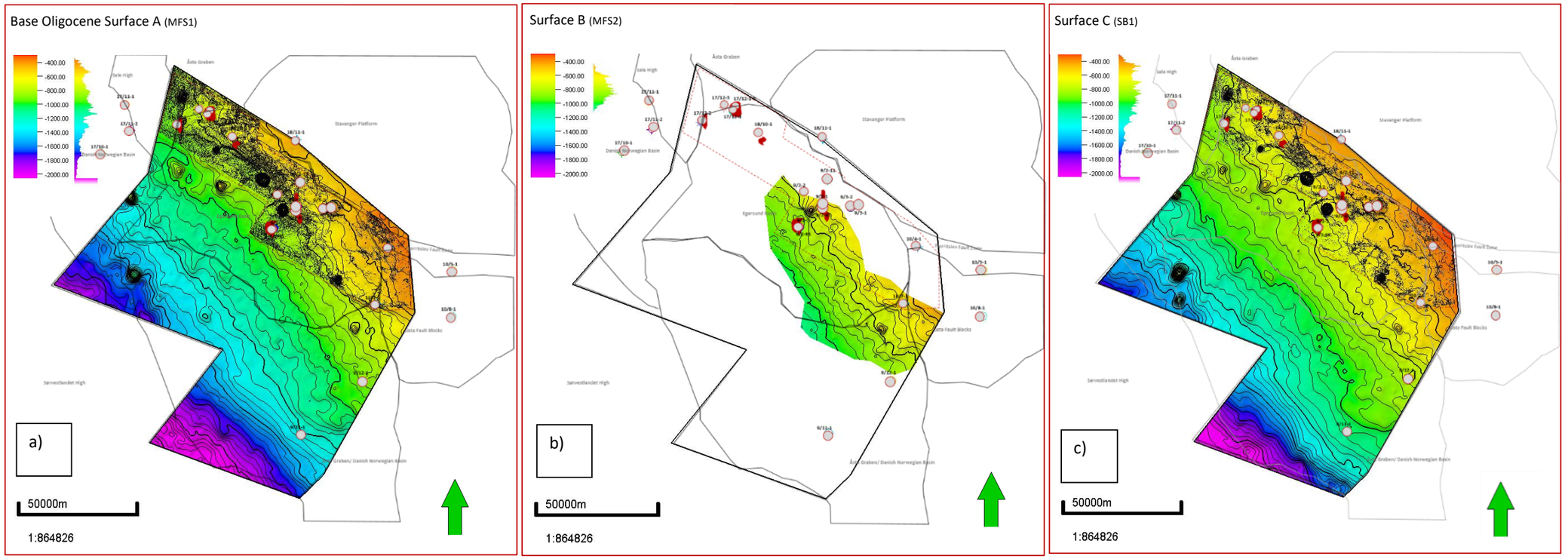

Figure 35. Surface maps. a) Surface A. b) Surface B. c) Surface C. d) Surface D. e) Surface E and f) Surface F. All of the surface maps display the boundaries nearby areas and structures, together with the location of the wells in this study, the location of the oil and gas fields in the Egersund Basin (red areas), the location of the area of the 3D seismic data (red stippled area) and the study area, for which most of the interpreted surfaces extends over. Surface A, C and F includes a variance map in the area of the 3D seismic data, which are based on the interpretations of the top, middle and base Oligocene surfaces.

5.1.1.3 Subdivision of surfaces within the 3D cube

The focus was mainly on interpreting the base, the middle and the top surface of the Oligocene interval within the 3D seismic area. The deposition of Oligocene age within this specific area is relatively thin, which is assumed to be due to the location on the shelf. This makes it difficult to identify other surfaces than these three surfaces.

As illustrated in Figure 37, for each of these three surfaces, there was created a time structural map superimposed by variance map and a RMS amplitude map. The structural maps show the topographic elevation throughout the extent of the surface. Using the 3D seismic data, the surfaces are more accurate and detailed than the surfaces created using the 2D seismic lines. The variance map is useful to reveal discontinuities in the seismic data. This helps with outlining the extent of the salt and its positions, detecting faults and possible geomorphology, e.g., channels. All of these features were observed in the variance maps from the 3D seismic data (37b). But after more investigation, the channel features appearing on the surfaces, was not found in the same interval in the seismic. Channels are rather observed in younger strata, closer to the seabed today (Figure 36), which is also confirmed by time slices in the top layers of the 3D seismic cube. Some of these rivers were mapped out at the time slice with a time depth of 244 ms. In Figure 36, the variance map of the Top Oligocene surface is presented with and without the shallow mapped channels.

The overlying shallow channels anomalies makes it difficult to interpret geomorphologies from the variance maps. However, a few faults and the characteristic black rounded circles indicative of salt

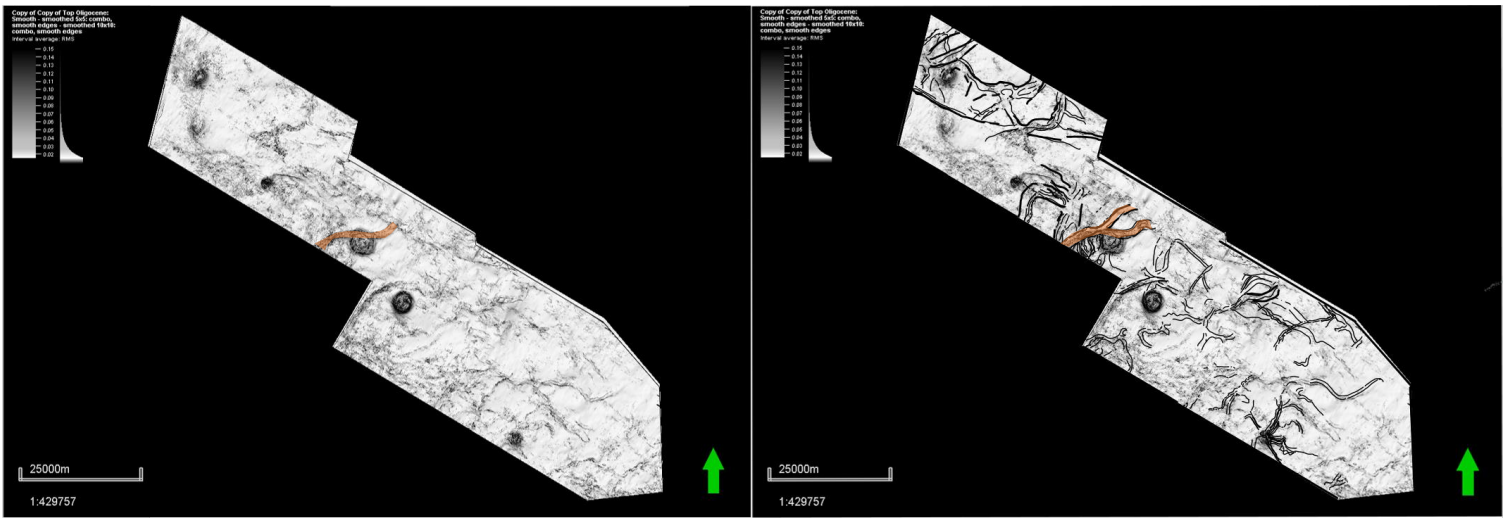

Figure 36. The map to the left comprises many of the same features as the map to the right, indicating that these features are anomalies of shallow channels above the Oligocene interval, and is therefore seen as anomalies or disturbances on the left map. The orange color highlights one of the many channels.

diapirs or salt stocks are recognized, which are easily observed (Figure 37b). The various variance maps of different ages do have some variations, like the Base Oligocene surface display more disturbance in the southwestern half of the study area (Figure 37b.3). This disturbance is not as clearly observed in the Middle Oligocene variance map, apart from a smaller area northwest of the largest salt diapir (Figure 37b.2). The Top Oligocene variance map highlights the channel anomalies in greater detail than the other maps below.

The RMS amplitude maps is overlain by the variance and illustrated in Figure 37c. The RMS amplitude detects amplitude variations for example created by channels with density changes with their surroundings. The red colors have lower amplitudes than the yellow colors. The Base Oligocene RMS amplitude map shows a bright amplitude anomaly in the southeastern part of the 3D seismic area (Figure 37c.3). This curved anomaly feature appears smaller and positioned further to the northeast for the Middle Oligocene RMS amplitude surface (Figure 37c.2). Here, more anomalies are also observed along the southwestern part of the 3D seismic cube. The Top Oligocene RMS amplitude map shows only a small area of high amplitudes in the northeast corner of the 3D seismic area, while the rest of the seismic cube consist of lower amplitudes (Figure 37c.1).

The areas of high amplitude might indicate sandy deposits, while the lower amplitude areas are most likely shaly deposits. The curved geomorphological feature on the base and middle Oligocene surfaces may suggest a retrograding lobe or delta (Figure 37c.2 and 37c.3). The other identified area of high amplitude is difficult to interpret in terms of geomorphology. However, some of the features might indicate deposition from growing salt diapirs, creating possible mass wasting further out in the basin, outside the control of 3D seismic data (Figure 37c.2). This downhill movement from the salt diapirs, can be caused due to gravity. On the Top Oligocene RMS amplitude map, it is observed a potential channel along the edges of the bright amplitude area (Figure 37c.1), which is most likely caused by progradation from the Stavanger Platform and Lista Fault Blocks.

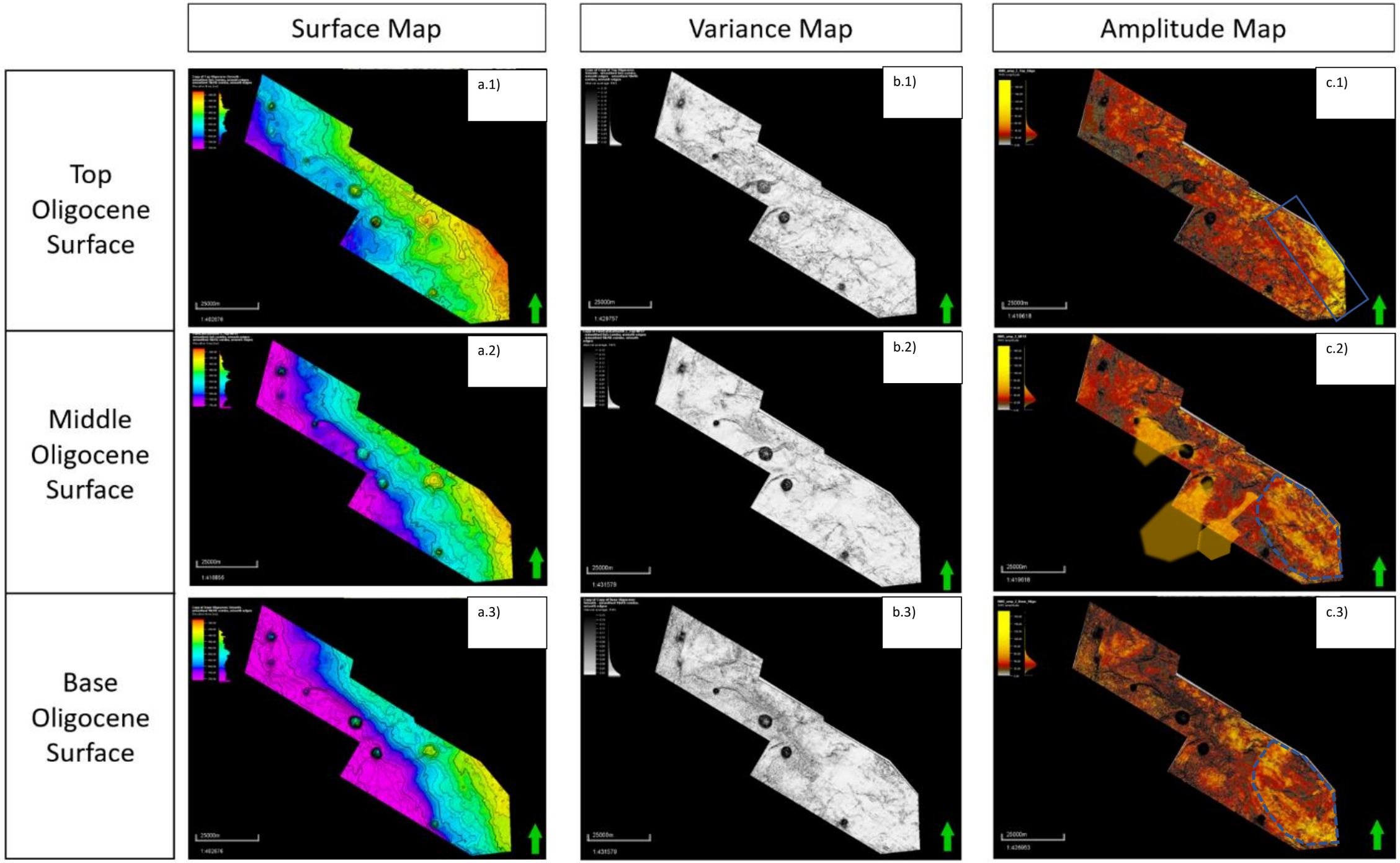

Figure 37. Different maps of the top (1), middle (2) and base (3) Oligocene. The column to the left (a) displays the surface maps, the middle(b) column displays the variance maps and the right (c) column show RMS amplitude maps, which are overlain by the variance of the different surfaces. The RMS amplitude map for the Middle Oligocene Surface display an illustration of the interpreted mass wasting in the area and how it could be deposited outside the area of the 3D seismic. The blue stippled outlines in the RMS amplitude maps for base and middle Oligocene, display the curved features, that could be interpreted as lobes or deltas. On the RMS amplitude map for the top Oligocene surface, a channel feature of high amplitude is outlined.

5.1.2 Subdivision of Units

Five 2D seismic lines were chosen to observe and interpret the vertical and lateral extent and changes of the different units. These lines were picked to present most of the study area, e.g., Egersund Basin and Åsta Graben. They were all interpreted from the base of Oligocene to the top of the Oligocene interval. The chosen 2D seismic lines run in southwest-northeast direction, and their extent are indicated in Figure 38. All these cross-sections are presented in Figures 39 to 43, without any interpretation and with the interpreted surfaces and units.

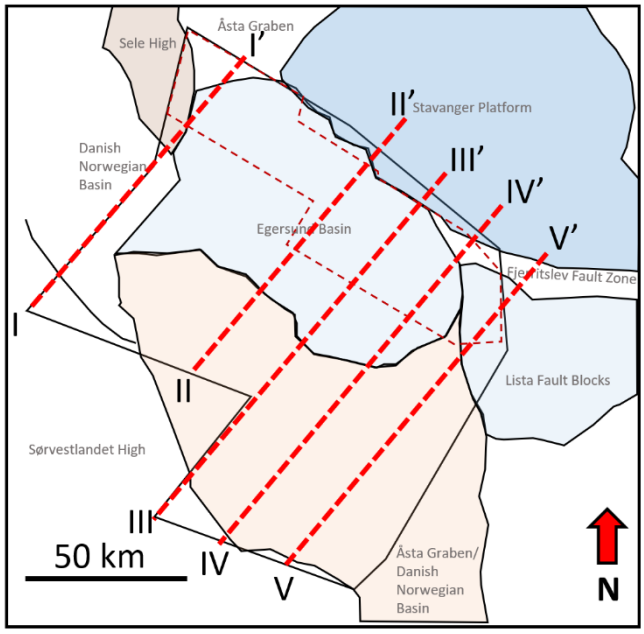

Figure 38. Location of the chosen 2D seismic lines within the study area and the location of the area of the 3D seismic survey. As observed in this figure, the chosen seismic lines extend from the Stavanger Platform in the northeast to the edge of the Åsta Graben in the Norwegian-Danish Basin.

Figure 39 display the cross-section I–I', which extends from the boundary between the Egersund Basin and Åsta Graben in the NE to the area of Sørvestlandet High in the SW. Cross-section II–II', shown in Figure 40, extends from the Stavanger Platform in NE to most western area of the Åsta Graben/Danish Norwegian Basin in SW direction. The last three cross-sections (III–III', IV–IV' and V–V') ranges from the edge of the Stavanger Platform in NE to the edge of Åsta Graben/Danish Norwegian Basin in SW (Figures 41, 42 and 43). But the last seismic line V – V' (Figure 43), does not cross the Egersund Basin, but the Lista Fault Block to the east, where it crosses the eastern part of the 3D seismic data cube.

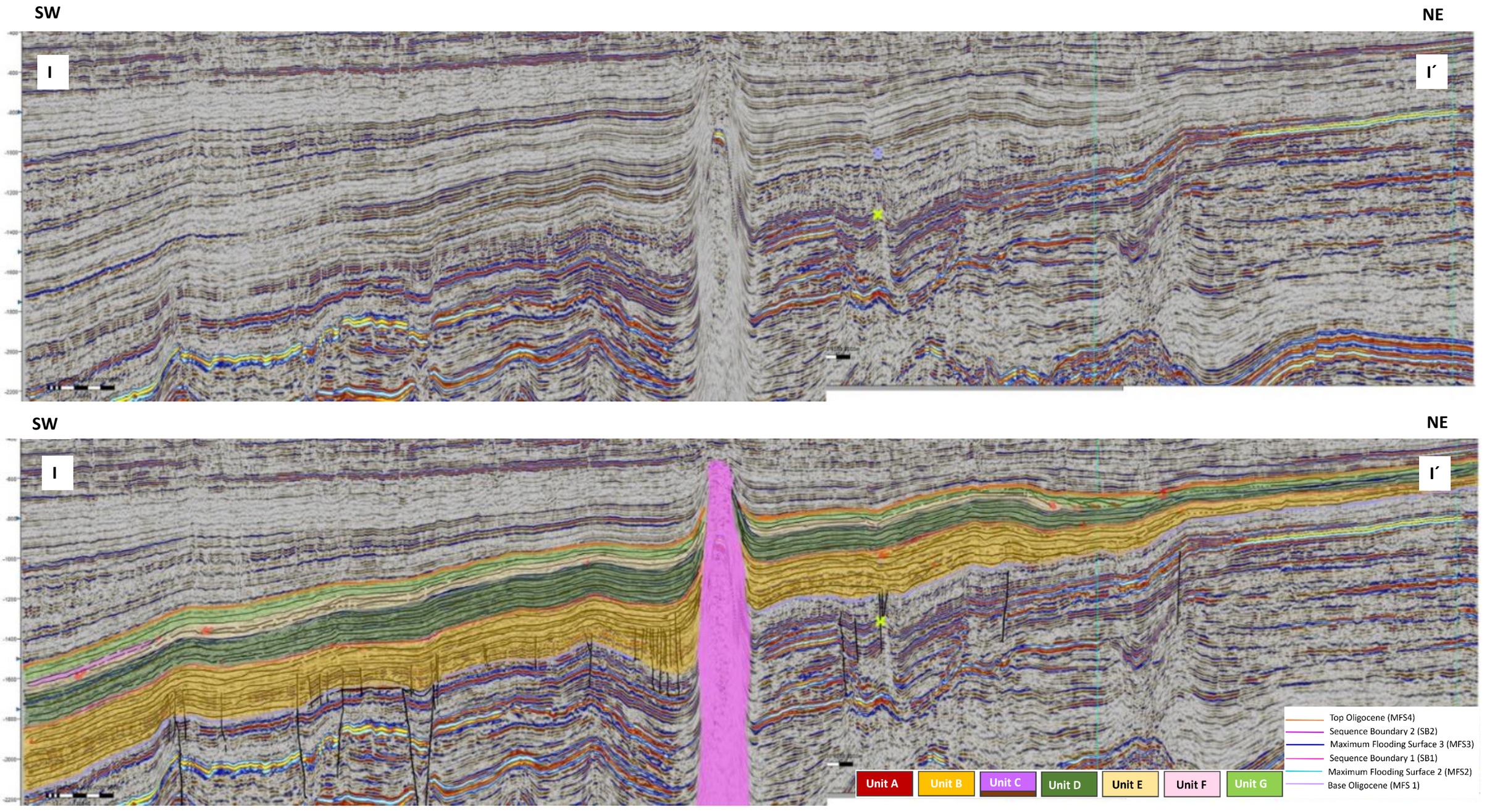

Figure 39. 2D seismic line I-I'. a) Display the 2D seismic line without interpretation. b) Display the 2D seismic line with interpretation. The location in shown in Figure 38, with the neon green vertical lines in NE, displaying the area of the 3D seismic within this 2D seismic line. The colored intervals are the interpreted units, and the colored lines between them are the different surfaces.

SW NE

II II´

SW NE

II II´

Unit A Unit B Unit C Unit D Unit E Unit F Unit G

Top Oligocene (MFS4)
Sequence Boundary 2 (SB2)
Maximum Flooding Surface 3 (MFS3)
Sequence Boundary 1 (SB1)
Maximum Flooding Surface 2 (MFS2)
Base Oligocene (MFS 1)

Figure 40. 2D seismic line II-II'. a) Display the 2D seismic line without interpretation. b) Display the 2D seismic line with interpretation. The location in shown in Figure 38, with the neon green vertical lines in NE, displaying the area of the 3D seismic within this 2D seismic line. The colored intervals are the interpreted units, and the colored lines between them are the different surfaces. The yellow vertical line illustrates the position of Well 9/2-11 (See Figure 33 for closer figure).

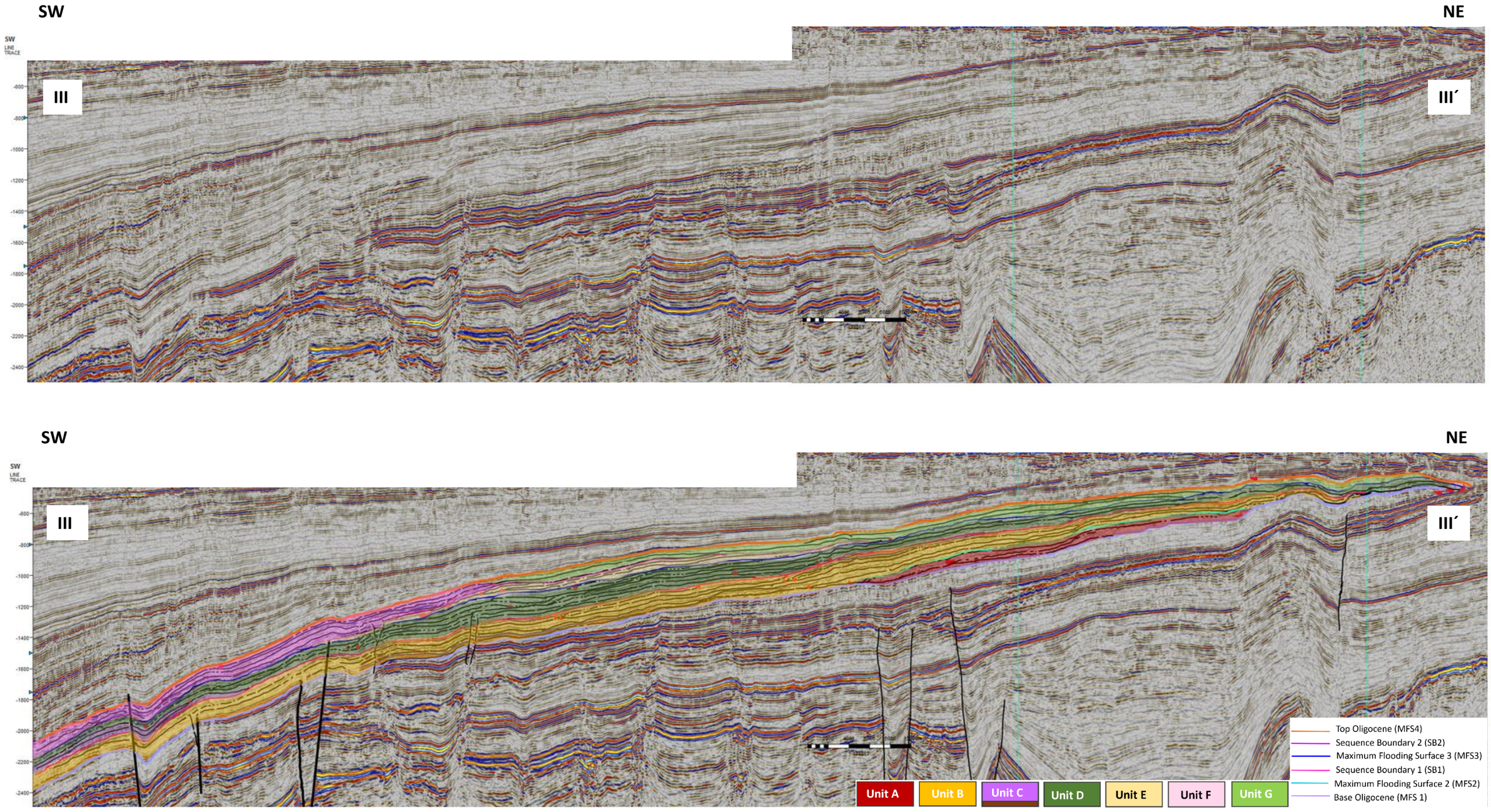

Figure 41. 2D seismic line III-III'. a) Display the 2D seismic line without interpretation. b) Display the 2D seismic line with interpretation. The location in shown in Figure 38, with the neon green vertical lines in NE, displaying the area of the 3D seismic within this 2D seismic line. The colored intervals are the interpreted units, and the colored lines between them are the different surfaces.

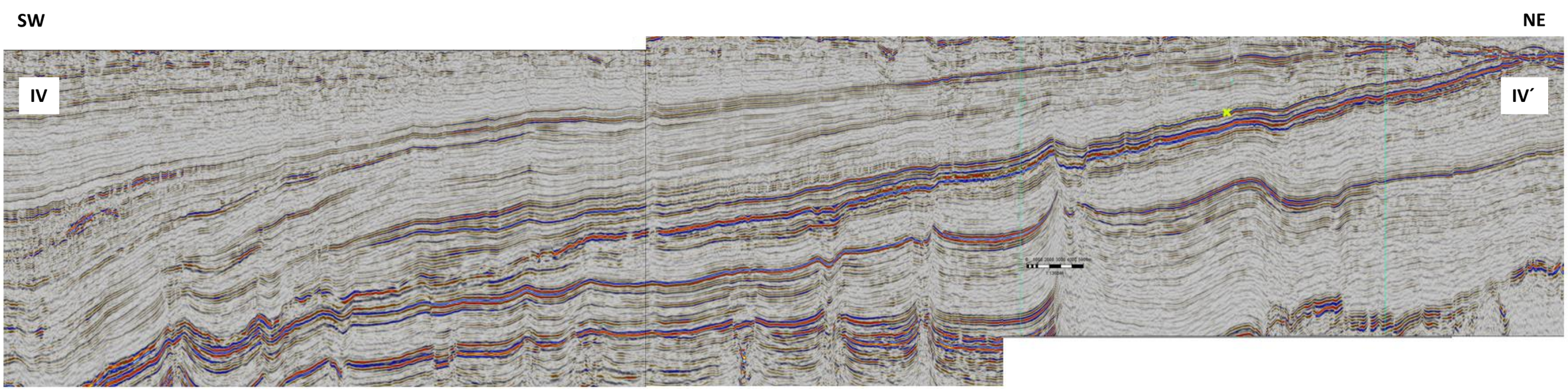

Figure 42. 2D seismic line IV-IV'. a) Display the 2D seismic line without interpretation. b) Display the 2D seismic line with interpretation. The location in shown in Figure 38, with the neon green vertical lines in NE, displaying the area of the 3D seismic within this 2D seismic line. The colored intervals are the interpreted units, and the colored lines between them are the different surfaces.

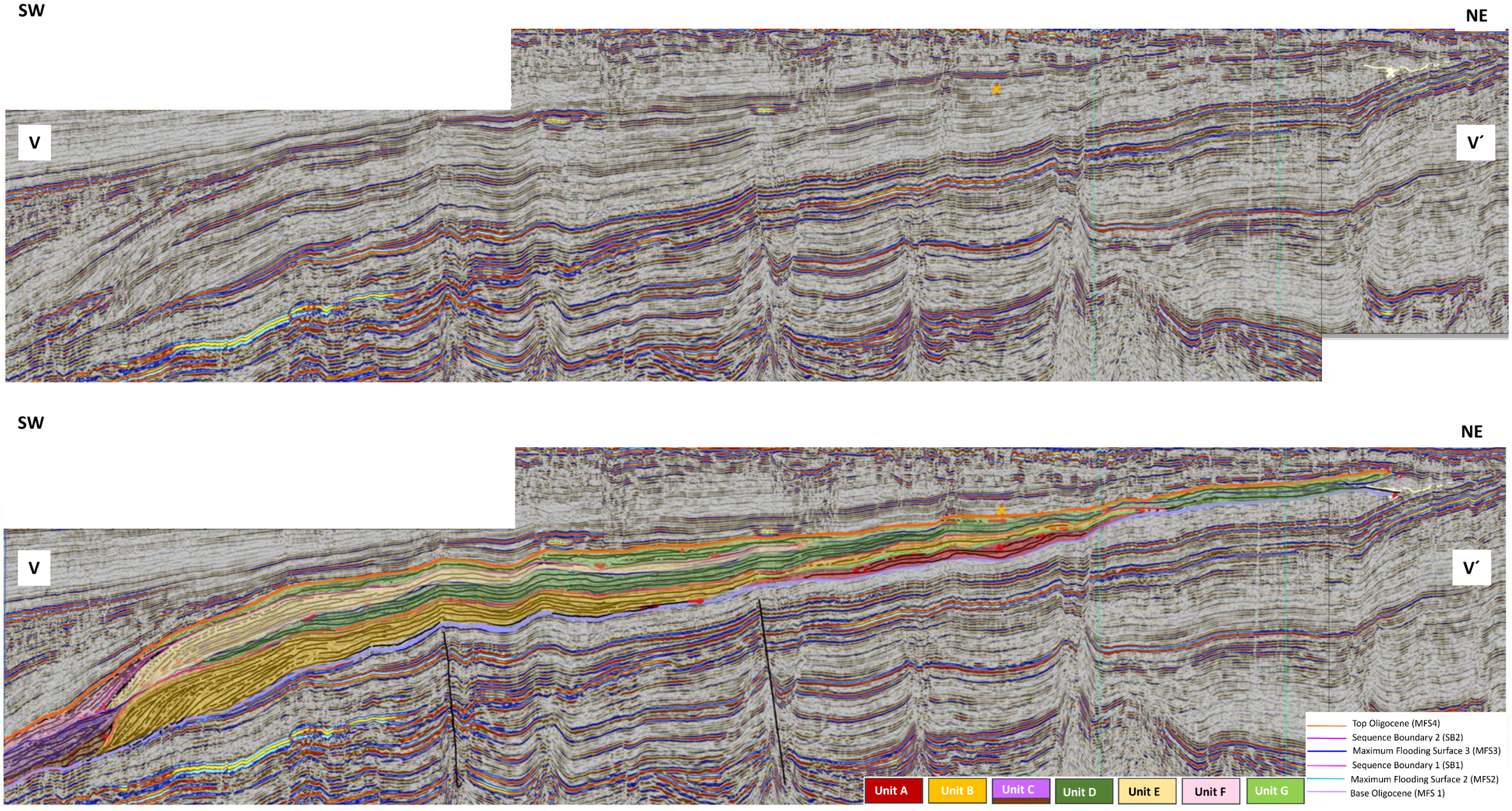

Figure 43. 2D seismic line V-V'. a) Display the 2D seismic line without interpretation. b) Display the 2D seismic line with interpretation. The location in shown in Figure 38, with the neon green vertical lines in NE, displaying the area of the 3D seismic within this 2D seismic line. The colored intervals are the interpreted units, and the colored lines between them are the different surfaces.

5.1.2.1Unit A

Seismic Unit A consists of strata of Early Oligocene age. It is bounded by the underlying Base Oligocene surface (MFS1), and by a maximum flooding surface at the top of this sequence (MFS2) (Figures 40-43). This unit is located relatively high up on the shelf and is one of the units with more limited extent.

5.1.2.1.1 Observations

This unit can be recognized by terminating downlapping reflectors onto the underlying Base Oligocene surface (MFS1) in southwestern direction on the 2D seismic line II, III, IV and V (Figure 40-43). This unit also contain observation of onlaps onto the same surface higher up on the shelf, relatively close to the Stavanger Platform in the northeast. The reflectors within Unit A are semi-continuous and sub-parallel, with relatively low amplitudes (Figure 40-43). This unit is gradually thinning laterally in northwestern direction, which is basinwards (Figure 44).

The thickness map (Figure 44) of Unit A displays the thickness variations of the interpreted unit including the area with the downlapping features. It is possible to observe a thicker zone in the middle of this unit, representing the main depocenter, with thinning in both NE and S-SW direction.

5.1.2.1.2 Interpretations

This unit can be interpreted as thin interval of prograding deposition occurring in the beginning of the Oligocene epoch. An indication of erosion close to the Stavanger platform can be seen (Figure 44) and is consistent with no observed deposition of this unit this far up on the shelf. The area of deposition is located in the upper part of the shelf, indicating that there has been a major transgression before this time, and that the system has started to build out towards the basin in southwest direction. It is difficult to observe any backstepping features within Unit A, but the reflectors on top of this unit onlaps further up onto the shelf and downlaps further out towards the basin (Figures 40-43). These observations suggest that a transgression has occurred before the deposition of the next unit, which also could explain the potential erosion. It is also a challenge to determine if the upper bounding surface of this unit is a sequence boundary or a maximum flooding surface. This surface is called MFS2, based on the suggested transgression, as mentioned earlier in sub-chapter 5.1.1.2. Unit A is interpreted as a Highstand Systems Tract (HST1), based on the main feature within the unit being downlapping reflectors onto MFS1.

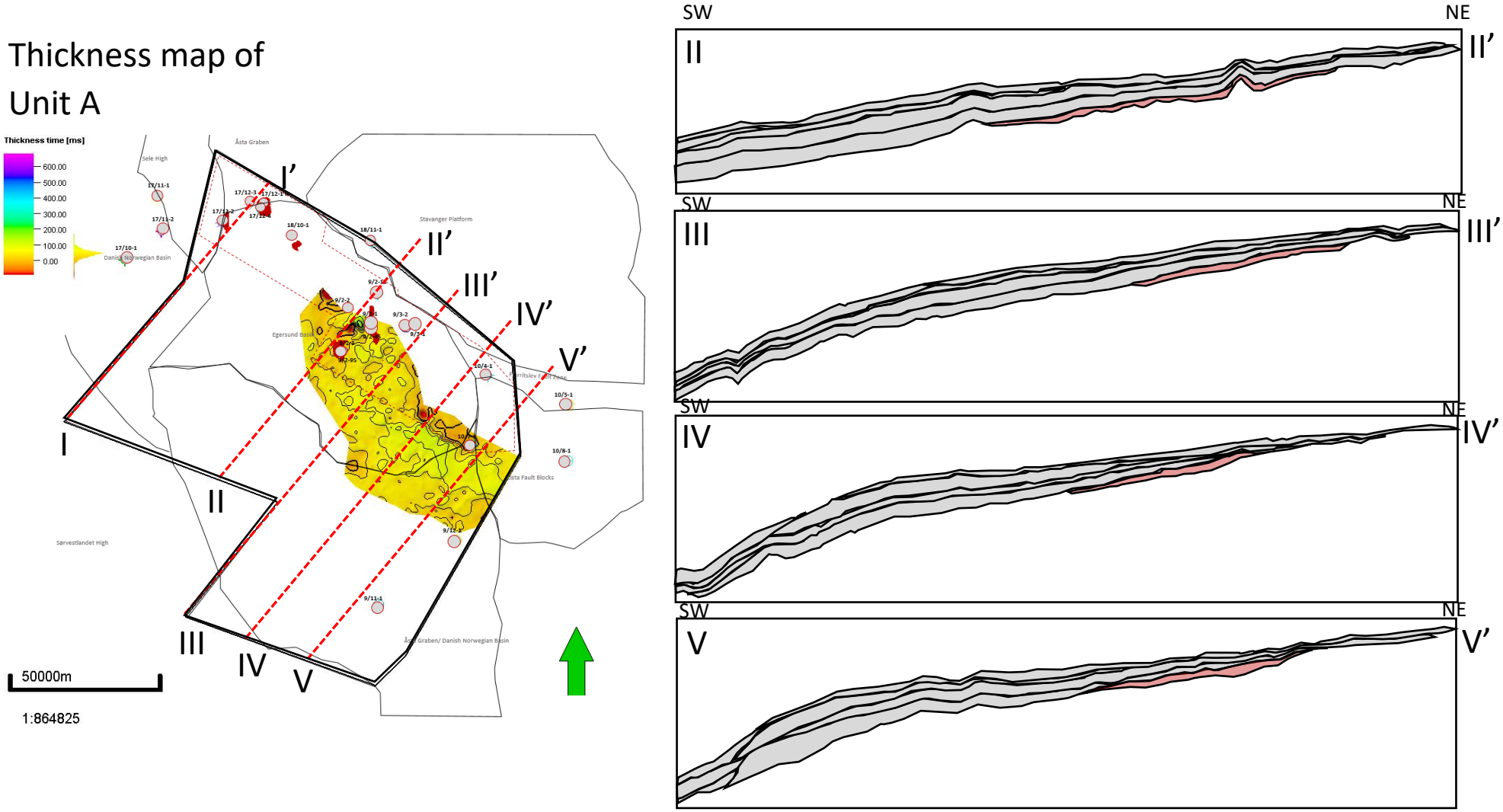

Figure 44. Unit A. Thickness map between the underlaying Base Oligocene surface and the overlying MFS2 surface of Unit A. 2D seismic cross-sections, line II to V, where the interval of red color is Unit A.

5.1.2.2 Unit B

Seismic Unit B is deposited after unit A but is still of Early Oligocene age. It is bounded by the sequence boundary, SB2 at top, and at the base by the Base Oligocene surface (MFS1) and Unit A (MFS2 surface) in the western part of Unit B.

5.1.2.2.1 Observations

Figure 39 to 40 shows the progradational patterns/features observed in the 2D seismic lines within Unit B in the southwestern part, which is clearly visible on seismic line IV and V, where several downlapping reflectors is observed (Figures 42 and 43). The limited lateral extent of this unit makes it difficult to recognize downlapping reflectors on the seismic line I and II. Unit B onlaps onto the base Oligocene surface (MFS1) in a northeast direction and thus onto the Stavanger Platform in almost all the 2D seismic lines. However, in seismic line II, the reflectors within this unit are truncated (Figure 40). Some internal offlapping reflections is observed in the southwestern part of unit B (Figures 42 and 43), else divergent reflector configuration is seen in this unit throughout the study area (Figures 39 to 43). The seismic reflectors within Unit B are semi-continuous to continuous with low amplitude in the southwest and medium amplitude in the northeast. Unit B is a relatively thick unit with abundant deposition during the time between early Oligocene to late early Oligocene (Figure 45). This unit is thickening basinward and thinning landward towards the Stavanger Platform in the northeast (Figure 45). An exception for this trend in thickness is observed in seismic line III, where Unit B appears to be getting thinner in the southwestern part of the cross-section and the study area (Figure 41 and 45).

The thickness map of Unit B (Figure 45) displays a significant depocenter in the area located in the south. In addition, a general thickening towards the west/southwest is observed. At the thickness map in the area of the southwestern part of seismic line III, a transition from thicker deposition to the west is “separated” from the areas of thinner thickness to the east. Unit B is one of the thickest units of Oligocene deposition throughout the study area with an average thickness of around 150 ms (290 m).

5.1.2.2.2 Interpretations

As mentioned earlier, Unit B is one of the thickest units within the Oligocene interval, which means that large amount of sediments was delivered to the basin during this time interval. The most likely source of this high sediment supply is the southern part of the Norwegian mainland (See Figure 50). The 2D seismic lines clearly show the thickness change from thinner in northeast and

significantly thicker in the southwestern part of the unit, where the prograding and downlapping features are seen (Figures 39-43). The deposited sediments are thinner closer to the Stavanger Platform, and truncated in some areas, this could be explained by limited accommodation space and erosion of the unit when post-Oligocene sediments were deposited or bypassed the platform. The shelf edge development of the downlapping reflectors located in the most southwestern part indicate progradation and some aggradation of clinoforms (Figures 42 and 43). The areas of greatest thicknesses in the thickness map are indicating the main depocenters during the time of deposition of the Unit B. Based on the progradational clinoforms and thickening of the unit in basinward direction, that occurs during relative sea level fall (See Figure 49), Unit B is interpreted as a Highstand Systems Tract (HST2).

Thickness map of Unit B

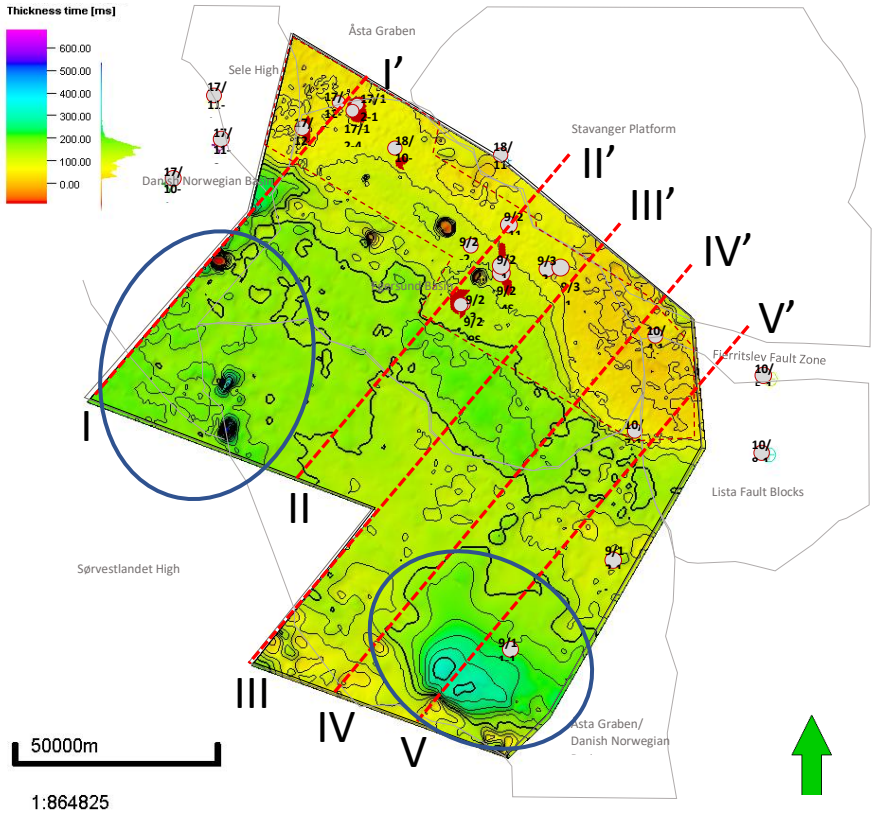

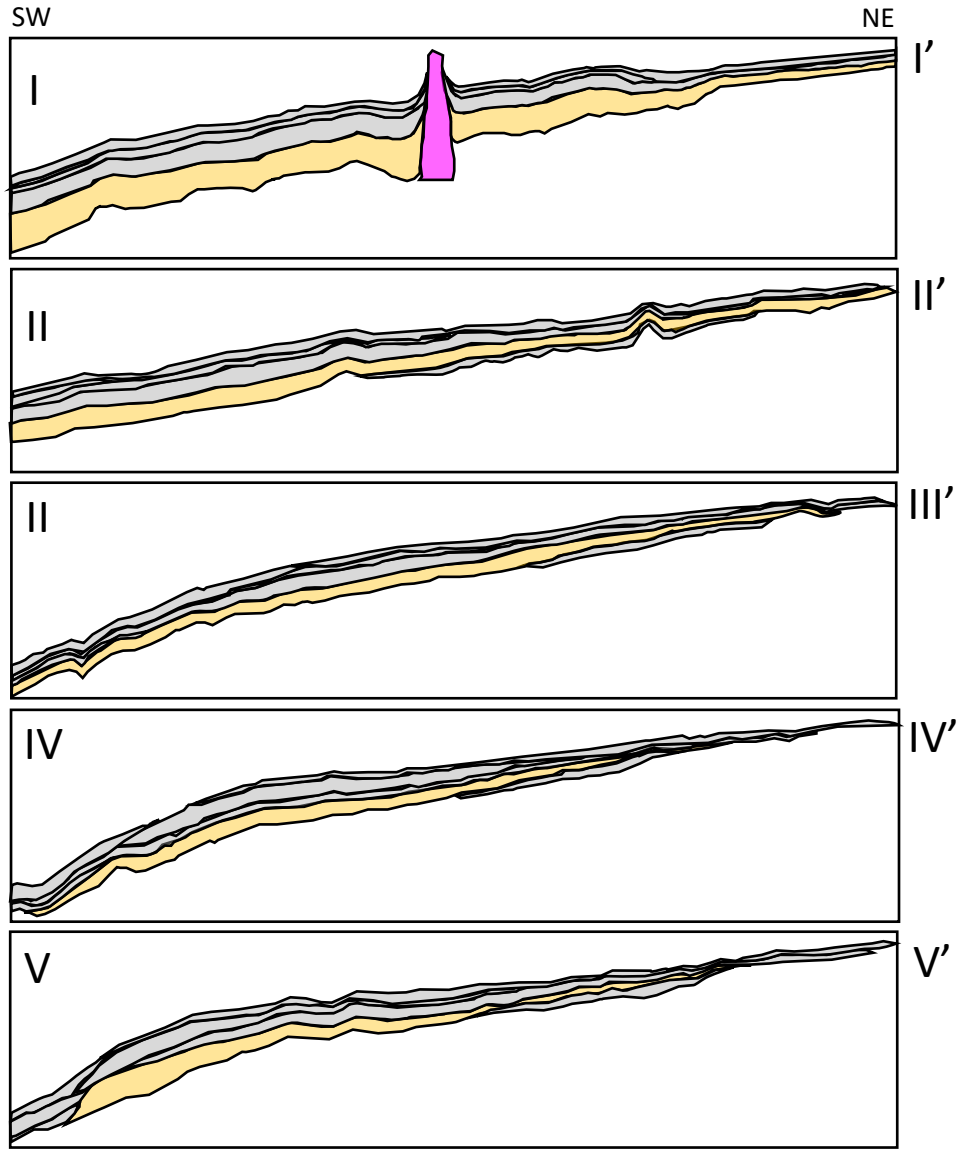

Figure 45. Unit B. Thickness map between the underlaying Base Oligocene surface and the overlying SB1 surface for Unit B. The blue circles indicate areas of significant deposition. 2D seismic cross-sections, line I to V, where the interval of yellow color is Unit B. These cross-section display the external forms of the unit and makes it easier to observe the thickness differences throughout the seismic lines.

5.1.2.3 Unit C

Seismic Unit C comprises sediments deposited during the latest Early Oligocene time, Rupelian stage. This unit is bounded by the Base Oligocene surface (MFS1) at the base and by the maximum flooding surface 3 (MFS3) at the top, and it is located in the southwestern part of the interpreted 2D seismic lines III, IV and V (Figures 41-43).

5.1.2.3.1 Observations

Internal reflectors within Unit C, onlaps onto the SB1 surface in the northeast. Unit C is cropped by the extent of the available 2D seismic data in the southwestern direction (Figures 39-43)). In seismic line V, some downlapping reflectors are observed at the bottom part of this unit, which is the reason for this unit to be interpreted. This part displays a wedge geometry with thinning towards the southwest (basinwards), strong amplitude reflectors are observed at both the top and base of it. This feature is only observed in seismic line V (Figure 43). On top of this wedge-shaped geometry there is an interval of medium to strong amplitude reflectors throughout the area (Figures 41, 42 and 43). This part displays a more pinching out geometry against the depocenter of Unit B. Unit C is interpreted to have the thickest interval in southeast, based on the 2D seismic lines III, IV and V. Seismic line I and II lack Unit C. In general, observations from the seismic lines suggest that this unit is thickening towards the basin and thinning towards (the top of) Unit B.

The time thickness map (Figure 46) is generated for the interval between the MFS1 and SB1, which means that the map includes both Unit C and Unit D. An overall thickening along the basinward part of the thickness map (Figure 46, blue circled area) is observed, and this area of thickening corresponds to Unit C. According to this thickness map, Unit C reaches a thickness of around 200 ms (380 m).

5.1.2.3.2 Interpretations

Unit C is as mentioned not interpreted on seismic line I and II, and this could be explained by the extent of the 2D lines and that this data is not optimally placed to interpret this unit. The reason why it is not observed in these seismic lines is probably because the unit is deposited closer to the basin. The bottom of Unit C may be interpreted as basin-floor fan, based on the geometry. It is thickening towards the clinoforms to the northeast and thinning basinwards. The overlying sediments, separated from the interpreted basin-floor fan by strong amplitude reflectors in the 2D seismic data in seismic line V, can be interpreted as a late lowstand slope fan based on the onlapping reflectors the wedge shape and the prograding features. The external shape of this slope fan is

observed thinner in the area of onlapping reflectors and thickening basinwards. Based on this, and the fact that basinal deposition is only possible during a lowstand when the shelf is exposed and the sediment bypasses the shelf to be deposited on the slope and in the basin (Sosson et al., 2010), Unit C is interpreted to be a Lowstand Systems Tract (LST1).

5.1.2.4 Unit D

Seismic Unit D is deposited during the latest Early Oligocene to Middle Oligocene time. It is bounded by SB2 at the base and by MFS2 at the top, and it is mostly located between Unit B and Unit E as Unit C is only locally preserved.

5.1.2.4.1 Observations

Backstepping features is typically observed in the southwestern part of the unit, where downlapping reflectors is seen retrograding in a landward direction (Figures 39-43). Unit D is truncated by post-Oligocene strata in the northeast, at the Stavanger Platform. The unit is mostly characterized by strong amplitude reflectors and some medium amplitude reflectors (Fig). The seismic lines III, IV and V, clearly display a thinning basinward towards the southwest and towards the Stavanger Platform to the northeast (Figures 41-43 and 46). The middle part of Unit D illustrates the greatest thickness seen in the different seismic lines. It is difficult to observe the thinning towards the basin in the seismic lines I and II, probably because the 2D seismic lines does not cover as an extensive area as seismic lines III, IV and V.

From the time thickness map (Figure 46) it is difficult to observe the thinning of Unit D towards the basin, because the Unit C is included in the map, and also because of the first two seismic lines (I and II) show a minimal change in thickness before the 2D seismic lines ends (Figures 39 and 40). Around the area of seismic line IV and V, it is possible to observe a slightly thinning sediment package. In the northeast direction, is also illustrated a gradual thinning from thick deposition of around 150 ms (290 m) to 0 m at the edge of the Stavanger Platform (Figure 46).

5.1.2.4.2 Interpretations

Unit D is thinning towards NE and the Stavanger Platform, this is possibly caused by erosion of the sediments deposited here when younger sediments have bypassed and eroded this platform. The observed backstepping, is most likely caused by rise in relative sea level. Reflectors of strong amplitude infer a more condensed and fine-grained deposition, which is indicative of a transgressive sedimentation. Based on these factors, Unit D is interpreted as a Transgressive Systems Tract (TST1).

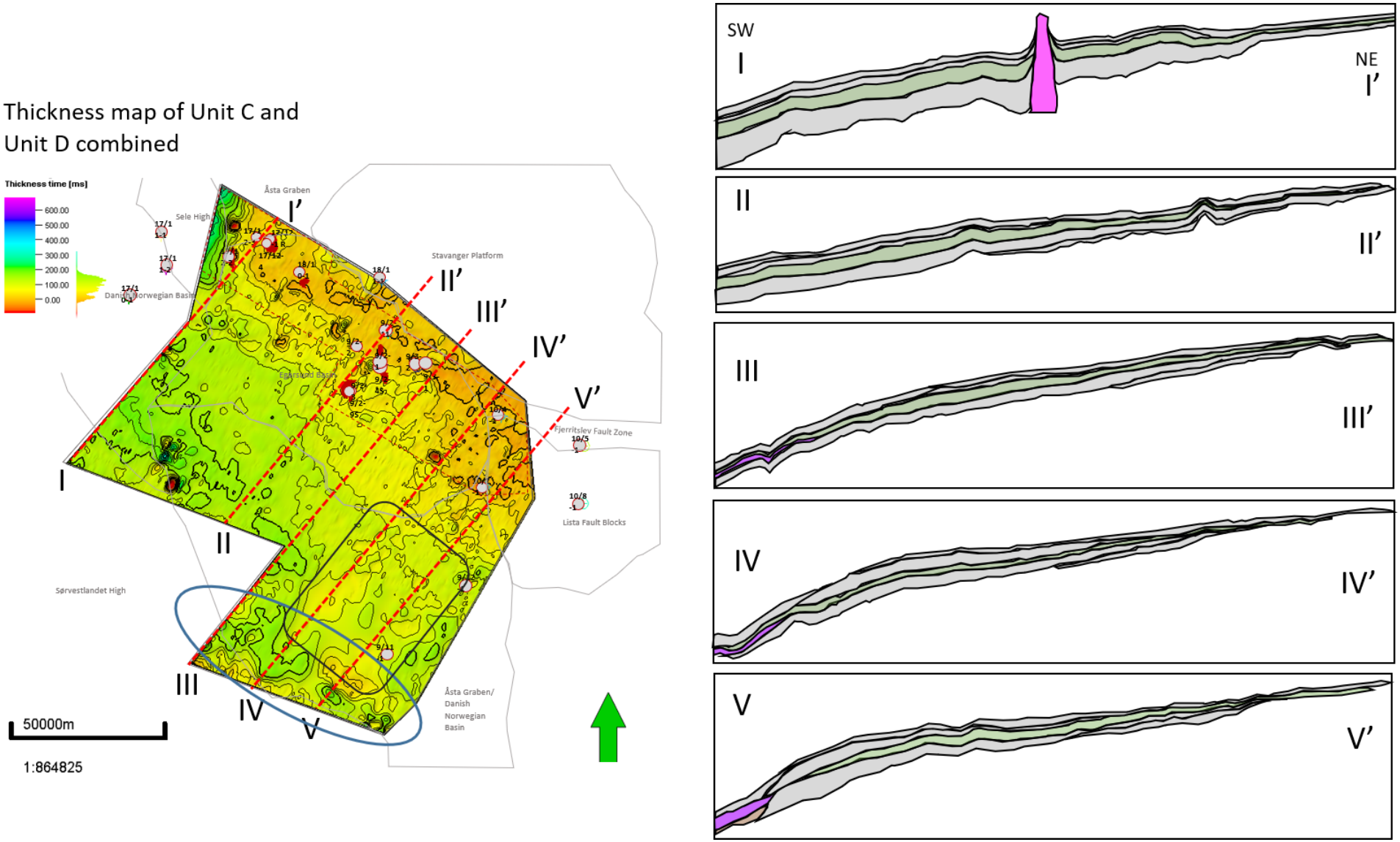

Figure 46. Unit C and Unit D. Thickness map between the SB1 surface and the overlying MFS3 surface. The observed increase thickness at the southern, distal part of the study area (circled with a blue line) correlates to Unit C, interpreted as LST1. The rest of the study area is displaying the thickness variations of Unit D. Within the black square, relatively thin deposition can be observed, indicative of the TST1 pinching out in basinward direction. But the depocenter of Unit D is located in the southwesterly parts of the study area, where a relatively thick succession of the unit is deposited. 2D seismic cross-sections, line I to V, where the interval of purple (and brown) color is Unit C, and the succession displayed in green color is Unit D.

5.1.2.5 Unit E

Seismic Unit E is deposited from ~Middle Oligocene to ~Middle Late Oligocene or Middle of Chattian. Unit E is bounded by MFS3 at the base and by SB2 at the top.

5.1.2.5.1 Observations

Reflectors downlapping onto the underlying surface, MFS3, are observed in the southwestern part of this unit on 2D seismic lines (Figures 39-43). The dip of these reflectors changes from steeply dipping in seismic line V into gentler downlapping in the northern seismic lines I, II and III. In Unit E, the reflectors are characterized as semi-continuous, sub-parallel to divergent, and have low to medium amplitude seismic configuration. The geometry or shape of Unit E is observed as thickening towards the deepest part of the study area in the southwest (Figure 47). While the unit pinches out or onlap onto Unit D and the MFS3 surface further landward and up onto the shelf in northeast direction.

Since Unit E progressively onlaps further in on the shelf, the regional extent of this surface is limited. The time thickness map displays the extent of this unit, which does not extend into the 3D seismic data area and is only interpreted in the 2D seismic lines (Figures 39-43). The southernmost part of the interpreted surface shows an increase in the thickness that infer the location of the main depocenter. The greatest thickness ~ 200 ms (380 m), marking this as a considerable depocenter (Figure 47).

5.1.2.5.2 Interpretations

Unit E is interpreted to be a Highstand Systems Tract (HST2), based on the observed prograding and downlapping reflectors within this unit and the general thickening towards the basin. Another aspect considered for this assumption, is that the underlying Unit D was interpreted as a TST. The top of Unit E is an erosional unconformity, interpreted as sequence boundary 2 (SB2).

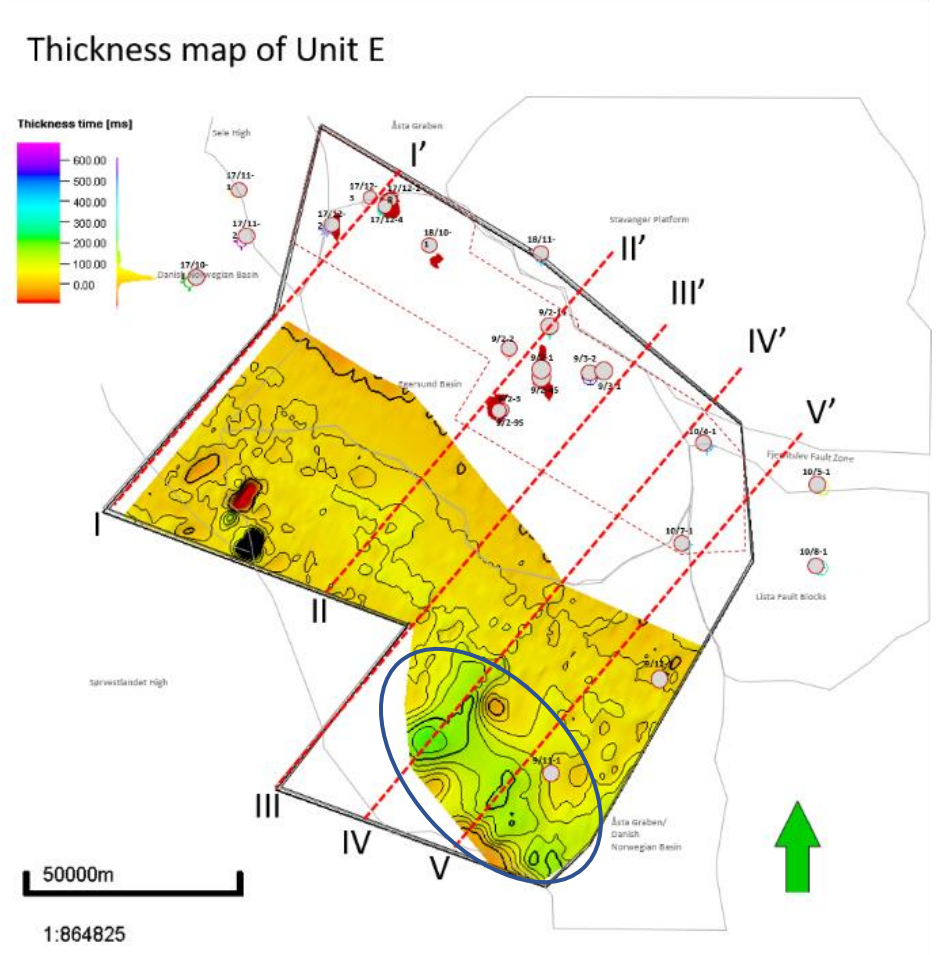

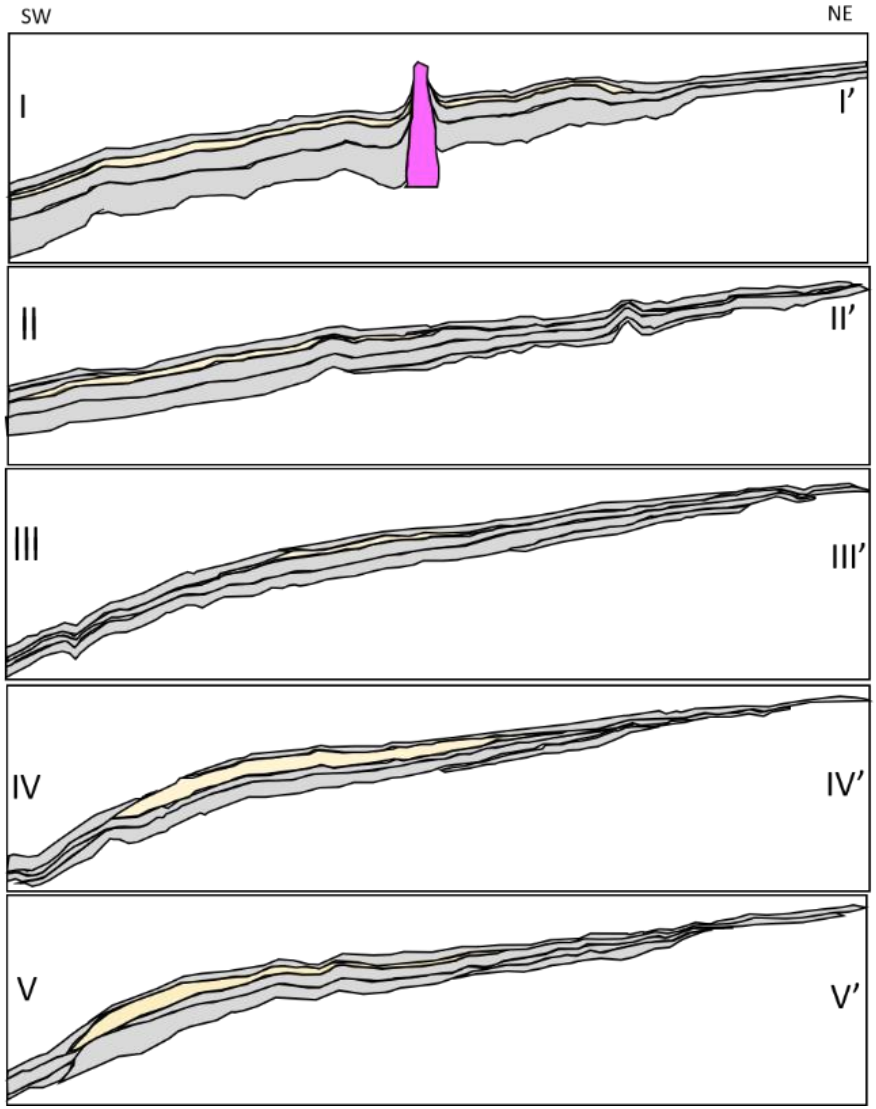

Figure 47. Unit E. Thickness map between the underlaying MFS3 surface and the overlying SB2 surface. The thickness map of Unit E does not cover the area of the 3D seismic data, it is only interpreted from the 2D seismic lines in the area of the edge of the Egersund Basin and in the Åsta Graben. The blue circled area marked on the thickness map, indicate the main depocenter during deposition of Unit E. This is also the area of the most prograding downlapping features. 2D seismic cross-sections, line I to V, where the interval of light-yellow color is Unit E.

5.1.2.6 Unit F

Seismic Unit F is of Late Oligocene age and more specifically the Chattian stage. It is bounded by MFS4 at the top and by MFS3 at the base.

5.1.2.6.1 Observations

Reflectors within Unit F onlaps onto the surface, SB2, to the northeast. This unit is not observed in the 3D seismic data, but only in the southwestern part of the 2D seismic lines (Figures 39-42). The entire extent of this unit cannot be observed with the available data due to the limitations of the 2D seismic lines, especially for seismic line I (Figure 39 and 48). The reflectors are characterized as semi-continuous, sub-parallel to divergent, with low to medium amplitude recognized in the 2D seismic data. Unit F has aggrading to prograding reflectors (Figures 40-43) and the unit thickens basinward and thins landward towards the northeast, where the onlapping terminates. A wedge geometry can only be observed in seismic line V (Figure 48 and 43), where the reflectors downlap onto MFS3.

Figure 48 display the combined thickness map of Unit F and Unit G. The most representative area for Unit F is the southwestern and southern edges of the study area, where this unit has its thickest deposition and preservation. The deposition of Unit F ranges in thicknesses from approximately 100 ms (190 m) to 200 ms (380 m).

5.1.2.6.2 Interpretations

The depocenters for Unit F seems to be mainly in the southwestern and southern corner of the study area, , based on the position of the unit thickness anomalies. Unit F has been interpreted as a Lowstand Systems Tract (LST2), based on the onlapping reflectors onto the sequence boundary together with the aggrading and prograding pattern, which could have been caused by increased accommodation space, likely due to base-level rise.

5.1.2.7 Unit G

Seismic Unit G is of the latest Chattian age, and thereby deposited during the latest late Oligocene age. It is bounded by the surface SB3 at the base and by the Top Oligocene surface, also known as MFS4 at the top (Figures 39-43).

5.1.2.7.1 Observations

Unit G is truncated on the Stavanger Platform in the northeast, by younger strata, but some of the reflectors within this unit onlap onto MFS3 further out onto the shelf (observed in Figures 39-43). The seismic character of Unit G is semi-continuous, sub-parallel, low to medium amplitude

reflectors. The backstepping reflectors have been observed, together with thickening strata in landward direction, before it thins rapidly towards the platform area again.

The time thickness map shows both thickness of Unit F and Unit G, which means that the thickness at the southwestern part of the study area display a greater thickness, than what Unit G consists of. The depocenter of Unit G seems to be in the middle of the study area (Figure 48), oriented in a NW-SE direction. This depocenter thins significantly towards the Stavanger Platform where the thickness is interpreted to be between 50 ms (100 m) to 0 m.

5.1.2.7.2 Interpretations

The depocenter of Unit G was clearly mapped along the middle of the interpreted area. The backstepping features are indicative of a period of relative sea level rise, and therefore was Unit G interpreted as a Transgressive Systems Tract (TST2). The TST is characterized by depositional transgression, because the rise in base level outpaces the sediment supply. The thinning and pinching out towards the basin, together with the thickening of the unit away from the basin match well with the interpretation of a TST unit. TST2 is bounded on top by a maximum flooding surface (MFS4).

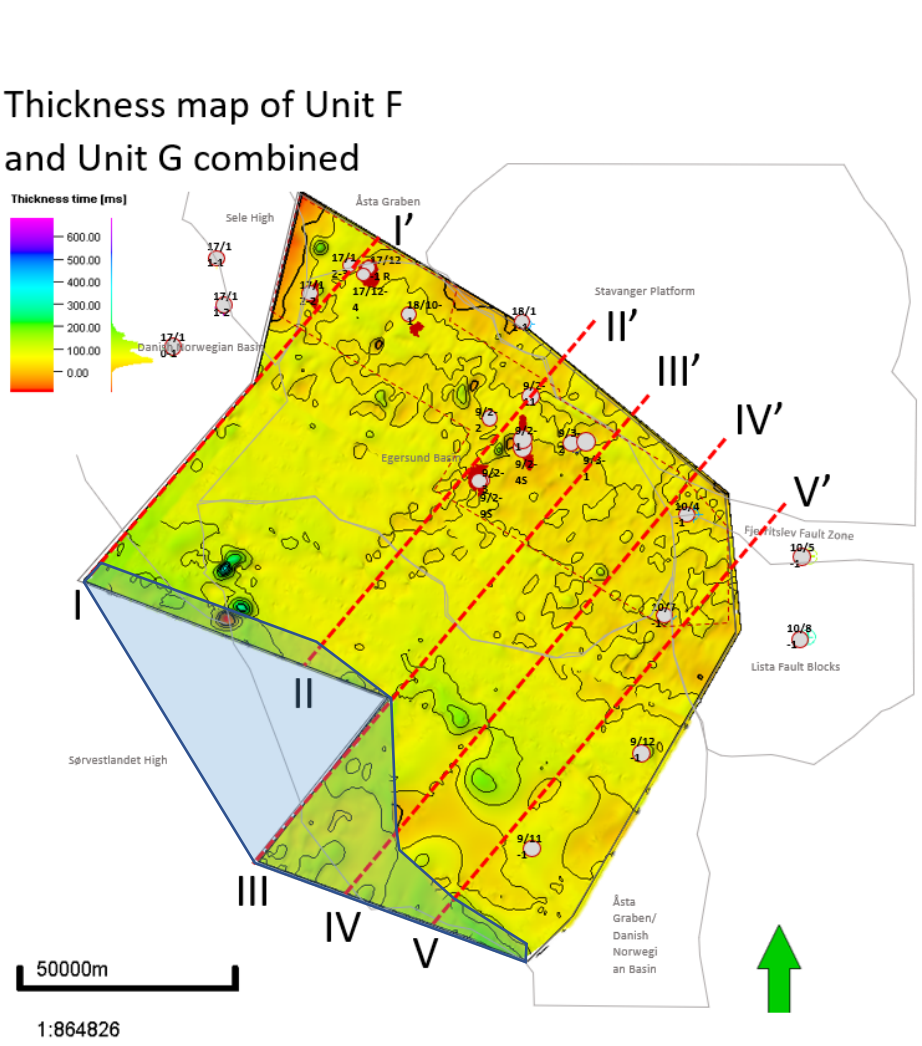

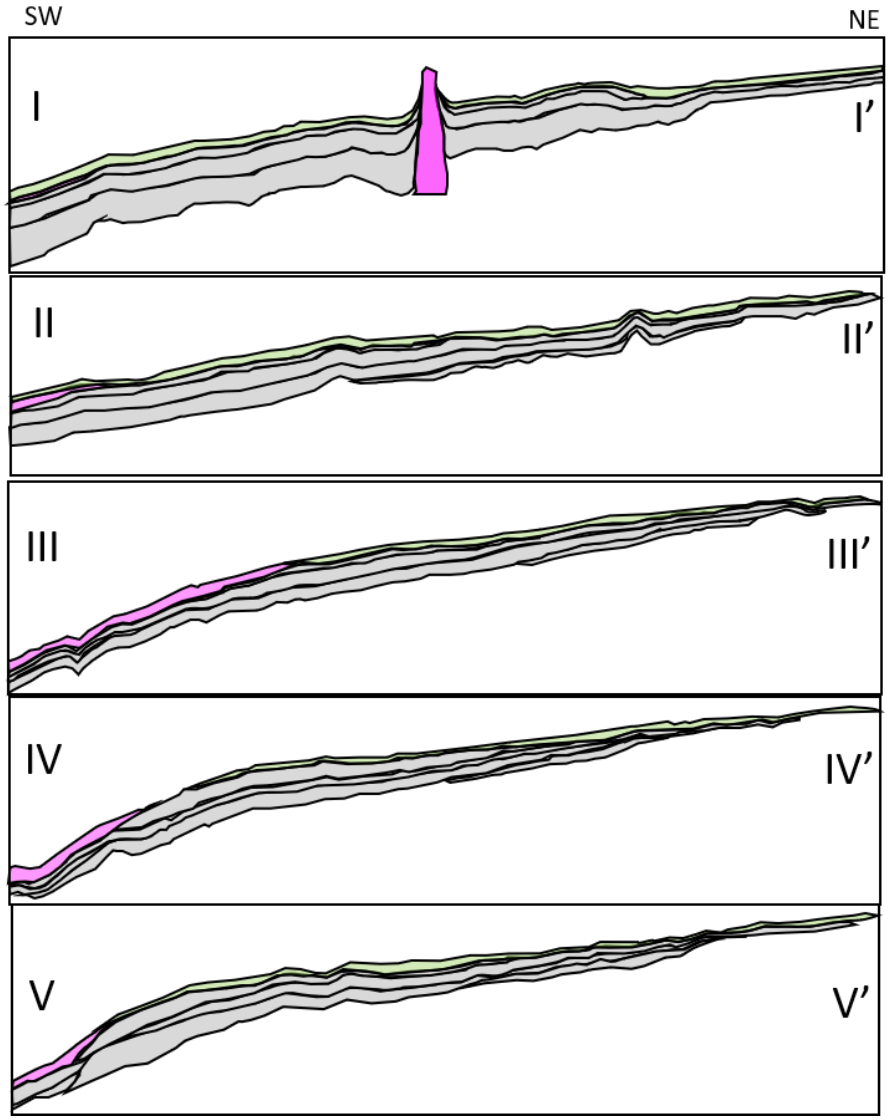

Figure 48. Unit F and Unit G. Thickness map between the SB2 surface, together with the MFS3 (where SB2 is not present) and the overlying Top Oligocene surface (MFS4). The thickness map shows the combined thickness of Unit F and Unit G. Unit F is illustrated in the blue outlined area. This area shows a generally thicker deposition than the rest of the thickness map, which illustrate the deposition of the transgressive unit G. 2D seismic cross-sections, line I to V, where the interval of pink color is Unit F and the light-green color illustrates Unit G. The pinkish-purple structure in the seismic line I is a salt diapir that has pierced through the Oligocene succession. Indicative of halokinetic movements during and after deposition of the Oligocene sediments.

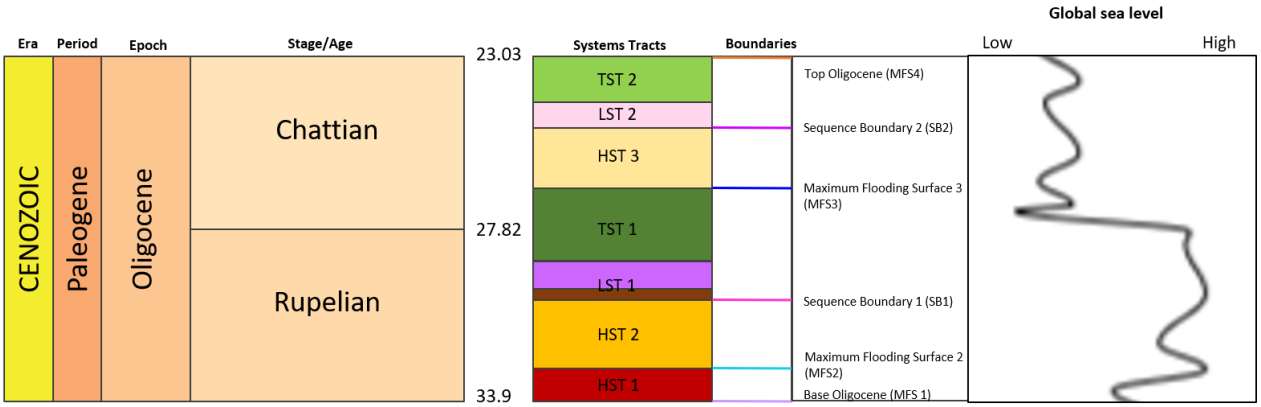

Figure 49. Conceptual chronogram displaying the interpreted systems tracts and their bounding surfaces, together with the global sea-level curve modified from Hardenbol et al. (1998).

Based on the interpretations from the previous sub-chapters, the Oligocene interval has been divided into seven systems tracts (Figure 49). The Rupelian consists of one smaller interval of highstand systems tract, which is overlying the base surface of Oligocene (MFS1), before a more extensive deposition occurred and created the second, much larger and thicker highstand systems tract (HST2). HST2 is bounded by a maximum flooding surface at the base and by a sequence boundary at top. Later in Rupelian lowstand deposition occurred at the edge of the terminating sigmoidal reflectors belonging to HST2. In the 2D seismic line V, this systems tract (LST1) can be divided into two individual types of lowstand deposition. During the transition from Rupelian to Early Chattian, a transgression occurred, based on the backstepping seismic reflectors and high GR in the well logs. Before another significant outbuilding occurred, which is interpreted based on downlapping reflectors in the distal parts of the study area. This deposition is interpreted as HST2. At the end of this outbuilding, LST2 was deposited, based on the onlapping reflectors onto the SB1 and HST2. After this maximum regression episode, the deposition began to transgress and formed the TST2, which is overlain by the top Oligocene surface, which is interpreted to be a maximum flooding surface (MFS4).

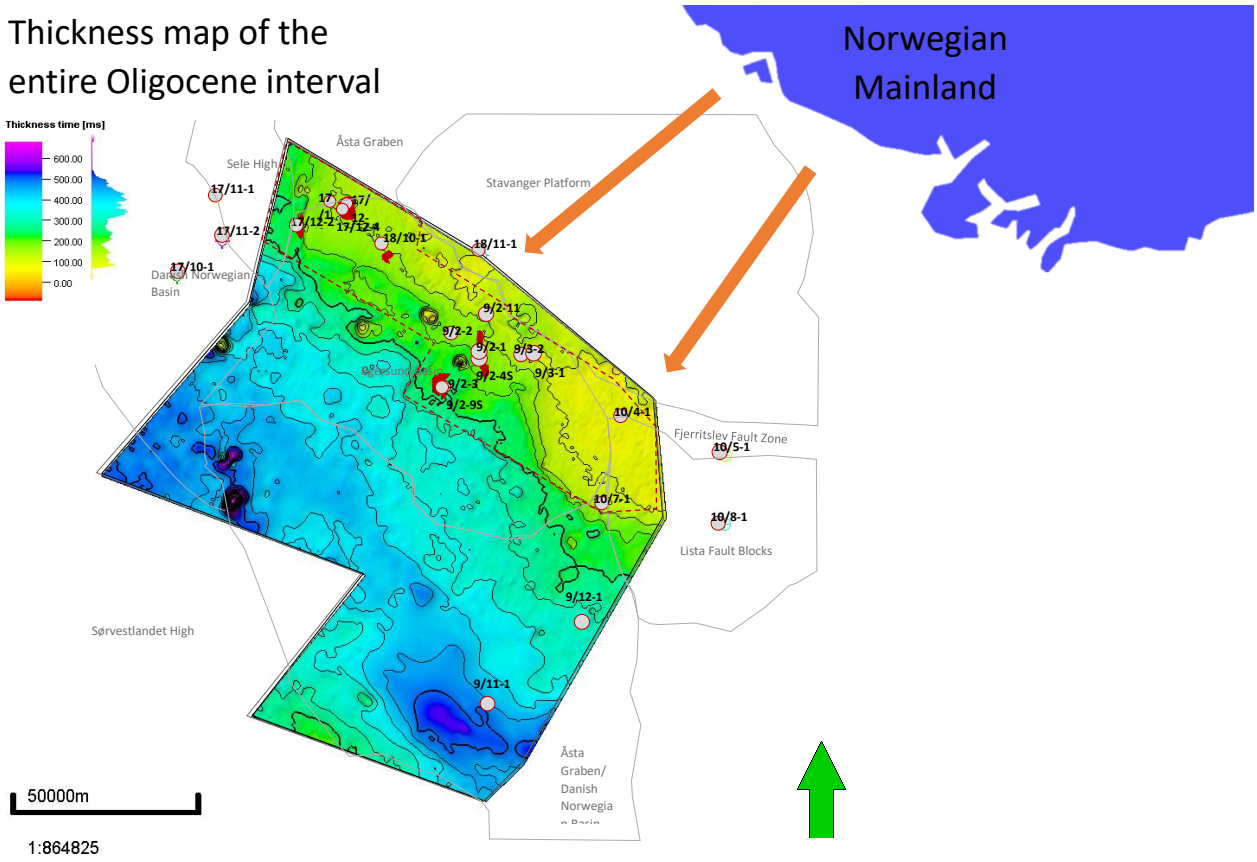

Figure 50. Direction of sediment supply (marked by the orange arrow), during Oligocene and the thickness map displaying the main depocenters. The areas of thickest deposition is located in the south and southwestern parts of the study area.

The overall thickness of the Oligocene interval in the study area is displayed in Figure 50. The areas of greatest thickness observed in the thickness map is in the most southern part of the study area and in the western area. The thickening in the south part correlate with the deposition of the prograding clinoforms of significant thickness. During the Oligocene time the sediment supply came from the continuous uplifting Norwegian mainland to the northeast. This is consistent with the areas of thicker sedimentation in the study area. The thickest areas display a thickness of approximately 500 ms (950 m), and the shallowest area display a thickness of around 100 ms (190 m).

5.2 Seismic Facies Analysis

Seven Seismic facies categories have been identified from the 2D and 3D seismic data. These seismic facies have been classified based on external geometry of the surfaces bounding the seismic facies, internal reflector configuration, seismic reflectivity and continuity. Table X have been created to define the seismic character variations caused by geological changes and to obtain information related to the depositional environments and processes together with the direction of sediment transport. Vertical and horizontal seismic resolution constrains the sizes of recognizable depositional geometries in the seismic data.

Table 4. The seven seismic facies recognized in the study area. They were identified based on the characteristics of the internal configuration, amplitude strength and continuity, based on Mitchum et al. (1977). Observations are mainly from the 2D seismic data.

Seismic facies	Depositional facies	Internal configuration	Amplitude	Continuity	Sedimentary facies interpretation	Seismic sequences
SF1	Incised valley	Complex fill	High to moderate	Semi-continuous	Platform interior	Unit C, Unit D
SF2	Shelf-margin clinoforms	Foreset angles of 2-5degrees	Moderate	Semi-continuous	Shelf-slope area, prograding	Unit A
SF3	Polygonal fault system	Small offset faults	Moderate	Semi-continuous	Compaction of host sediments or due to friction	Unit B
SF4	Prograding clinoforms	Sigmoidal clinoforms	Moderate	Semi-continuous	Shelf-slope area, prograding	Unit B, Unit E
SF5	Onlapping reflectors	Parallel to divergent	High to moderate	Semi-continuous	Slope and basin floor	Unit C
SF6	Parallel to subparallel reflectors	Parallel to subparallel	High	Continuous	Shelf	Unit B, Unit D, Unit E
SF7	Chaotic facies	Chaotic	Variable	Discontinuous	Shelf, gravitational collapsed	Unit E, Unit G

5.2.1 Seismic Facies 1 (SF1)

Seismic facies 1 (SF1) consists of lens or mounded shaped features (Figure 51b). Figure 51a show the extent and location of this feature, which is located on the Stavanger Platform and dipping gently in southeasterly direction.

This feature can be interpreted as an incised valley, based on the erosional surface (Figure 51a), and within the incised valley complex fill pattern is observed (Mitchum et al., 1977). This might be a result of multiple cycles of incision and deposition (Tesson, 2005). The fill within this feature (incised valley) occurs to be downlapping from west to east in some of the seismic lines, while other seismic lines display downlapping reflectors from easterly direction. The erosional surface of the incised valley truncates several reflectors within the Oligocene interval to the west.

Following the 2D seismic lines in southeasterly direction, it is possible to observe that this feature is progressively deepening, this could be explained by an interval of relative sea-level fall and that the Stavanger Platform at this time were a zone of bypass (Weimer and Link, 1991).

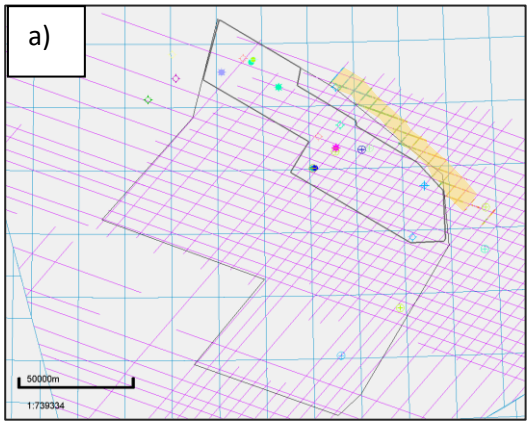

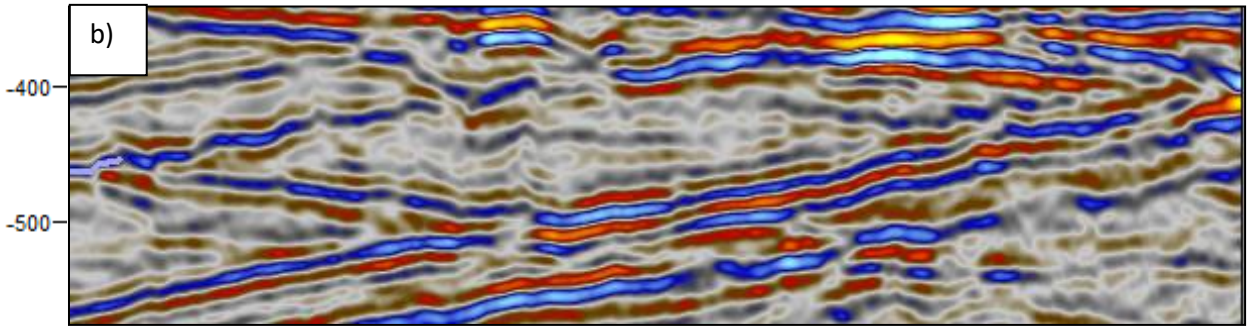

Figure 51. Seismic Facies 1. Seismic feature at the Stavanger Platform, interpreted as an incised valley. a) The location and the interpreted extent of this seismic facies marked yellow area. b) How the seismic feature looks like in one of the 2D seismic lines in the northeastern part of the interpreted area (yellow). Erosional surfaces can be observed at the top, side and base of this structure. In this example, the internal reflectors seem to be downlapping.

5.2.2 Seismic Facies 2 (SF2)

Clinoforms with foreset angles of 2-5 degrees and a height of 50-100 m is forming the seismic facies 2 (SF2). The clinoforms show a gentle sigmoidal shape with an ascending shelf-edge trajectory (Figure 52b). This can be characteristic of shelf-margin clinoforms. The approximal extent and position of this seismic facies is shown in Figure 52a.

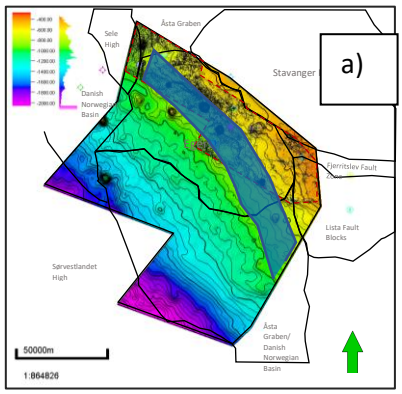

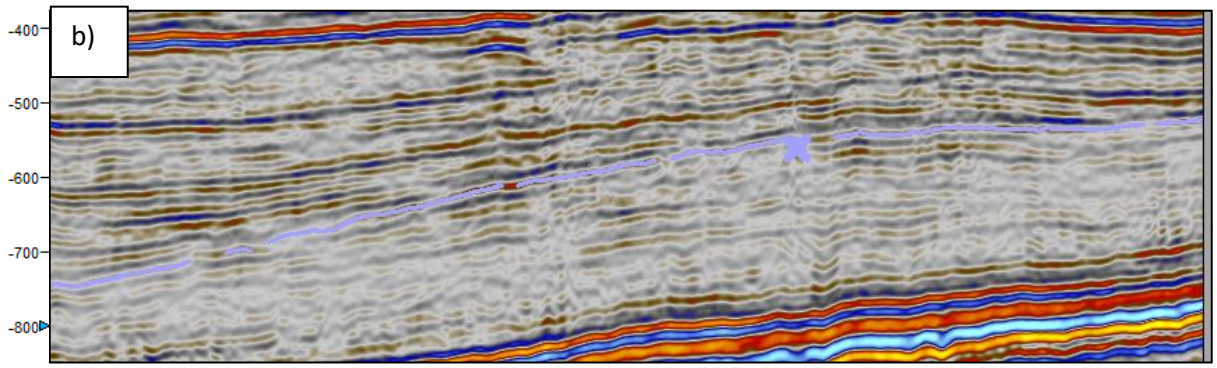

Figure 52. Seismic Facies 2. a) The approximate position and extent of the interpreted Seismic Facies 2. b) clinoforms with foreset angles of 2-5 degrees.

5.2.3 Seismic Facies 3 (SF3)

Seismic facies 3 (SF3) consists of layers containing small-offset polygonal faults (Figure 53b). It is distributed in the westerly corner of the study area (Figure 53a) in Åsta Graben and the Danish Norwegian Basin, just above the interpreted Base Oligocene surface. Polygonal fault systems are mostly developed in fine-grained sedimentary successions (Cartwright et al., 2003), dominantly found in mudstone-dominated lithologies.

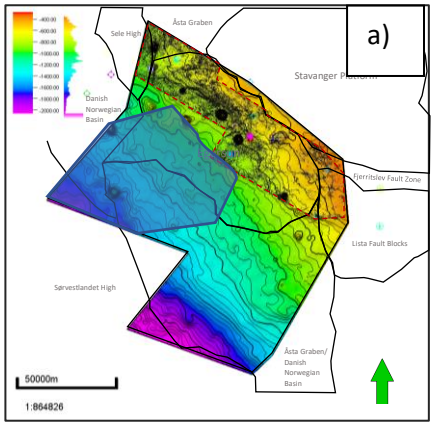

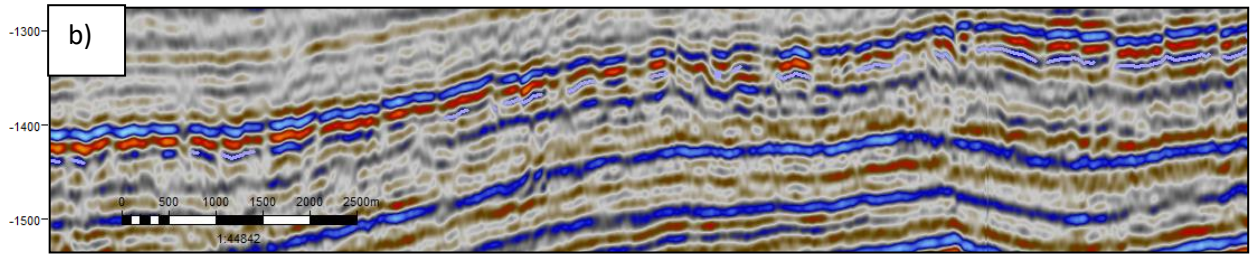

Figure 53. Seismic Facies 3. a) the areas of extensive small-offset polygonal faults. b) The polygonal faults displayed in the 2D seismic data.

5.2.4 Seismic Facies 4 (SF4)

Seismic facies 4 (SF4) is progradational deposits and consists of sigmoidal to sigmoidal-oblique clinoforms (Figure 54). This seismic facies is located in the southern part of the study area, and is found in Unit B and Unit E. (Figures 42 and 43). Internal reflectors are downlapping, and these terminations represent outbuilding of sediments from relatively shallow to relatively deep waters, with relatively high angle and height of more around 100 m. The sigmoidal geometry of this seismic facies suggests rapid base-level rise or rapid basin subsidence (Mitchum et al., 1977).

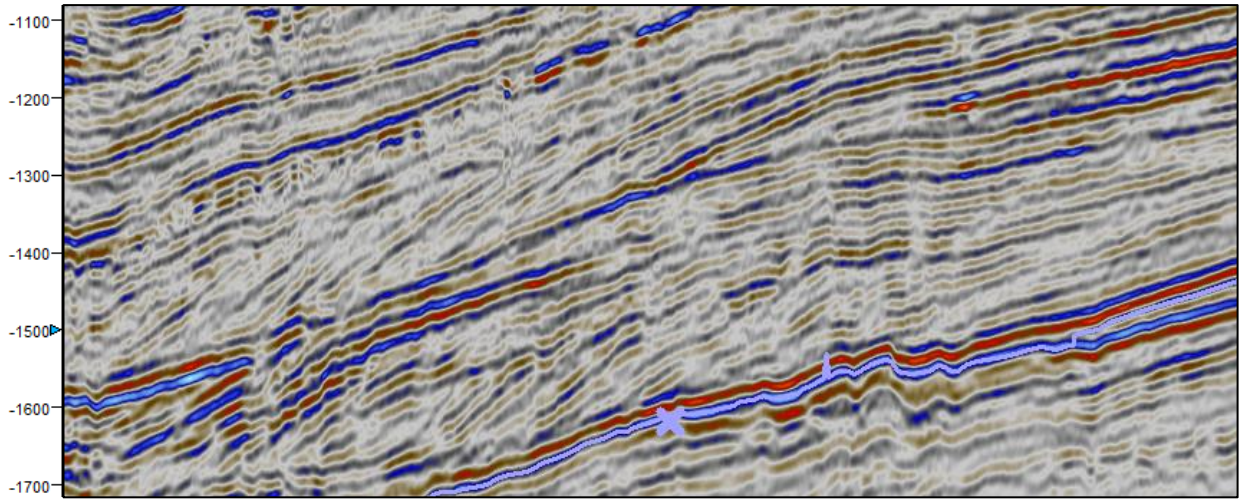

Figure 54. Seismic Facies 4. Prograding sigmoidal clinoforms

5.2.5 Seismic Facies 5 (SF5)

Seismic facies 5 (SF5) consists of onlapping, parallel to slightly divergent reflector patterns with relatively high continuity and high to variable amplitudes (Figure 55). The external form of this feature appears mounded to wedge shaped. This seismic facies is interpreted to display lowstand slope fan.

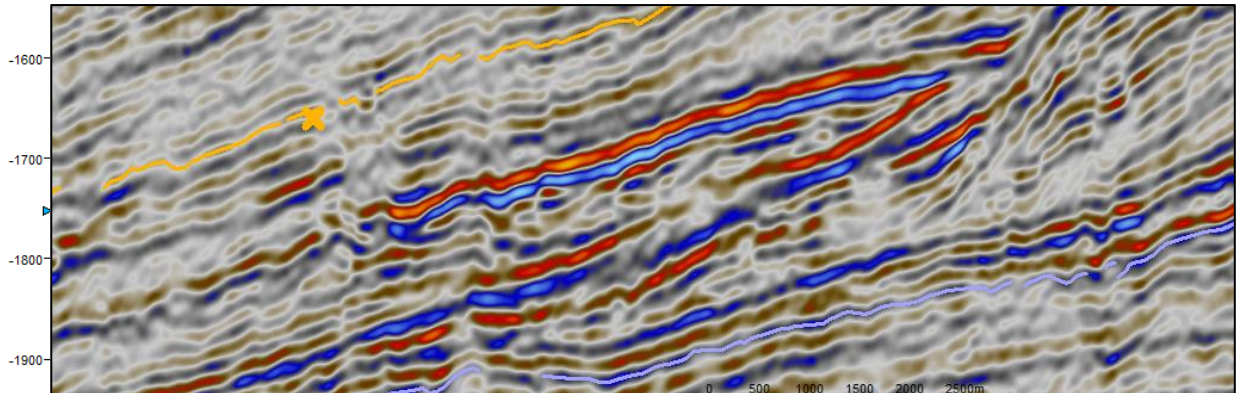

Figure 55. Seismic Facies 5. Onlapping, parallel to divergent reflector pattern

5.2.6 Seismic Facies 6 (SF6)

Seismic facies 6 (SF6) consists of continuous, parallel to sub-parallel reflectors with high reflectivity (Figure 56). This seismic facies is related to Unit B and Unit D. Seismic facies 6 varies from thin, single seismic wavelets to more complex waveforms expressed as doublets or high amplitude sets.

This type of seismic facies is interpreted to represent pelagic to hemipelagic claystones in the shelfal area. According to Mitchum et al. (1977), the parallel to subparallel reflection configuration illustrate constant sedimentation rates on a steadily subsiding shelf.

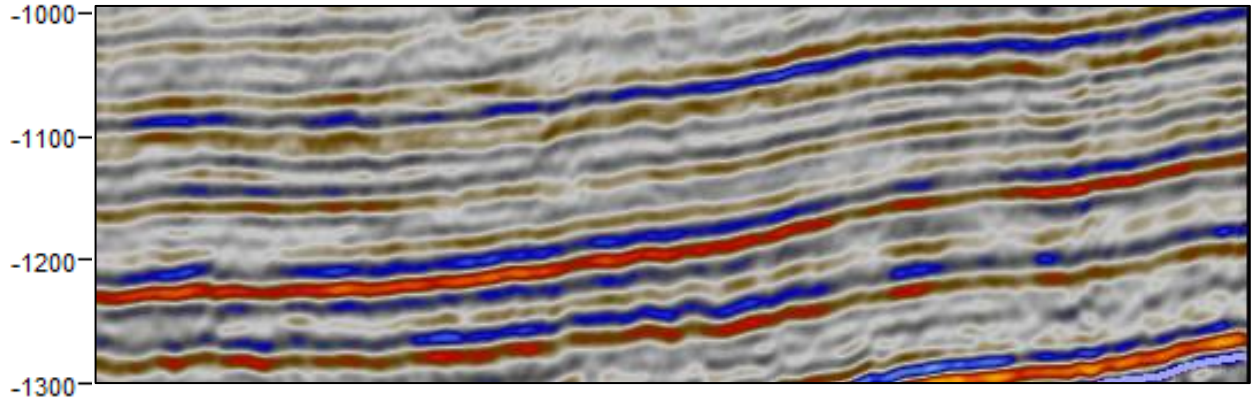

Figure 56. Seismic Facies 6. Parallel to sub-parallel reflectors

5.2.7 Seismic Facies 7 (SF7)

Seismic facies 7 (SF7) consists of low amplitude, low reflectivity and relatively poor reflection continuity. The external form of the deposits is of mound-shaped bodies. The chaotic pattern is interpreted as mass-transport deposits (Posamentier and Kolla, 2003). The reflector on both sides of this chaotic feature is subparallel.

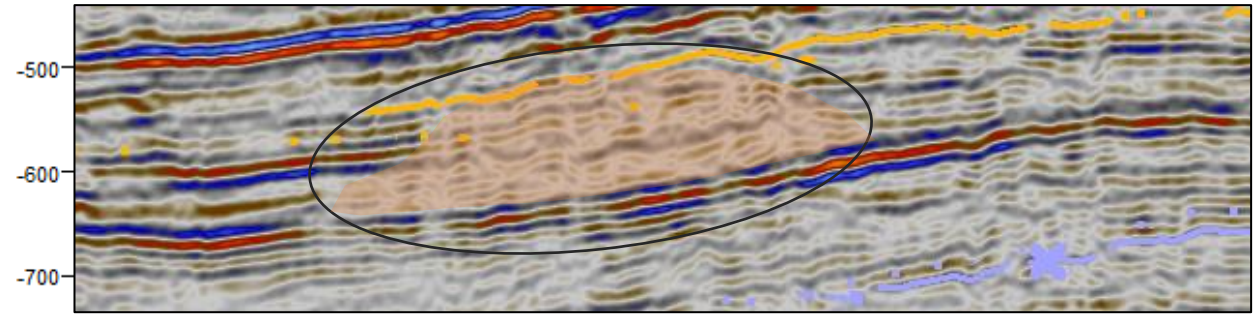

Figure 57. Seismic Facies 7. Poor continuity, chaotic reflectors.

6. Discussion

The Oligocene interval of the area of Egersund Basin and its surroundings in the southern part of the Norwegian North Sea has been divided into seven seismic units (Unit A to Unit G) bounded by six key stratigraphic surfaces. This was done by using integration seismic data and well logs.

Seismic stratigraphic analysis of the internal characteristics of each unit reveal a regional flooding during the Middle Oligocene period. The global sea-level curve from Hardenbol et al. (1998) display mostly relatively high sea-level for the Early Oligocene, Rupelian time and a lower sea-level during the Late Oligocene. The global sea-level curve shows a sea-level fall at the transition between Rupelian and Chattian age, which is consistent with outbuilding of sediments in the beginning of Chattian times.

The ages of the seismic surfaces have been extrapolated from well tops and compared with proposed ages from previous studies (Jarsve et al., 2014; Eidvin et al., 2014; Danielsen et al.,). The LST's has not been penetrated by any obtained wells, it is therefore difficult to say anything about the sediments of this deposition.

6.1 Sequence Hierarchy

The seven interpreted seismic units in the Oligocene strata, discussed in the previous chapter, represent the systems tracts bounded by key stratigraphic surfaces. These units can be classified into two complete sequences and incomplete sequence of shorter extent and smaller scale.

The incomplete sequence 1 consists only of Unit A, which is bounded at the base by Base Oligocene (MFS1) and by MFS2 at the top. Both downlapping reflectors and backstepping features are observed within this unit, but a clear sequence boundary is difficult to determine. Since this sequence is of a smaller scale, it is interpreted to be of a low rank, with a higher frequency in the rock record, where sequence stratigraphic surfaces occur more often than in orders of higher rank (Figure x (HiRACHY figure). Sequence 2 comprises Units B, C and D, and it is bounded by MFS1 and MFS2 (where this surface is present) at the base and by the MFS3 at the top. Sequence 3 consists of Units E, F and G, bounded at the base by the surface MFS3 and at the top by the Top Oligocene surface (MFS4). Both Sequence 2 and 3 comprise higher ranked orders, based on the model of the genetic stratigraphic sequences (Galloway, 1989), the stratigraphic cycles were determined to be of third-order cycles. This suggests that each sequence was formed in response to

thermal subsidence and a regional tectonic event (Miall, 2016), that could be related to seafloor spreading in the North Atlantic Ocean and the uplift of the Fennoscandian shield.

6.2 Temporal variability of the post-rift deposition

The sediment supply during Oligocene is interpreted to originate from the southern part of the Norwegian mainland, based on the progradational trends and previous regional studies in the Norwegian North Sea (Eidvin et al., 2014; Jordt et al., 1995 and Jarsve et al., 2014). All units are interpreted to have been deposited during this time of the mainland uplift, while the basins in the North Sea underwent thermal subsidence. The units are depositions of the Hordaland Group, which are, as previously explained, mainly fine-grained sediments of shales or claystones. But some coarse-grained deposition has been observed in the area of the Egersund Basin and its surroundings. So, areas and well logs indicative of sandy deposition might correlate to the coarse clastics of the Vade Formation.

In the study area, Unit A represents a lower ranked highstand systems tract (HST1) which underwent normal regression. This resulted in progressive addition of sediments, explained by the prograding, downlapping features within the unit. Unit A (Figure 44) is observed in the more proximal part of the interpreted shelf in the area of the Egersund Basin and towards the Norwegian-Danish basin in the south/southwest. This unit is suggested to have been deposited during the earliest of Oligocene and Rupelian time. Seismic Facies 2 (SF2) can be related to unit A in the northeastern part of the unit's extent.

The prograding clinoform features deposited in Unit B have formed during a late stage of relative sea level rise, are interpreted to have been formed due to the sediment supply being greater than the accommodation space (Catuneanu et al., 2011). Based on the sigmoidal shape, coarser sediments are believed to have been deposited on the shelf, while finer mud-prone sediments were most likely deposited onto the basin-floor. This can be backed up by well 9/12-1, which shows upwards decrease in GR and sandy deposits for the interval of Unit B at the well's position on the shelf. These sandy deposits might belong to the previously mentioned Vade Formation. This unit is related to most of the Early Oligocene or Rupelian, and to the Seismic Facies 3 (SF3) and Seismic Facies 4 (SF4; Figure 54). This unit represents the deposition of the Highstand Systems Tract 1 (HST1); Figures 45 and 49)). The depocenter of this unit (Figure 45) moved further to the south/southeast, compared to underlying Unit A. This represents a progradation of sediments

basinwards into the Norwegian-Danish Basin. The shelf-edge trajectory is most clearly observed in seismic line V (Figure 43), display the progradational and some aggradational patterns of Unit B south/south-westwards. Hence, the sediment source was predominantly from the southern part of the Norwegian mainland bypassing the Stavanger Platform into the study area.

Unit C, deposited during the latest of Rupelian, has no given well positioned in the area of accumulation in the distal, southwestern parts of the 2D seismic lines. Deposition of this unit began by relative sea-level fall and ended by, relative sea-level rise. Based on the area of deposition relatively to Unit B, together with the characteristics of the Seismic Facies 5 (SF5; Figures 46 and 55), the lower part of Unit C is interpreted to be a basin-floor fan, which is observed in the southwestern part of the 2D seismic line V (Figure 43). It is deposited during a time of sea-level lowstand according to Posamentier and Kolla (2003). Later the upper part of Unit C was deposited, with more parallel to divergent internal seismic reflectors, and with a wedge external form. This upper part was interpreted to be a slope fan, since it is building further up on the slope. Unit C progrades towards the southwest, which is displayed on the thickness maps, where the depocenter of this unit is at the distal parts of the study area in the same direction.

In the study area, Unit D represents a period of sea-level rise, consisting of rates of base level rise (increase in accommodation space) greater than the rate of sedimentation. This was likely caused by ongoing subsidence in the area. The retrogradational stacking pattern observed in this unit can be explained by those occurrences, and it is interpreted as the Transgressive Systems Tract 1 (TST1; Figures 46 and 49). Several of the obtained well logs illustrate an upward increase in GR, indicating deposition of finer material, which is common for the sedimentation occurring during rise in sea-level. Seismic Facies included in Unit D is the Seismic Facies 2 (SF2) and the Seismic Facies 6 (SF6). The depocenters of this unit prograded gradually towards the Stavanger Platform in the northeast.

Progradational pattern for Unit E during the Early to Middle Chattian times, is observed in the seismic sections and shown in Figures 39 to 43 and Figure 54. Where the sedimentation rates outpace the rates of relative sea-level rise (Catuneanu et al., 2011). This unit is associated with the Seismic Facies 4 (SF4), Seismic Facies 6 (SF6) and in some areas also Seismic Facies 7 (SF7) in this regressive system.

Unit F, deposited during the latest of Chattian time, is interpreted as a lowstand systems tract (LST2; Figure 48), which represents the time of maximum regression and the shift in depositional trends from seaward-directed to landward-directed. Seismic Facies 5 (SF5) can be related to this unit, based on its onlapping characteristics. The depocenter during depositing of Unit F was located at the slope-shelf transition in the most distal parts if the study area.

Unit G, the youngest interpreted seismic unit within the Oligocene epoch, was deposited during a rise in base level that exceeded the sediment supply and lead to retrogradation of the depositional system. This unit is interpreted as another transgressive systems tract (TST2; Figure 49). Unit G is related to the Seismic Facies 6 (SF6) and in some areas to the Seismic Facies 7 (SF7). The depocenter (Figure 48) of Unit G is illustrated by the observed backstepping features, where the unit increase in thickness in landward direction, but close to the platform, the unit gets progressively thinner, which could possibly be explained by the uplift and erosion to the northeast.

6.3 Controlling factors

The stratigraphic units can be explained in terms of variations in sediment supply and rate of change in accommodation space. Tectonics have played a role in the changes of rate of accommodation space during the Oligocene times in the Egersund Basin and its surrounding areas. Significant uplift of mainland Norway during the Early Oligocene were accompanied by a lowered eustatic sea level and subsidence of the basin floor (Faleide et al., 2008). This led to a considerable increase in sediment supply along the Norwegian continental shelf. The Eocene-Oligocene boundary correlate with the Base Oligocene unconformity surface, which corresponds in time with eustatic sea-level fall (e.g. Jarsve et al., 2014; Haq, Hardenbol and Vail, 1987; Miller et al., 2005), coincident with significant glaciation in Antarctica (Pekar and Christie-Blick, 2008).

The time thickness maps (Figures 44, 45, 46, 47, and 48) of sedimentary deposits in the Oligocene epoch indicate that the depositional pattern does not change much during this period, with the sedimentary depocenters being located in the south/southwestern parts of the studied area, for all the interpreted units. The evolution of the deposition demonstrate that the sediments were mainly sourced from the Norwegian mainland and possibly from the area of the Stavanger Platform. Eidvin et al., 2014, identified a depocenter in the Norwegian-Danish Basin, which received sediments from the southern Scandes Mountains, which correlates with the interpretations of this study.

Huuse (1986) studied the Late Cenozoic paleogeography of the eastern North Sea Basin, and suggested that in post-Eocene time, the central and eastern North Sea Basin was progressively filled by large deltas building out from the eastern basin margin. These deltas were, according to Huuse (1986) fed by ancient rivers from the southern Norway. From the RMS attribute maps, curved, high amplitude features were observed in the area of the 3D seismic data. Based on the previous studies provided by e.g Huuse (1986), these features are believed to be large deltas prograding from the northeast/east direction. Huuse (1986) also illustrated a typical delta of the North Sea Cenozoic in the schematic cross-section in Figure 58, which is similar to the interpreted clinoforms within the study area located in the Åsta Graben.

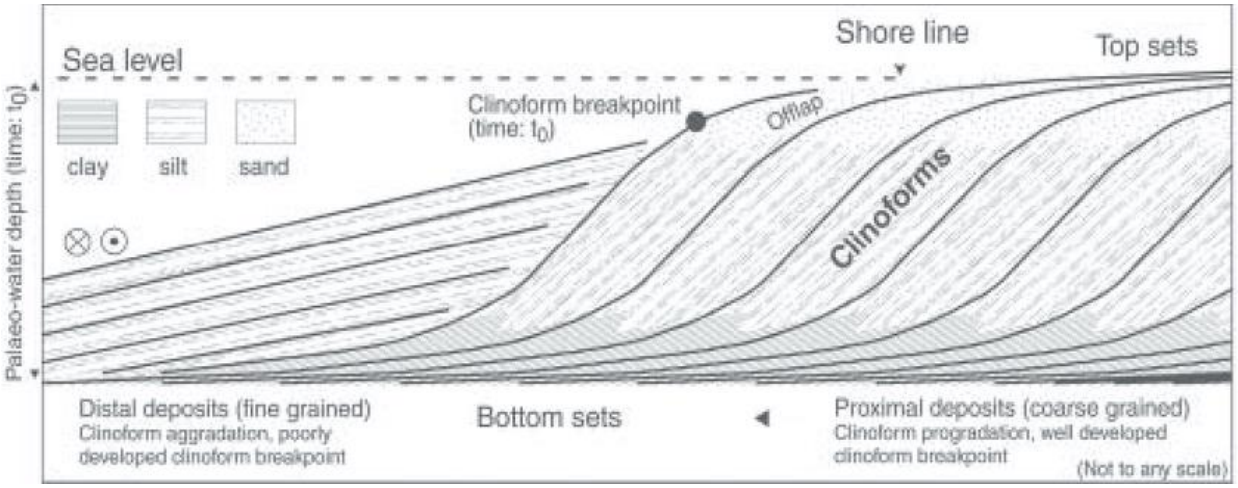

Figure 58. Typical delta of the North Sea Cenozoic, displaying thick progradational succession. This schematic cross-section is not to scale. From Huuse (1986)

7. Conclusion

The Oligocene interval in the Egersund Basin and the surrounding areas in the southern to central parts of the Norwegian North Sea, was divided into seven main units: Unit A (the earliest Early Oligocene or Rupelian), Unit B (Early Oligocene, Rupelian), Unit C (late Early Oligocene), Unit D (latest Early Oligocene to early Late Oligocene (Chattian)), Unit E (Chattian), Unit F (late Chattian) and Unit G (latest Chattian/Late Oligocene).

Stratigraphic unit interpretations were determined based on the well correlation and seismic interpretation. Three units, Unit A, Unit B and Unit E, were interpreted as highstand systems tracts. Two lowstand systems tracts were interpreted in Unit C and Unit F in the distal part of the study area, based on the 2D seismic data. Unit D and Unit G were interpreted as transgressive systems tracts. For the Oligocene strata in the Egersund Basin and its surrounding, two complete sequences were identified, and one lower ranked order sequence were interpreted within Unit A. The two complete sequences are related to third-order cycles, based on the time span of Oligocene of almost 10 Ma and the occurring tectono-eustacy.

Depositional sequences are controlled mainly three regime variables, which are influenced by sediment supply, eustatic sea level and tectonic setting. The onset of Oligocene was affected by the regional event of seafloor spreading in the North Atlantic Ocean (Jarsve et al., 2014). The global sea-level curve displays a generally high sea level during the Rupelian, and a transition to relatively low sea level during the Chattian period. The Fennoscandian Shield and mainland Norway underwent uplifting during the Oligocene period, contributing to abundant sediment supply from the northeast of the Egersund Basin. Differential subsidence together with the mainland uplift, resulted in falls and rises in relative sea level throughout the Oligocene succession, which led to progradation and retrogradation of sediments. Large scale progradation of mostly fine sediments occurred in Early Oligocene, while in the Late Oligocene input of coarser sediments have been observed.

The Oligocene interval display a thickening succession towards the deeper parts of the basin (Norwegian-Danish Basin) in a southwest direction, with a gradual thinning of deposition towards the Stavanger Platform to the northeast. The thickest deposition within the study area display a thickness of approximately 500 ms (950 m), and the shallowest area of Oligocene deposition, at the edge of the Stavanger Platform, display a thickness of around 100 ms (190 m).

Based on the thin succession of Oligocene deposition within the extent of the Egersund Basin, 2D seismic lines outside this area were utilized to provide a better understanding of the sequence stratigraphic framework of the Oligocene in this area.

References

http://www.sepmstrata.org/Terminology.aspx?id=chronostratigraphy (20.03.19)

Allen, G.P. and Posamentier, H.W., 1993. Sequence stratigraphy and facies model of an incised valley fill: the Gironde estuary, France. Journal of Sedimentary Petrology 63, Vol. 3, pp. 378–391.

Anell, I., Thybo, H., and Stratford, W., 2010. Relating Cenozoic North Sea sediments to topography in southern Norway: The interplay between tectonics and climate. *Earth and Planetary Science Letters, 300*, 19-32.

Blum, M. D.,1994. Genesis and architecture of incised valley fill sequences: a Late Quaternary example from the Colorado River, Gulf Coastal Plain of Texas. In: Weimer, P., Posamentier, H. W. (eds.), Siliciclastic sequence stratigraphy: recent developments and applications. American Association of Petroleum Geologists Memoir **58**, 259-283.

Brown, L, F, Jr., and Fisher, W, L. 1977. Seismic Stratigraphic Interpretation of Depositional Systems: Examples from Brazilian Rift and Pull Apart Basins. In: Payton, C. E. (ed.), Seismic Stratigraphy – Applications to Hydrocarbon Exploration. AAPG Memoir 26, pp. 213–248.

Carter, R. M., Fulthorpe, C. S., Naish, T. R., 1998. Sequence concepts at seismic and outcrop scale: the distinction between physical and conceptual stratigraphic surfaces. Sedimentary Geology 122, pp.165–179.

Cartwright, J., James, D., and Bolton, A. (2003). The genesis of polygonal fault systems: a review. Subsurf. Sedim. Mobilizat. 216, 223–243. doi: 10.1144/GSL.SP.2003.216.01.15

Catuneanu, O. 2002. Sequence Stratigraphy of Clastic Systems: Concepts, Merits, and Pitfalls. Journal of African Earth Sciences 35, pp. 1–43. DOI: 10.1016/S0899-5362(02)00004-0

Catuneanu, O., 2006. Principles of Sequence Stratigraphy Elsevier, Amsterdam, pp. 375

Catuneanu, O., Abreu, V., Bhattacharya, J.P., Blum, M.D., Dalrymple, R.W., Eriksson, P.G., Fielding, C.R., Fisher, W.L., Galloway, W.E., Gibling, M.R. and Giles, K.A., 2009. Towards the standardization of sequence stratigraphy. Earth-Science Reviews, 92(1-2), pp.1-33.

Catuneanu, O., Galloway, W, E., Kendall, C, G, S, C., Miall, D, A., Posamentier, H, W., Strasser, A., Strasser, A., and Tucker, M, E. 2011. Sequence Stratigraphy: Methodology and Nomenclature. Newsletters on Stratigraphy, Vol. 44, pp. 173-245.

Coward, M P, Dewey, J F, Hempton, M and Holroyd, J. 2003. Tectonic evolution. 17-33 in *The Millennium Atlas: petroleum geology of the central and northern North Sea.* Evans, D, Graham, C, Armour, A, and Bathurst, P (editors and co-ordinators). London: The Geological Society of London.)

Cross, T.A., and Lessenger, M.A., 1988. Seismic stratigraphy: Annual Review of Earth and Planetary Sciences, v. 16, p.117-131.

Danielsen, Michelsen, & Clausen. (1997). Oligocene sequence stratigraphy and basin development in the Danish North Sea sector based on log interpretations. *Marine and Petroleum Geology, 14*(7), 931-950.

Davidson, I., Alsop, I., Birch, P., Elders, C., Evans, N., Nicholson, H., Rorison, P., Wade, D., Woodward, J., Young, M., 2000b. Geometry and late-stage structural evolution of Central Graben salt diapirs, North Sea. Mar. Pet. Geol. 17, 499-522.

Deegan, C. E and Scull, B. J, (compilers), 1977. A proposed standard lithostratigraphic nomenclature for the Central and Northern North Sea. Rep. Inst. Geol. Sci., No. 77/25: Bull. Norw. Petrol. Direct., No. 1, HMSO, London

Dooley, T. P., Jackson, M.P.A, Hudec, M. R., 2009. Inflation and deflation of deeply buried salt stocks during lateral shortening. J. Struct. Geol. 31, 582-600.

Doré, A., Lundin, E., Jensen, L., Birkeland, &., Eliassen, P., & Fichler, C. (1999). Principal tectonic events in the evolution of the northwest European Atlantic margin. *Geological Society, London, Petroleum Geology Conference Series, 5*(1), 41-61.

Eidvin, T., & Rundberg, Y. (2001). Late Cainozoic stratigraphy of the Tampen area (Snorre and Visund fields) in the northern North Sea, with emphasis on the chronology of early Neogene sands. *Norsk Geologisk Tidsskrift, 81*(2), 119-160.

Eidvin, T., & Rundberg, Y. (2007). Post-Eocene strata of the southern Viking Graben, northern North Sea; integrated biostratigraphic, strontium isotopic and lithostratigraphic study. *Norsk Geologisk Tidsskrift, 87*(4), 391-450.

Eidvin, T., Goll, R.M., Grogan, P., Smelror, M., Ulleberg, K., 1998b. The Pleistocene to Middle Eocene stratigraphy and geological evolution of the western Barents Sea continental margin at well site 7316/5-1 (Bjørnøya West area). Nor. Geol. Tidsskr. 78, 99-123.

Eidvin, T., Goll, R.M., Grogan, P., Smelror, M., Ulleberg, K., 1998b. The Pleistocene to Middle Eocene stratigraphy and geological evolution of the western Barents Sea continental margin at well site 7316/5-1 (Bjørnøya West area). Nor. Geol. Tidsskr. 78, 99-123.

Eidvin, T., Jansen, E., Riis, F., 1993. Chronology of Tertiary fan deposits of the western Barents Sea: implications for the uplift and erosional history of the Barents Shelf. Mar. Geol. 112, 109-131.

Eidvin, T., Riis, F., & Norge Oljedirektoratet. (1992). *En biostratigrafisk og seismostratigrafisk analyse av tertiære sedimenter i nordlige deler av Norskerenna, med hovedvekt på øvre pliocene vifteavsetninger* (Vol. 32, NPD-contribution (trykt utg.)). Stavanger: Oljedirektoratet.

Eidvin, T., Riis, F., Gjeldvik, I.T., 2013a. The Lower Miocene Skade Formation in the northern North Sea (Extent and thickness, age from fossil and Sr isotope correlations, lithology, paleobathymetry and regional correlation). NGF Abstr. Proc. no 1 (2013), 28-29.

Eidvin, T., Riis, F., Gjeldvik, I.T., 2013b. Middle Miocene sandy deposits of the Nordland Group, northern North Sea (Suggested called Eir Formation, extent and thickness, age from fossil and Sr isotope correlations, lithology, paleobathymetry and regional correlation). NGF Abstr. Proc. no 1 (2013), 30-31.

Eidvin, T., Riis, F., Rasmussen, E. S. & Rundberg, Y. 2013. Investigation of Oligocene to Lower Pliocene deposits in the Nordic offshore area and onshore Denmark. NPD Bulletin 10, 62.

Eidvin, T., Riis, F., Rasmussen, E.S., 2014. Oligocene to Lower Pliocene deposits of the Norwegian continental shelf, Norwegian Sea, Svalbard, Denmark and their relation to the uplift of Fennoscandia: A synthesis. *Marine and Petroleum Geology, 56*, 184-221.

Eidvin, T., Riis, F., Rasmussen, E.S., Rundberg, Y., 2013d. Investigation of Oligocene to Lower Pliocene deposits in the Nordic area. NPD Bull. No 10

Embry, A.F., 1995. Sequence boundaries and sequence hierarchies: problems and proposals. Sequence Stratigraphy on the Northwest European Margin, 5, pp.1-11.

Embry, A.F., 2009. Practical sequence stratigraphy. Canadian Society of Petroleum Geologists, 81.

Emery, D. & Myers, K. 2009. Sequence stratigraphy, John Wiley & Sons, pp. 304.

Erratt, D., Thomas, G., & Wall, G. (1999). The evolution of the Central North Sea Rift. *Geological Society, London, Petroleum Geology Conference Series, 5*(1), 63-82.

Faleide J.I., Bjørlykke K., Gabrielsen R.H. (2010) Geology of the Norwegian Continental Shelf. In: Petroleum Geoscience. Springer, Berlin, Heidelberg, pp.467-499.

Faleide, J.I., Solheim, A., Fiedler, A., Hjelstuen, B.O., Andersen, E.S., & Vanneste, K., 1996. Late Cenozoic evolution of the western Barents Sea-Svalbard continental margin. In: Solheim, A., et al. (Eds.), Impact of glaciations on basin evolution: data and models from the Norwegian margin and adjacent areas. *Global and Planetary Change, 12*(1), 53-74.

Fjeldskaar, W., Prestholm, E., Guargena, C., Gravdal, N., 1993. Isostatic and tectonic development of the Egersund Basin. Doré, A.G., Augustson, J.H., Hermanrud, C., Stewart, D.J., Sylta Ø (Eds.), basin Modelling: Advances and Applications, Elsevier, Amsterdam, pp. 549-562.

Fyfe, J A, Gregersen, U, Jordt, H, Rundberg, Y, Eidvin, T, Evans, D, Stewart, D, Hovland, M, and Andersen, P. 2003. Oligocene to Holocene. 279-287 in *The Millennium Atlas: petroleum geology of the central and northern North Sea.* Evans, D, Graham, C, Armour, A, and Bathurst, P (editors and co-ordinators). London: The Geological Society of London.)

Gabrielsen, R.H., Kyrkjebø, R., Faleide, J.I., Fjeldskaar, W. and Kjennerud, T., 2001. The Cretaceous post-rift basin configuration of the northern North Sea. *Petroleum Geoscience*, Vol. 7, 137-154.

Galloway, W, E. 1989. Genetic Stratigraphic Sequences in Basin Analysis I: Architecture and Genesis of Flooding-Surface Bounded Depositional Units. The American Association of Petroleum Geologists Bulletin, Vol. 73, pp. 125–142.

Glennie, K.W., and Underhill, J.R., 1998. Origin, Development and Evolution of Structural Styles. 42-84 in *Petroleum geology of the North Sea, basic concepts and recent advances* (fourth edition). Glennie, K.W. (editor). (Oxford: Blackwell Scientific Publications.)

Glennie, K.W., Higham, J., Stemmerik, L., 2003. Permian. In: Evans, D., Graham, C., Armour, A., Bathurst, P. (Eds.), The Millennium Atlas: Petroleum Geology of the Central and Northern North Sea. The Geological Society of London, London, pp. 91-103.

Gregersen, U., & Johannessen, P.N., 2007. Distribution of the Neogene Utsira Sand and Hutton Sand, and the succeeding deposits in the Viking Graben area, North Sea. *Marine and Petroleum Geology, 24*(10), 591-606.

Halland, E., Johansen, W., Riis, F., & Norge Oljedirektoratet. (2011). *CO_2 storage atlas: Norwegian North Sea*. Stavanger: Norwegian Petroleum Directorate.

Haq, B. U., Hardenbol, J. & Vail, P. R. 1987. Chronology of fluctuating sea levels since the Triassic. Science 235, 1156–67.

Hardenbol, J., Thierry, J., Farley, M.B., De Graciansky, P.C. and Vail, P. (1998). Mesozoic and Cenozoic sequence chronostratigraphic framework of European basins. In: *Mesozoic and Cenozoic Sequence Stratigraphy of European Basins* (Ed. By P.C. Graciansky) SEMP *Spec. Publ., 60, 3-13.*

Helland-Hansen, W. & Martinsen, O. J. 1996. Shoreline trajectories and sequences: description of variable depositional-dip scenarios. Journal of Sedimentary Research, 66.

Helland-Hansen, W. and Hampson, G., J. 2009. Trajectory Analysis: Concepts and Applications. Basin Research, Vol. 21, pp. 454-483. DOI: 10.1111/j.1365- 2117.2009.00425.x

Helland-Hansen, W., 2009. Towards the standardization of sequence stratigraphy. Earth- Science Reviews, 94(1-4), pp.95-97.

Helland-Hansen, W., Gjelberg, J. G., 1994. Conceptual basis and variability in sequence stratigraphy: a different perspective. Sedimentary Geology **18**, 451-467.

Hodgson, N.A., Farnsworth, J., Fraseer, A.J., 1992. Salt-related tectonics, sedimentation and hydrocarbon plays in the Central Graben, North Sea, UKCS. Geol. Soc. Lond. Spec. Publ. 67, 31-63.

Holmes, R., 1997. Quaternary stratigraphy: the offshore record. 72-94 in *Reflections in the ice age in Scotland*. Gordon, J.E. (editor). (Glasgow: Scottish Association of Geography Teachers and Scottish Natural heritage.)

Hunt, D. and Tucker, M.E., 1992. Stranded parasequences and the forced regressive wedge systems tract: deposition during base-level fall. Sedimentary Geology, 81(1-2), pp.1-9. DOI: 10.1016/0037-0738(94)00123-C

Husmo, T., Hamar, G., Høiland, O., Johannessen, E.P., Rømuld, A., Spencer, A., Titterton, R., 2003. Lower and middle Jurassic. In: Evans, D., Graham, C., Armour, A., Bathurst, P. (Eds.). The Millennium Atlas: Petroleum Geology of the Central and Northern North Sea. The Geological Society of London, London, pp. 129-155.

Huuse, Mads. (1986). Late Cenozoic palaeogeography of the eastern North Sea Basin: Climatic vs tectonic forcing of basin margin uplift and deltaic progradation. Bull. Geol. Soc. Denmark. 5. 2002-12.

Isaksen, D. and Tonstad, K. eds., 1989. A revised Cretaceous and Tertiary lithostratigraphic nomenclature for the Norwegian North Sea. Norwegian Petroleum Directorate.

Jackson, C., & Lewis, M. (2016). Structural style and evolution of a salt-influenced rift basin margin; the impact of variations in salt composition and the role of polyphase extension. *Basin Research, 28*(1), 81-102.

Jackson, C.A.L., & Lewis, M.M. (2013). Physiography of the NE margin of the Permian Salt Basin: New insights from 3D seismic reflection data. *Journal of the Geological Society, 170*(6), 857-860.

Jackson, C.A.L., Chua, S.T., Bell, R.E., & Magee, C. (2013). Structural style and early stage growth of inversion structures: 3D seismic insights from the Egersund Basin, offshore Norway. *Journal of Structural Geology, 46*, 167-185

Jacobsen, V.W., 1982. Sedimentation and paleogeography. In: R.C. Olsen and I.F. Strass (Editors), 1982. The Norwegian Danish Basin. Norwegian Petroleum Directorate, NPD Paper No. 31, pp. 54-66.

Jarsve, E., Nystuen, T., Faleide, J., Gabrielsen, R., Eidvin, B., & Thyberg. (2014). The Oligocene succession in the Eastern North Sea: Basin development and depositional systems. *Geological Magazine, 108*(4), 668-693.

Jervey, M.T., 1988. Quantitative geological modeling of siliciclastic rock sequences and their seismic expressions. In: C.K. Wilgus et al., eds., Sea level changes: an integrated approach: Society of Economic Paleontologists and Mineralogists Special Publication 42, pp. 47-69.

Jordt, H., Faleide, J, I., Bjorlukke, K., and Ibrahim, M, T. 1995. Cenozoic Sequence Stratigraphy of the Central and Northern North Sea Basin: Tectonic Development, Sediment Distribution and

Provenance Areas. Marine and Petroleum Geology, Vol. 12, pp. 845–879. DOI: 10.1016/0264-8172(95)98852-V

Knox, R.W., and Holloway, S. 1992. Paleogene of the Central and Northern North Sea. *Lithostratigraphic nomenclature of the UK North Sea, Vol.1.* Knox, R.W. O'B, and Cordey, W.G. (editors). (Nottingham: British Geological Survey.)

Laberg, J.S., Stoker, M.S., Dahlgren, K.I.T., de Haas, H., Haflidason, H., Hjelstuen, B.O., Nielsen, T., Shannon, P.M., Vorren, T.O., van Weering, T.C.E., Ceramicola, S., 2005b. Cenozoic alongslope processes and sedimentation on the NW European Atlantic margin. Mar. Pet. Geol. 22, 1069-1088

Leckie, D. A., 1994. Canterbury Plains, New Zealand – Implications for sequence stratigraphic models. American Association of Petroleum Geologists Bulletin **78**, 1240-1256.

Mannie, A., Jackson, C., & Hampson, G. (2014). Structural controls on the stratigraphic architecture of net-transgressive shallow-marine strata in a salt-influenced rift basin: Middle-to-Upper Jurassic Egersund Basin, Norwegian North Sea. *Basin Research, 26*(5), 675-700.

Martin, J., Paola, C., Abreu, V., Neal, J., & Sheets, B. (2009). Sequence stratigraphy of experimental strata under known conditions of differential subsidence and variable base level. *AAPG Bulletin, 93*(4), 503-533

Martini, E., 1971. Standard Tertiary and Quaternary calcareous nannoplankton zonation. Farinacci, A. (Ed.), Proceedings for the II Planktonic Conference, Edizioni Tecnoscienza No. 2, Rome, 1970 (1971), pp. 739-785

Miall, A. D. (2016). *Stratigraphy: A Modern Synthesis* (1st ed. 2016 ed.). Cham: Springer International Publishing.

Michelsen, O., Danielsen, M., Heilmann-Clausen, C., Jordt, H., Laursen, G.V., and Thomsen, E., 1995. Occurrence of major sequence stratigraphic boundaries in relation to basin development in Cenozoic deposits of the southeastern North Sea. *Norwegian Petroleum Society Special Publications, 5*(C), 415-427.

Mitchum, R, M, Jr., Vail, P.R., 1977. Seismic Stratigraphy and Global Changes of Sea Level. Part 7: Stratigraphic of Seismic Reflection Patterns in Depositional Sequences. In: Peyton, C.E. (Ed.), Seismic Stratigraphy—Applications to Hydrocarbon Exploration. AAPG Memoir 26, pp. 135-144.

Mitchum, R. M. Jr., P. R. Vail and J. B. Sangree, presence of a stratigraphic trap at Hortense Field 1977, Seismic Stratigraphy and Global Changes of Sea Level, Part 6: Stratigraphic Interpretation of Seismic Reflection Patterns in Depositional Sequences, In: Payton, C. E. cd., Seismic Stratigraphy - Applications to Hydrocarbon Exploration: AAPG Memoir 26, pp.117-133.

Mitchum, R. M. Jr., P. R. Vail and S. Thompson III, 1977, Seismic Stratigraphy and Global Changes of Sea Level, Part 2: The Depositional Sequence as a Basic Unit for StratigraphicAnalysis,

In: Payton, C. E. cd., Seismic Stratigraphy - Applications to Hydrocarbon Exploration: AAPG Memoir 26, pp.53-62.

Mitchum, R. M., Jr., Van Wagoner, J.C., 1991. High-frequency sequences and their stacking patterns: sequence stratigraphic evidence of high-frequency eustatic cycles. Sedimentary Geology **70**, 131-160.

Mitchum, R.M, Jr., Vail, P.R., and Sangree, J.B., 1977. Seismic stratigraphy and global changes of sea level: Part 6. Stratigraphic interpretation of seismic reflection patterns in depositional sequences: Section 2. Application of seismic reflection configuration to stratigraphic interpretation. In: Payton, C.E. (Ed.), Seismic Stratigraphy—Applications to Hydrocarbon Exploration. AAPG Memoir 26, pp. 205-212

Møller, J. J., & Rasmussen, E. S. (2003). Middle Jurassic - Early Cretaceous rifting of the Danish Central Graben. *Geological Survey of Denmark and Greenland Bulletin,* (1), 247-264.

Nichols, G. 2009. *Sedimentology and Stratigraphy*, second edition. West Sussex, UK: Wiley-Blackwell, 419 pp.

Norwegian Petroleum Directorate (NPD)- FactPages. 2017.

Nummedal, D., Swift, D. J. P., 1987. Transgressive stratigraphy at sequence-bounding unconformities: some principles derived from Holocene and Cretaceous examples.

Nystuen, J.P., 1998. History and development of sequence stratigraphy. In: *Sequence Stratigraphy – Concepts and Applications (*Ed. By F. M. Gradstein, K. O. Sandvik and N. J. Milton), pp. 31-116. Elsevier, Amsterdam.

Pekar, S. F., Christie-Blick, N., Kominz, M. A. & Miller, K. G. 2002. Calibration between eustatic estimates from backstripping and oxygen isotopic records for the Oligocene. Geology 30, 903–6.

Plint, A. G., 1988. Sharp-base shoreface sequences and" offshore bars" in the Cardium Formation of Alberta: their relationship to relative changes in sea-level. Sea-level Changes: An Integrated Approach: SEPM Special Publication, 42, pp.357-370.

Posamentier, H, W., and Allen, G, P., 1999. Siliciclastic Sequence Stratigraphy: Concepts and Applications. SEPM Concepts in Sedimentology and Paleontology, No. 7, 210 pp.

Posamentier, H, W., and Kolla, V. 2003. Seismic Geomorphology and Stratigraphy of Depositional Elements in Deep-Water Settings. Journal of Sedimentary Research, Vol. 73; No. 3, pp. 367–388. DOI: doi.org/10.1016/j.earscirev.2008.10.003

Posamentier, H, W., Jervey, M, T., and Vail, P, R. 1988. Eustatic Controls on Clastic Deposition. I. Conceptual Framework. In: Wilgus, C. K., Hastings, B. S., Kendall, C, G, St. C., Posamentier, H.W., Ross, C. A., Van Wagoner, J. C. (Eds.). Sea Level Changes – An Integrated Approach. SEPM Special Publication 42, pp. 110–124.

Posamentier, H.W. and Vail, P.R., 1988. Eustatic controls on clastic deposition II—sequence and systems tract models. In: Wilgus, C. K., Hastings, B. S., Kendall, C.G.St.C., Posamentier, H. W., Ross, C. A., Van Wagoner, J.C. (Eds.), Sea Level Changes – An Integrated Approach. SEMP Special Publication **42**, 125-154.

Ramsayer, G, R. 1979. Seismic Stratigraphy: A Fundamental Exploration Tool. In: Proceedings of the Offshore Technology Conference, Houston, Texas, April–May 1979, Vol. 3, pp. 1859–1867. DOI: 10.4043/3568-MS

Rich, J. L., 1951. Three critical environments of deposition and criteria for recognition of rock deposited in each of them: Geological Society of America Bulletin, v. 62, p. 1-20.

Roksandic, M, M. 1978. Seismic Facies Analysis Concepts. Geophysical prospecting 26, pp. 383-398. DOI: 10.1111/j.1365-2478.1978.tb01600.x

Rundberg, Y., Eidvin, T., 2005. Controls on depositional history and architecture of the Oligocene-Miocene succession, northern North Sea Basin. In: Wandaas, B.T.G., et al. (Eds.), Onshore-offshore Relationships on the North Atlantic Margin, NPF Special Publication, vol. 12, pp. 207-239.

Ryan, M.C., Helland-Hansen, W., Johannessen, E.P. and Steel, R.J., 2009. Erosional vs. accretionary shelf margins: the influence of margin type on deepwater sedimentation: an example from the Porcupine Basin, offshore western Ireland. Basin Research, 21(5), pp.676-703.

Salvador, 1994. International Stratigraphic Guide: A Guide to Stratigraphic Classification Ch. 2, 3

Shanmugam, G., 1988. Origin, recognition and importance of erosional unconformities in sedimentary basins, in Kleinspehn, K. L., and Paola, C., eds., New Perspectives in Basin Analysis: New York, Springer-Verlag, p. 83–108.

Sheriff, R.E. and Geldart, L.P., 1995. Exploration seismology. Cambridge university press. pp. 146.

Schlumberger, 2016. Petrel Seismic-to-Simulation Software Interpreter's Guide to Seismic Attributes. Schlumberger, Houston.

Sloss, L., Krumbein, W., and Dapples, E., 1949.Integrated facies analysis. In: Longwell, C. (ed.), Sedimentary facies in geologic history. Geological Society America, Memoir 39, pp.91-124.

Sørensen, S., and Tangen, O, H. 1995. Exploration Trends in Marginal Basins from Skagerrak to Stord. Petroleum Exploration and Exploitation in Norway. NPF Special Publication, No. 4, pp. 97-114. DOI: 10.1016/S0928-8937(06)80039-1

Sørensen, S., Morizot, H., Skottheim, S., 1992. A tectonostratigraphic analysis of the southeast Norwegian North Sea basin. Spec. Publ. Nor. Pet. Soc. NPF 1, 19-42.

Sosson, M., Kaymakci, N., Stephenson, R. A., Bergerat, F. and Starostenko, V. (eds) Sedimentary Basin Tectonics from the Black Sea and Caucasus to the Arabian Platform. Geological Society, London 2010, Special Publications, 340, 1-10. DOI: 10.1144/SP340.1

Steel, R. J., Olsen, T., 2002. Clinoforms, clinoform trajectories and deepwater sands. In: Armentrout, J. M., Rosen, N. C. (eds.), Sequence Stratigraphic Models for Exploration and Production: Evolving Methodology, Emerging Models and Application Histories. Proceeding of the 22nd Annual Bob F. Perkins Research Conference. Gulf Coast Section, Society of Economic Paleontologists and Mineralogists (GCS-SEMP), 367-381.

Tesson, M., Labaune, C. and Gensous, B., 2005. Small rivers contribution to the Quaternary evolution of a Mediterranean littoral system: The western gulf of Lion, France. Marine Geology, 223-223, 299-311.

Tvedt, A., Rotevatn, A., & Jackson, C., 2016. Supra-salt normal fault growth during the rise and fall of a diapir: Perspectives from 3D seismic reflection data, Norwegian North Sea. *Journal of Structural Geology,91*, 1-26.

Tvedt, A., Rotevatn, A., Jackson, C.A.L., Fossen, H., & Gawthorpe, R.L., 2013. Growth of normal faults in multilayer sequences: A 3D seismic case study from the Egersund Basin, Norwegian North Sea. *Journal of Structural Geology, 55*, 1-20.

Underhill, J.R., & Partington, M.A. (1993). Jurassic thermal doming and deflation in the North Sea: Implications of the sequence stratigraphic evidence. In: *Geological Society, London, Petroleum Geology Conference Series,4(1), 337-345.*

Vail, P. R., Mitchum, R, M, Jr., and Thompson, S. 1977. Seismic Stratigraphy and Global Changes of Sea Level, Part Four: Global Cycles of Relative Changes of Sea Level. In Payton, C.E., ed., Seismic stratigraphy; applications to hydrocarbon exploration: American Association of Petroleum Geologists Memoir 26, pp. 83-98.

Van Wagoner, J, C. 1995. Sequence Stratigraphy and Marine to Non-Marine Facies Architecture of Foreland Basin Strata, Book Cliffs, Utah, U.S.A. In: Van Wagoner, J. C., Bertram, G.T. (Eds.), Sequence Stratigraphy of Foreland Basin Deposits. AAPG Memoir 64, pp. 137–223.

Van Wagoner, J, C., Mitchum R., M, Jr., Campion, K, M., and Rahmanian, V, D. 1990. Siliciclastic Sequence Stratigraphy in Well Logs, Core, and Outcrops: Concepts for High- Resolution Correlation of Time and Facies. American Association of Petroleum Geologists Methods in Exploration, Series 7, 55 pp.

Van Wagoner, J, C., Posamentier, H, W., Mitchum, R, M., Vail, P, R., Sarg, J, F., Loutit, T, S., and Hardenbol, J. 1988. An Overview of the Fundamentals of Sequence Stratigraphy and Key Definitions. In: Wilgus, C, K., Hastings, B. S., Kendall, C, G, St, C., Posamentier, H.W., Ross, C. A., Van Wagoner, J, C. (Eds.). Sea Level Changes – An Integrated Approach. SEPM Special Publication, No. 42, pp. 39-45.

Van Wagoner,J. C., Mitchum, R. M., Posamentier, H. W., Vail, P. R., 1987. An overview of sequence stratigraphy and key definitions. In: Bally, A.W. (Ed.), Atlas of Seismic Stratigraphy, volume 1. AAPG Studies in Geology **27**, 11-24.

Vejbæk, O., Andersen, C., 2002. Post mid-Cretaceous inversion tectonics in the Danish Central Graben – regionally synchronous tectonic events. Bull. Geol. Soc. Den. 49, 129-144.

Vollset, J. and Doré, A.G. eds., 1984. A revised Triassic and Jurassic lithostratigraphic nomenclature for the Norwegian North Sea. Oljedirektoratet.

Wheeler, H. E., 1958. Time-stratigraphy. AAPG Bulletin, 42, pp.1047-1063.

Zachos, J., Pagani, M., Sloan, L., Thomas, E., & Billups, K. (2001). Trends, rhythms, and aberrations in global climate 65 ma to present. *Science, 292*(5517), 686-693.

Zanella, E, and Coward, M P. 2003. Structural framework. 45-59 in *The Millennium Atlas: petroleum geology of the central and northern North Sea.* Evans, D, Graham, C, Armour, A, and Bathurst, P (editors and co-ordinators). London: The Geological Society of London.)

Zanella, E., and Coward, P, M. 2003. Structural Framework. In D. Evans, et al. (Eds.). The Millennium Atlas: Petroleum Geology of the Central and Northern North Sea. The Geological Society of London, pp. 88-125.

Zecchin, M., & Catuneanu, O. (2012). High-resolution sequence stratigraphy of clastic shelves I: Units and bounding surfaces. *Marine and Petroleum Geology*, *39*(1), 1-25.

Ziegler, P.A., 1975. North Sea Basin History in the Tectonic Framework of North-West Europe. 131-149 in *Petroleum and the Continental Shelf of North-West Europe, Vol 1.* Woodland, A.W. (editor). (Barking: Applied Science Publisher.)

Ziegler, P.A., 1979. North Sea exploration. *AAPG Bulletin, 63*(3), 556.

Ziegler, P.A., 1981. Evolution of sedimentary basins in north-west Europe. 3-39 in *Petroleum geology of the continental shelf of North-West Europe*. Illing, L.V., and Hobson, G.D. (editors). (London: Heyden and Son.)

Ziegler, P.A., 1990. *Geological Atlas of Western and Central Europe,* pp. 1-239. Shell International Petroleum Maatschappij B.V., Netherlands.

Ziegler, P.A., 1992. North Sea rift system. Tectonophysics 208, 55-75.